A TALE OF TWO POISONS: OVERCOMING DELETERIOUS ANTICANCER SIDE EFFECTS AND ANTIBACTERIAL RESISTANCE

By

Alexandria Argelia Oviatt

Dissertation

Submitted to the Faculty of the

Graduate School of Vanderbilt University

in partial fulfillment of the requirements

for the degree of

DOCTOR OF PHILOSOPHY

in

Chemical and Physical Biology

May 13, 2022

Nashville, Tennessee

Approved:

Brian Bachmann, Ph.D.

James Dewar, Ph.D.

Brandt Eichman, Ph.D.

Kathy Friedman, Ph.D.

Neil Osheroff, Ph.D.

To my grandfather, Bernard L. Oviatt, Sr., who instilled in me a deeply abiding love for the written word and for learning.

ACKNOWLEDGEMENTS

There are numerous iterations of the idea that the destination matters far less than the journey it took to get there. I would apply the same thinking to getting a Ph.D.

Thankfully, I had a 5-star tour guide on this trip from clueless undergraduate STEMinist to budding woman in science. To Dr. Neil Osheroff, teacher, mentor, and advocate: thank you. If I am now "blossoming," it is in no small part because of you. Thank you for recognizing and believing in my potential from the beginning – and reminding me of it when I was less sure. Thank you, too, for acknowledging my weaknesses and helping me find ways to overcome them, even if that just meant stepping back to let me find my own voice. Thank you for your witty repartee, your belief in feeding us (in both scientific thought and top-notch cuisine), your time, and your devotion to your students. It has been my honor to be a part of your laboratory and to become a far better scientist and person as a result.

To my dissertation committee – Drs. Brian Bachmann, James Dewar, Brandt Eichman, and Kathy Friedman – thank you for editing the roadmap that Neil and I followed. Your expertise, and the willingness with which you shared it, have certainly shaped my graduate career for the better. Thank you for the many questions that refined my thinking, the advice that made my science better, and the encouragement.

For being the operator-and-mechanic-in-one that keeps our lab running smoothly, thank you to Jo Ann Byl. Thank you for the training, the day-to-day troubleshooting, the thoughtful questions, the freely-given advice, and the unending love and support. Thank you for spending long days in the cold room with me, for being there with suggestions when I finish ranting, and for sharing your kDNA. You are an invaluable asset and I cannot thank you enough for helping me get to the finish line.

How lucky I have been to join not just a lab but a family. Thank you to Jessica Collins, confidant and co-NBR (Nashville biscuit researcher), Dr. Esha Dalvie, who started this journey with me and ended it just the same, Soziema Dauda, our fearless undergraduate, Dr. Elizabeth Gibson, older lab sister

extraordinaire, Jeff Jian, who plays little brother to my older sister so well, Dr. Lorena Infante Lara, the one with whom I climb trees, Justin Lopez, *pew, pew*, and Dr. Elirosa Minniti, who reminded me that hugs should be freely given. My sincerest thanks for the laughs, the rants, the coffee shop trips, the Jeni's and the support.

For preparing me to take on graduate school, I must thank Drs. Christian Rojas and Jean Vadakkan. Your belief in my potential as a scientist gave me the opportunity to become just that. Your continued support, both in the form of recommendation letters and encouraging notes, has been so appreciated.

To Leonore Annenberg: you are long gone, but your legacy lives on in the people whose dreams you made reality. Thank you for giving me the opportunity to be a Barnard woman. To Dr. Gail Levin and co, thank you for giving me the benefit of the Annenberg legacy and for the advice along the way.

To Elaine Harper, my appreciation for your mentorship is unending. For paying some of my college applications fees, organizing college visits, giving me a summer job, and much more, thank you.

To my family: none of this would be possible without you. Thank you for having an unwavering belief that I could accomplish anything I dreamed up. Thanks to my parents for the love and especially for the built-in, lifelong best friend that you gave me in the form of a younger brother. To that younger brother – when did you become so wise? I would be remiss if I did not mention the friends who have become my family: you fill my life with so much love. To Katie and Ariel, who have been by my side for more than a decade; to the Sci-5 (Alison, Erica, Jessamine, and Nadia), who made me feel at home in the big city; to Sarah and Matthew, for the supper clubs that fed my soul; to Spencer, my favorite running partner; to Zack, the best person to survive a crash with; to Ashley, for the deep understanding; to Holly, for letting me sit next to you that first time; to Sam, a great friend and baker; and to Bernoulli Yoshi Stitch, the best pandemic puppy. Finally, to David, especially, thank you for being an extraordinary partner while I have been a thesis-writing misery.

TABLE OF CONTENTS

LIST OF TABLES

LIST OF FIGURES

Figure

Chapter I Page

Chapter III

Chapter IV

Chapter VI

LIST OF ABBREVIATIONS

(-)SC	negatively supercoiled
(+)SC	positively supercoiled
A	alanine
Asp	aspartic acid
ATP	adenosine triphosphate
bp	base pair
BSA	bovine serum albumin
Cipro	ciprofloxacin
D	aspartate
DMSO	dimethyl sulfoxide
DS	double-stranded
DTT	dithiothreitol
EDTA	ethylenediaminetetraacetic acid
F	phenylalanine
G	glycine
Gepo	gepotidacin
Glu	glutamic acid
Gyr	gyrase
H	histidine
hTIIα	human topoisomerase IIα
hTIIβ	human topoisomerase IIβ
L	leucine
Lin	linear
MGI	*Mycobacterium tuberculosis* gyrase inhibitor
Moxi	moxifloxacin
N	asparagine
NBTI	novel bacterial topoisomerase inhibitor
Nick	nicked
P	proline
Rel	relaxed
SDS	sodium dodecyl sulfate
Ser	serine
SPT	spiropyrimidinetrione
SS	single-stranded
T	threonine
TB	tuberculosis
V	valine
WT	wild-type
Y	tyrosine

CHAPTER I

INTRODUCTION

DNA Topology

Imagine for a moment that you have a rope that is 2 meters long, or approximately equal to the height of Michael Jordan. This rope is very thin – thinner than floss or fine thread – and you need to be able to pack it into a miniscule compartment that is only 10 μm in diameter (or 4 millionths of an inch). To complicate matters further, let's assume that your rope is actually double-stranded with each rope twisted about the other. Importantly, you must package this rope in such a way that any point along its length can be accessed and it does not become irreparably tangled.

Your cells do this with remarkable efficiency - far more so than you or I have ever managed to store a pair of corded headphones, a garden hose, or electronic cables. Each cell stores ~ 2 meters worth of DNA in a nucleus that measures approximately 5-10 μm across.[1] Although it is the one-dimensional sequence of your ~ 6 billion DNA bases[2] that provides the genetic code to make you, it is the three-dimensional structure of DNA that regulates the utilization of that code. Therefore, your cells must deal with ~2 meters of double-stranded DNA (the double helix) in the form of 46 chromosomes (as we are diploid) and, utilizing a slew of enzymes, regulate the accessibility of your genome.[1, 2]

Humans have linear DNA; however, the sheer length of the DNA, its extensive compaction, and cellular scaffolding preclude free rotation of the DNA ends.[3-7] Similarly, the fact that most bacteria have circular chromosomes means that there are no free ends to rotate in order to unwind or untangle the double helix.[8] As such, DNA is considered a closed topological system in which the three-dimensional relationships can only be altered when one or both strands of the double helix are broken (creating an open system).[3-5, 7, 9-15]These topological relationships, including DNA under- and overwinding, knotting, and tangling, can be defined mathematically (Figure 1.1).[3, 7, 11, 13, 16]

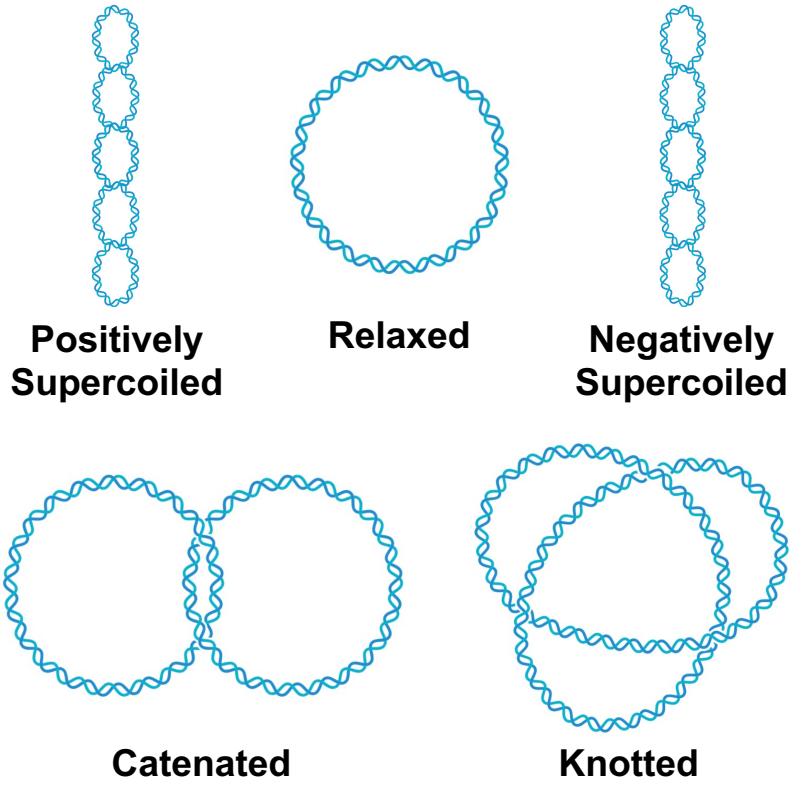

Figure 1.1. DNA Topology. Top: "Relaxed" DNA, under no torsional stress, is shown in the middle. Supercoiling as a result of overwinding (positively supercoiled, left) and underwinding (negatively supercoiled, right) are shown. Twist and writhe are interconvertible in these structures. Bottom: Twist and writhe are not interchangeable in intermolecular catenanes (tangles, left) or intramolecular knots (right). Made using Biorender.

Twist (Tw) is defined as the number of turns in a given length of DNA. Conventionally, the right-handed twist in B-form DNA is denoted as a positive integer. Writhe (Wr) is defined as the number of times a length of double-stranded DNA crosses itself. Depending on the handedness of the crossover (the direction of rotation needed to align the front and back portion of the DNA), each integer of writhe is either +1 (counter-clockwise rotation of the front portion) or -1 (clockwise rotation of the front portion).[3, 11, 13] Twist and writhe, when summed, define the linking number (Lk) of the DNA.

$$Lk = Tw + Wr$$

As DNA is a topologically closed system, linking number does not change unless the DNA is broken.[3, 4, 11, 13, 16-19] Additionally, twist and writhe are interconvertible when the DNA is not knotted or tangled. As an example, consider a pair of corded headphones. As the two strands are twisted around each other there comes a point when the twist is sufficiently high to convert to writhe or supercoils. If stretched taut, the writhe will again be removed and converted back into twist. As such, any DNA under torsional stress is said to be supercoiled – it writhes about itself or forms superhelical twists.

DNA is generally represented in the canonical Watson-Crick B-form in which the DNA is relaxed (i.e., it has no torsional stress). B-form DNA is defined by the 10.5 bases per right-handed turn of the helix.[20] Therefore, a relaxed molecule of DNA with 1050 base pairs would have a linking number of 100.

$$Lk = Tw\ (1050\ bases/\ 10.5\ bases/turn) + Wr\ (0)$$

$$Lk = 100$$

However, DNA is rarely found in its relaxed form. In most organisms DNA is slightly underwound.[3, 4, 13, 17-19] Under- and overwinding cause torsional stress (that can be converted to axial stress), resulting in a linking number that deviates from that of the relaxed form (overwinding is positive and underwinding is negative).[4, 11, 13, 17] DNA topology is therefore more frequently written as the *change* in linking number (ΔLk), or the difference between the actual linking number of DNA (Lk) and the linking number of the relaxed form (Lk_0).[3, 11, 13] As most eubacteria and eukaryotic organisms maintain DNA in an ~6% globally underwound state, the ΔLk is -6 (overwinding is positive and underwinding is negative).[3,

[11, 13] Using the same example of a 1050 base pair long stretch of DNA, the actual linking number can be calculated as below:

$$\Delta Lk = Lk - Lk_0$$

$$-6 = Lk - 100$$

$$Lk = 94$$

As such, this piece of DNA has 94 turns of the helix compared to the 100 turns if the same piece of DNA were relaxed. Maintaining the DNA in such a state provides the DNA more single-stranded character (Figure 1.2) and facilitates the opening of the double helix for DNA duplication (replication) and expression (transcription).[9, 21, 22] In humans, this underwinding [or negative supercoiling, (-)SC] is achieved by wrapping DNA around histones and other scaffolding proteins,[3, 17-19, 23] while the enzyme gyrase introduces negative supercoils in bacteria.[24-26]

Although negative supercoiling is useful for DNA access, hypernegative supercoiling can be detrimental. The twin-supercoiled domain model[27] can be used to explain formation of hypernegative supercoiling. In this model, rotation of transcription complexes moving along a DNA template becomes increasingly difficult as the RNA chain grows. As such, the machinery instead energetically favors forcing the DNA to rotate locally as the two strands of the helix are separated. Separation of the two strands compacts the turns of the helix ahead of the enzymatic machinery into a smaller stretch of DNA, thereby positively supercoiling the DNA. Compensatory (-)SC domains form behind the advancing enzyme complex. A similar model can be applied to replication as this process also requires melting of the double helix as the replication fork progresses. The build-up of (+)SCs ahead of advancing machineries can stall either process by preventing further separation of the two strands.[3, 5, 13] In the case of head-on conflicts, (+)SCs build-up between advancing replication and transcription machinery, stalling both processes.[28] Hypernegative supercoiling can arise from the abrupt removal of the (+)SC domain without concurrent removal of the (-)SCs behind the converging protein complexes.[28] This severe underwinding is associated with the formation of R-loops, regions of nascent RNA annealing to the template DNA behind the

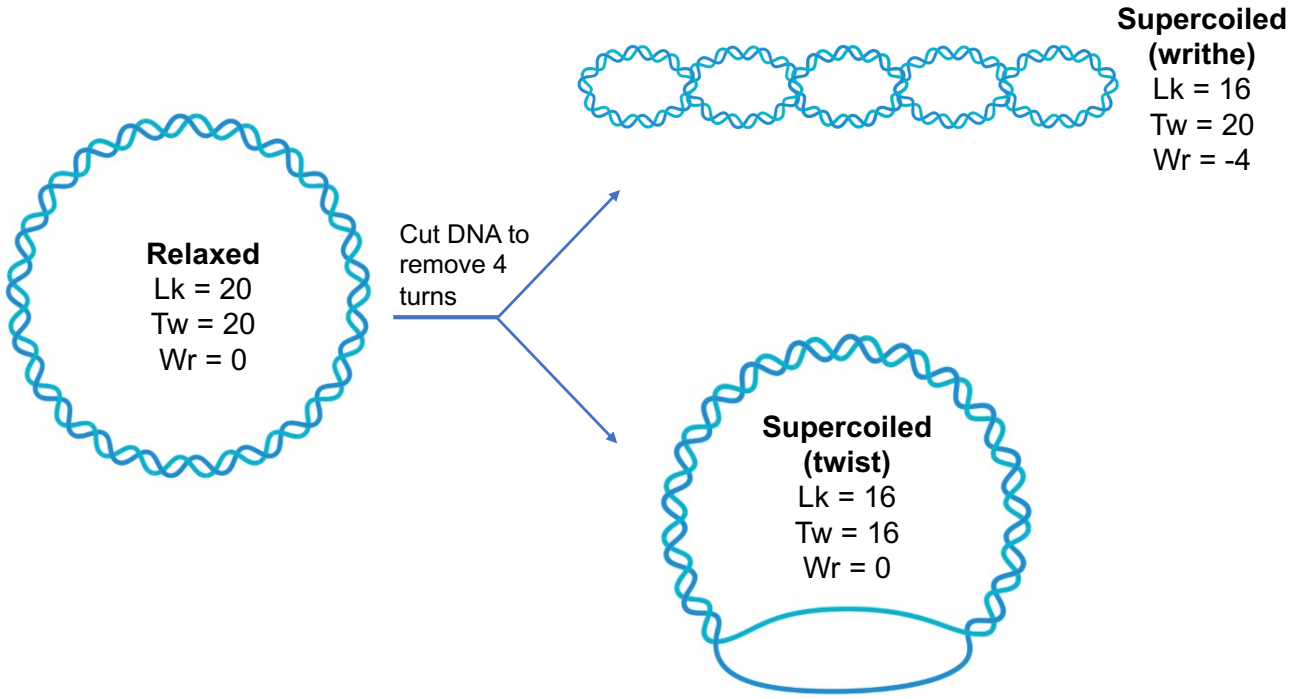

Figure 1.2. Negative Supercoiling Increases Single-stranded Character. A relaxed molecule of DNA with a Lk = 20 is shown on the left. Negative supercoiling of this molecule, or removal of 4 helical turns (ΔLk = -4), results in a molecule with Lk = 16 (right). Twist and writhe are interconvertible in supercoils, so DNA with Tw = 20, Wr = -4 is equivalent to DNA with Tw = 16, Wr = 0. When all of the torsional stress is in the form of twist, there is local denaturation of the DNA to facilitate opening of the helix. Adapted from Koster et al.[29] Made using Biorender.

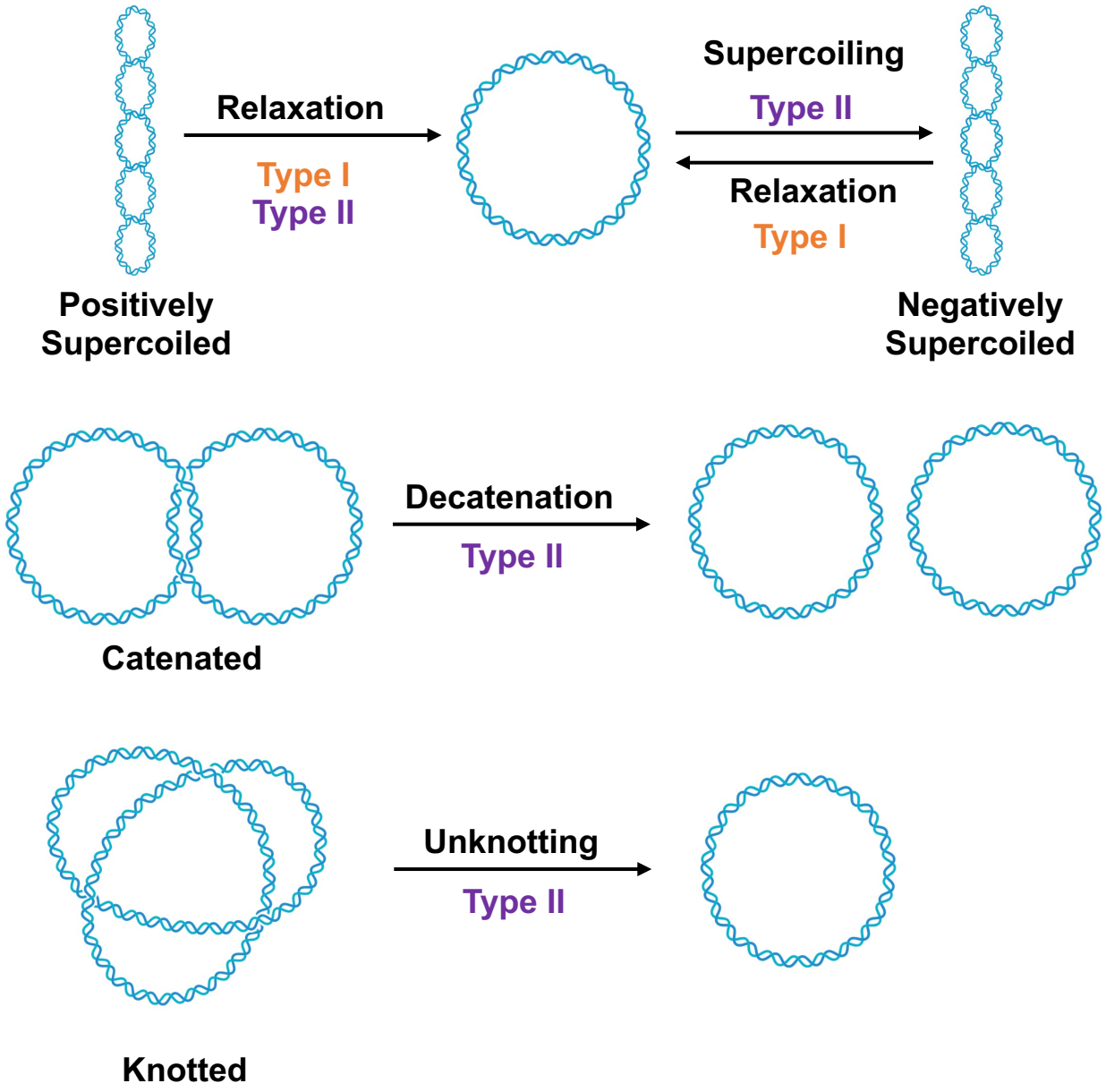

Figure 1.2. Type I vs. Type II Topoisomerase Action. Type I enzymes, because they cut a single strand, can only remove twist. Type II enzymes cut both strands and can work on writhe. Made using Biorender.

transcription machinery.[28, 30, 31] Failure to remove R-loops can then result in permanent stalling of replication and transcription.

Although the Tw and Wr in supercoils is interchangeable, the same is not true for DNA knots and tangles. In these topologies, DNA crossovers are constrained as writhe.[4, 32] DNA knots are formed during recombination processes used to increase genetic diversity and repair DNA. They involve a single DNA molecule (intramolecular) and stall DNA tracking systems if not removed.[3, 5, 9, 33, 34] Likewise, DNA tangles can impede DNA replication and transcription. Tangles are formed behind replication forks when part of the torsional stress created by (+)SC ahead of the machinery redistributes upon fork rotation.[35, 36] The links created between parent and daughter chromosomes (intermolecular) are called precatenanes and must be resolved for proper chromosome segregation during mitosis and meiosis.[3, 5, 9, 33, 34]

How do cells overcome these topological barriers to replication or transcription? As stated, the DNA ends are not free to rotate. Therefore, the closed topological system must be opened. Enter the topoisomerases.

Topoisomerases

Multiple enzymes, known collectively as topoisomerases, are encoded by all living organisms.[5, 13, 15, 37-42] Topoisomerases are essential to life and enable tight control of DNA topology by introducing transient breaks in the DNA backbone, thereby opening the topological system. These enzymes fall into two major classes, depending on the number of DNA strands that are broken (Figure 1.3). The first topoisomerase to be discovered was ω in 1971.[43] We now know ω as *Escherichia coli* topoisomerase I, an enzyme that cuts a single strand of DNA and the founding member of the Type I class (as it was the first described).[9, 44, 45] Nomenclature conventions denote type I enzymes with odd numbers. Conversely, type II enzymes cleave both strands and include proteins denoted by even numbers.[45-47] This difference allows the two classes to carry out different functions. Type I enzymes are able to work on Tw and therefore relax

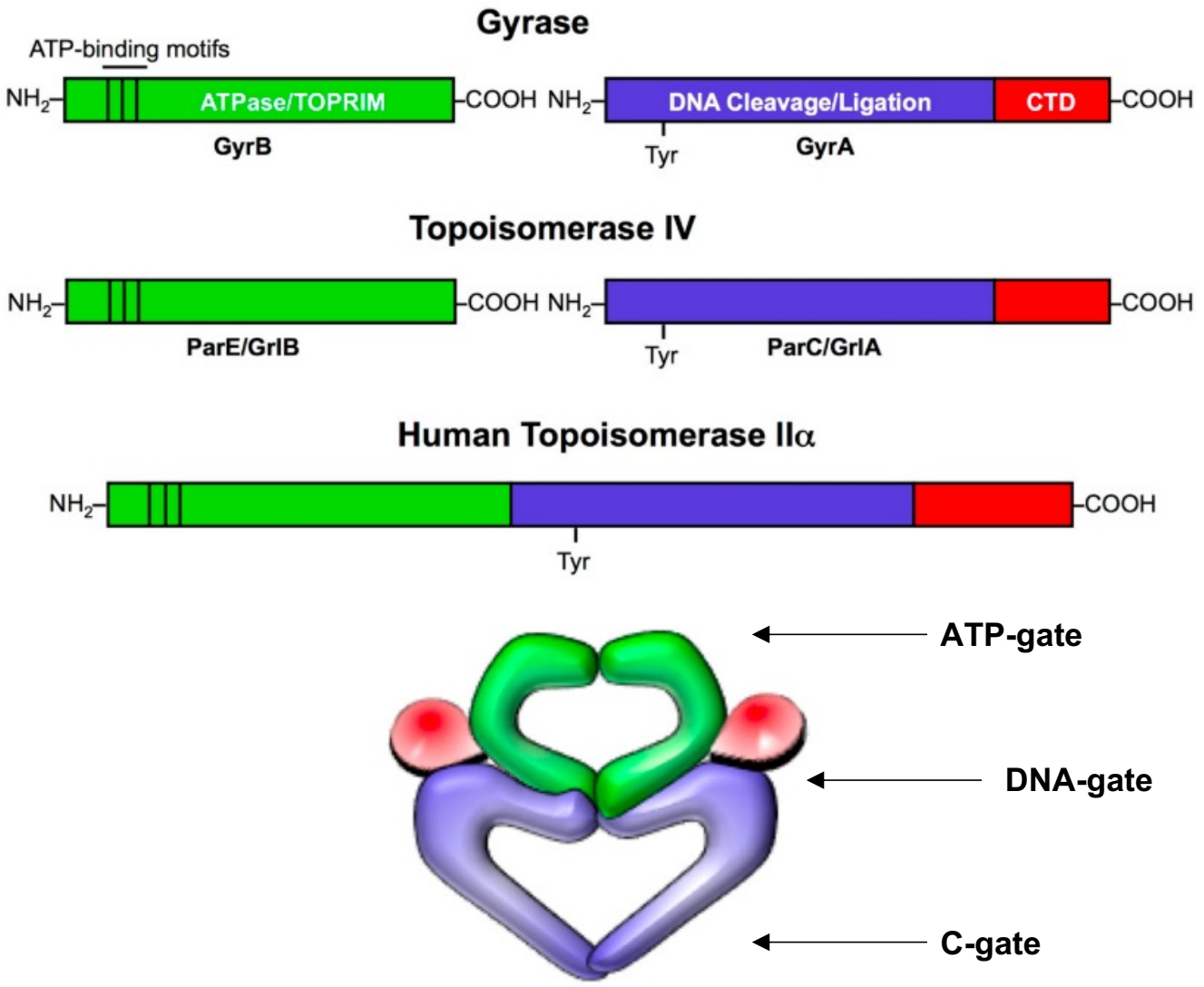

Figure 1.4. Type II Topoisomerase Domains and Structure. The bacterial type II topoisomerases, gyrase and topoisomerase IV, are heterotetramers (A_2B_2). The ATPase and TOPRIM (metal-binding) domains are located in the B subunit (green). The active site tyrosine is located in the A subunit (blue). The C-terminal domain (CTD, red) is also located in the A subunit and is key to the wrapping mechanism used by gyrase to negatively supercoil DNA. In humans, the A and B subunits are fused to form a homodimer. Adapted from Aldred et. al.[48]

supercoils for which Tw and Wr are interconvertible. Additionally, there is evidence that type I topoisomerases can decatenate sister chromatids by working on the hemicatenated DNA before replication fork convergence.[49, 50] Because type II enzymes generate a double-stranded break in the DNA, they can modulate supercoiling and unknot and untangle DNA by working on Wr. This dissertation will focus on the type II topoisomerases from humans and bacteria.

Type II Topoisomerase Catalysis

Structural studies have shown that type II topoisomerases are either homodimers (eukaryotes)[51-55] or heterotetramers (bacteria) (Figure 1.4).[45, 56-60] These enzymes utilize two active site tyrosine residues[12, 40] to create a transient double-stranded break in a DNA segment through which a separate segment is passed.[11, 13, 34, 37, 61-65] Both eukaryotic and bacterial type II enzymes have three protein gates that allow for transport of this separate segment: the N-terminal gate, the DNA gate, and the C-terminal gate.[55, 66, 67]

All type II enzymes utilize a similar catalytic cycle shown in a stepwise fashion in Figure 1.5. In addition to a requirement for the high-energy cofactor ATP,[68-71] these metalloenzymes necessarily utilize divalent metal cations.[72, 73] (1) The enzyme must first bind two DNA segments at a crossover.[74] The first segment bound by the enzyme is the double helix that will be cleaved by the enzyme, referred to as the "Gate-" or "G-segment."[53, 75] The second double helix, to be transported through the transiently cleaved G-segment, is referred to as the "Transport-" or "T-segment."[74, 76, 77] (2) The TOPRIM domain enables coordination of divalent metal ions used to sample the G-segment for bendability.[72, 73, 78, 79] The enzyme distorts bendable segments of the DNA to an angle of ~150° , inducing a conformational shift from B-form to A-form DNA at the site of cleavage.[78, 80, 81] (3) The bent G-segment is then cleaved, catalyzed by the nucleophilic attack of the active site tyrosine residues.[53, 73] The two tyrosine residues act in a coordinated manner to form the cleavage complex. Once the first strand has been cleaved, the second is cleaved >10-fold faster.[82] (4) Upon the binding of two ATP molecules, the enzyme closes the N-gate,

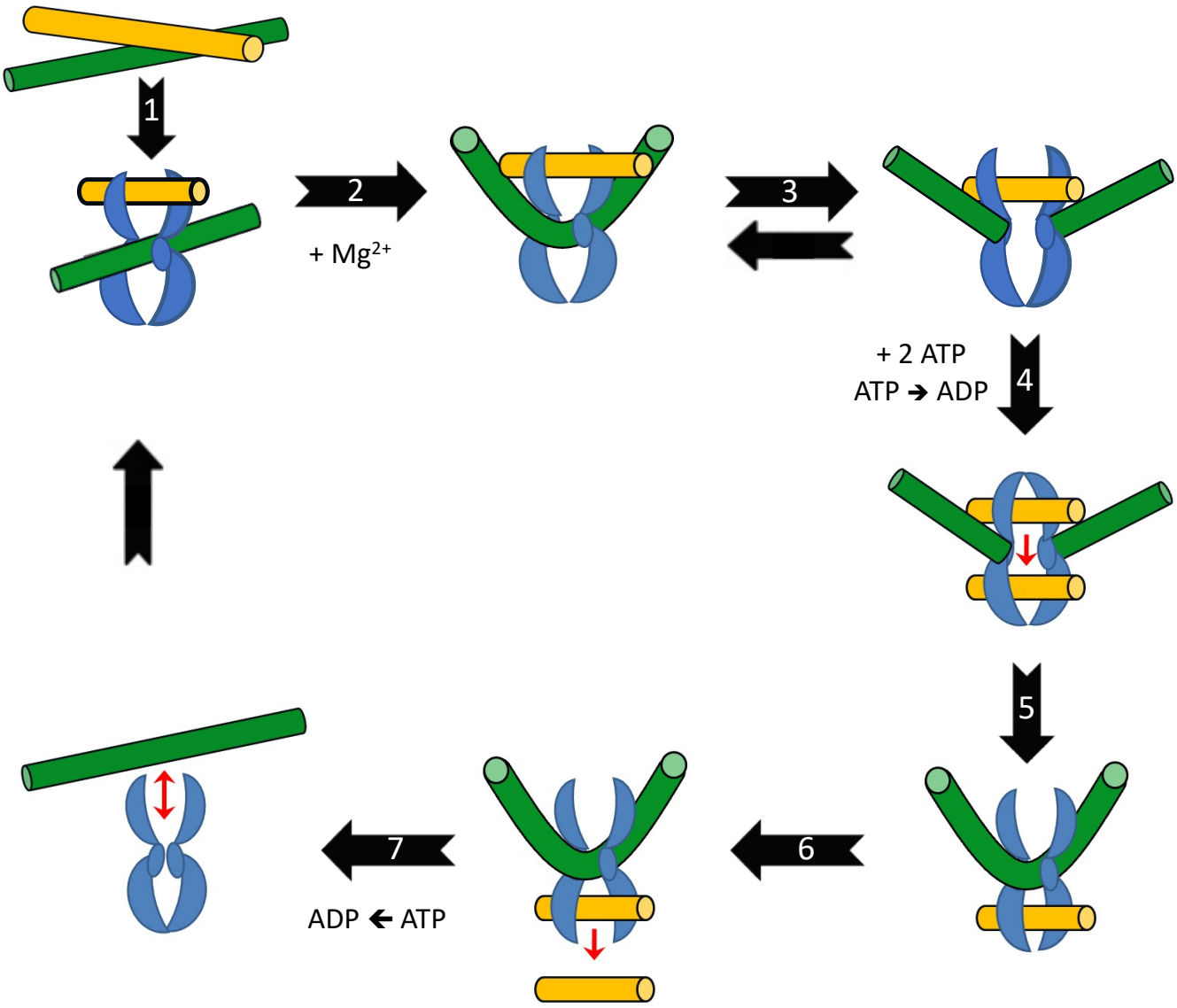

Figure 1.5. Type II Topoisomerase Catalytic Cycle. The type II topoisomerases regulate DNA topology by introducing a transient break in one or both DNA strands. To do so, (1) the enzyme (blue) first binds to a DNA crossover (either intra- or intermolecular). The T-segment is shown in yellow and the G-segment is shown in green. (2) Coordinated metal ions enable the enzyme to bend and (3) cut the G-segment. (4) Binding of ATP dimerizes the N-gate and allows passage of the T-segment through the DNA gate. (5) Ligation of the DNA, release of the T-segment, and (6) ATP hydrolysis allow enzyme turnover.

forcing the T-segment through the open DNA gate.[12, 37, 40] The DNA strand passage event appears to take place more rapidly if one of the ATP molecules is hydrolyzed.[83] (5) The G-segment is then ligated, and the T-segment is released through the open C-terminal gate.[12, 37, 40] (6) Following hydrolysis of the second ATP molecule, the G-segment can be released and (7) the enzyme conformation is reset, allowing for the capture of another DNA crossover.[12, 37, 40]

The DNA cleavage reaction (and subsequent ligation) utilizes a two-metal ion mechanism similar to that of primases and polymerases (Figure 1.6).[53, 72, 84-86] *In* vivo this ion is magnesium.[87-89] Not only are the divalent metal cations used for DNA bending, but they are also thought to stabilize the transition state of the DNA and/or aid in active site tyrosine deprotonation. The deprotonation is carried out by a general base, thought to be a histidine (purple), and removes the proton from the hydroxyl group of either tyrosine residue (blue). The oxyanion then performs an SN2 transesterification reaction at the scissile phosphate (bond in red) of the DNA backbone. The rightmost metal ion, as stated above, is thought to aid in deprotonation and transition state stabilization, while the leftmost cation stabilizes the leaving 3' oxygen (in red).[72, 86] Transesterification results in a covalent linkage between the tyrosine residue of the enzyme and the newly generated 5'-terminal phosphate of the DNA that conserves the bond energy of the backbone.[90-93] This covalently bound enzyme-DNA structure is called the *cleavage complex*[39, 45, 94, 95] and is an important state in the catalytic cycle of the enzymes. Ligation of the DNA gate is thought to be the result of the reverse transesterification initiated by general acid deprotonation of the free 3'-hydroxyl of the DNA segment.[44, 46, 51, 96]

Human Type II Topoisomerases

All living organisms encode at least one type II topoisomerase.[11-13, 63] Lower eukaryotes encode a single type II enzyme, while vertebrates express two isoforms of topoisomerase II, α and β.[34, 40, 97]Human topoisomerase IIα (hTIIα) and IIβ (hTIIβ) are encoded by two separate genes (17q21−22 and 3p24, respectively) and differ in molecular mass (170 and 180 kDa, respectively). Both isoforms share ~70%

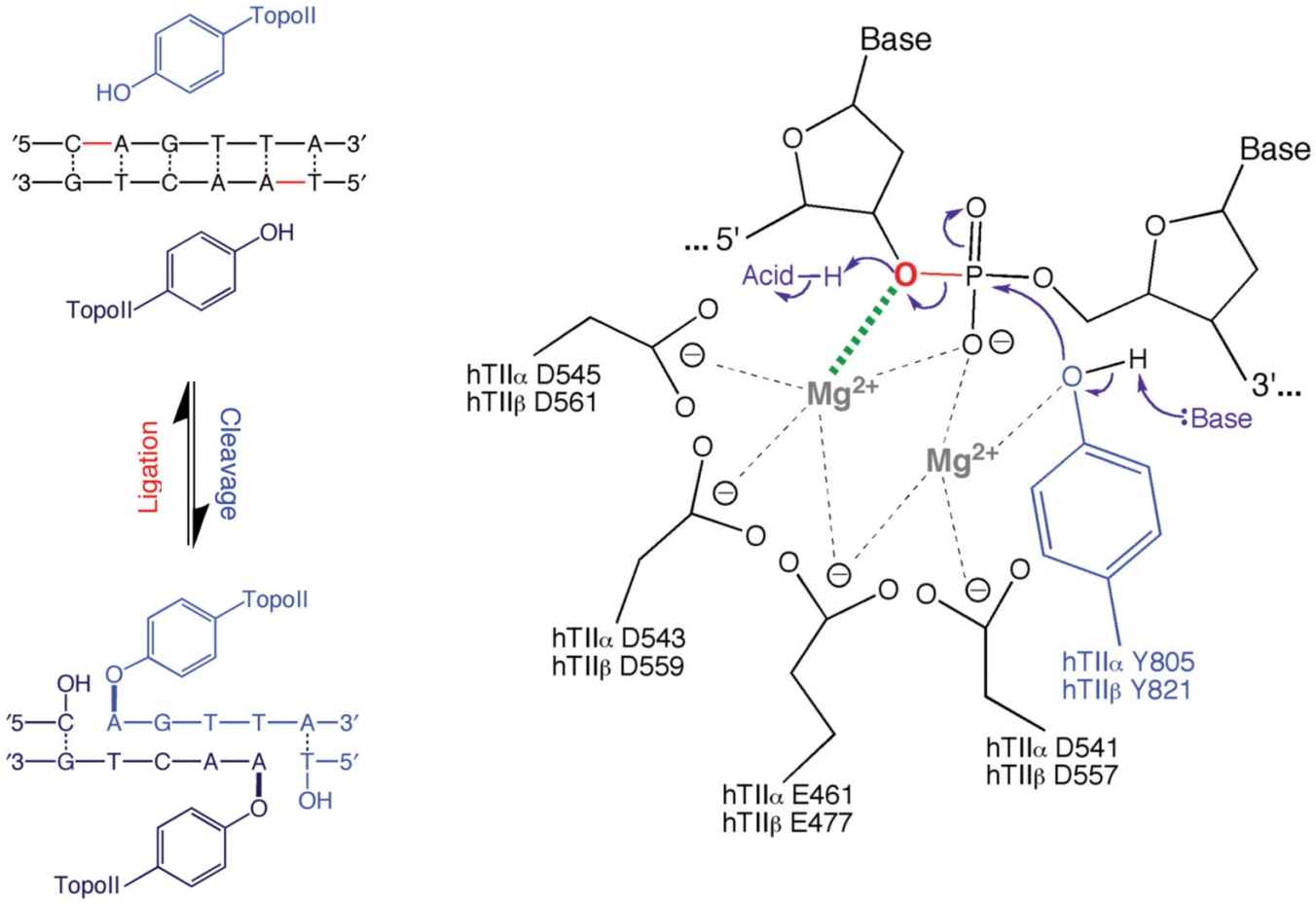

Figure 1.6. Transesterification Reaction Creates a Covalent DNA-Enzyme Bond. Left: A schematic showing ligated and cleaved DNA. The active site tyrosine residues (blue) form a covalent bond with the DNA backbone of both strands 4-base pairs apart. This is the cleavage complex. Right: The transesterification reaction that forms the cleavage complex is shown. The active site tyrosine is blue, the scissile bond is red, the magnesium ions are gray, and nucleophilic attack is denoted by purple arrows. Magnesium interactions are shown as dotted lines, and stabilization of the 3' leaving oxygen is specifically colored green. Enzyme residue numbering is shown only for the human enzymes. Adapted from Noble and Maxwell.[86]

sequence identity and display similar enzymatic properties; however, they differ significantly in their expression, cellular regulation, and functions.[34, 40, 61, 63, 97-99] Expression of topoisomerase IIα is linked to cellular growth and is essential for the survival of proliferating cells.[5, 34, 37, 40, 61, 97]Although the α isoform is virtually nonexistent in quiescent and differentiated tissues, rapidly proliferating cells contain ~500,000 molecules.[64, 97, 99, 100] Topoisomerase IIα is associated with replication forks and remains tightly bound to chromosomes during mitosis. The enzyme plays roles in DNA transcription and recombination,[64, 101] is important for fork convergence and termination of replication,[102] and is required for proper chromosome organization and segregation.[13, 64, 101, 102]In contrast to topoisomerase IIα, the β isoform is not required at the cellular level.[97] However, it is essential for neuronal development.[11, 12, 34, 97, 103]High levels of the β isoform are found in most cell types, independent of proliferation status.[11, 64, 97, 104] Topoisomerase IIβ dissociates from chromosomes during mitosis but appears to play an important role in the transcription of hormonally and developmentally regulated genes.[97, 105-107]

Bacterial Type II Topoisomerases

Bacteria, with some notable exceptions (such as *Mycobacterium tuberculosis*[108] and *Helicobacter pylori*,[109] which encode only gyrase), encode two type II topoisomerases: gyrase and topoisomerase IV.[38, 45, 95, 110] Both gyrase and topoisomerase IV are heterotetrameric (A_2B_2) proteins.[11, 34, 48, 110, 111] The A and B subunits have fused to form the protomer subunit in the human enzymes. The active-site tyrosine needed for cleavage and religation of the DNA is found in the A subunits (GyrA in gyrase; ParC or GrlA in Gram-negative or Gram-positive topoisomerase IV, respectively).[48, 111] The B subunits (GyrB in gyrase; ParE or GrlB in Gram-negative or Gram-positive topoisomerase IV, respectively) contain both the ATP hydrolysis and TOPRIM (metal ion binding) domains.[48, 111]

Gyrase was discovered in 1976 by Martin Gellert, the co-discoverer of DNA ligase.[68] He and collaborators were working on site-specific DNA recombination and realized that the structure of the DNA they used made an important difference in the recombination reactions.[112] Specifically, circular DNA

plasmids were good substrates for recombination but required ATP. Supercoiled circular plasmids were also good substrates and removed the need for ATP. This led the team to search for an ATP-dependent DNA supercoiling reaction, which led them to the enzyme gyrase. The name was created the first time that Gellert presented on the enzyme "over beer at a Gordon conference with a few friends"[112] and is the only type II topoisomerase to retain its historical name.

Gyrase utilizes a non-canonical strand passage mechanism to actively underwind DNA (Figure 1.7).[113-116] It does so by wrapping DNA around the GyrA box of the C-terminal domain of the enzyme,[116] creating a constrained (+)SC. The linking number cannot be changed, and therefore a compensatory (-)SC forms in the unbound DNA. Upon DNA gate opening and strand passage, the constrained (+)SC is converted to a (-)SC. Altogether, gyrase introduces two (-)SCs per catalytic cycle. The need to wrap a positive node around the C-terminal domain makes gyrase very good at relaxing (+)SCs. In fact, gyrase relaxes (+)SCs rapidly and processively – about 10 times faster than it introduces (-)SCs into relaxed DNA.[117] This intramolecular reaction necessarily has the G- and T-segments in close proximity (~140 bp apart), making it much easier for gyrase to wrap the DNA gate segment.[115] As such, gyrase tends to work ahead of replication forks to remove (+)SCs that accumulate ahead of DNA helicase and DNA polymerase.[41, 118-120] Though it can function to remove knots and tangles, gyrase is a poor decatenase.[121] Not only does gyrase remove (+)SCs, but it also works with topoisomerase I (ω protein) to maintain the superhelicity of the bacterial genome.[34, 41, 43, 120, 122, 123] It relaxes DNA and introduces (-)SCs to keep DNA in an underwound state that makes it accessible for replication and transcription machinery.

Topoisomerase IV utilizes a canonical strand passage mechanism without the need for wrapping.[115] However, the existence of topoisomerase IV was not known for more than a decade after the discovery of gyrase. ParC and ParE, the two subunits of Gram-negative topoisomerase IV, were initially understood to be partitioning enzymes needed for proper chromosome segregation in bacteria.[34] In 1990, Hideho Suzuki sequenced the genes encoding these partitioning enzymes in *E. coli*, revealing homologous

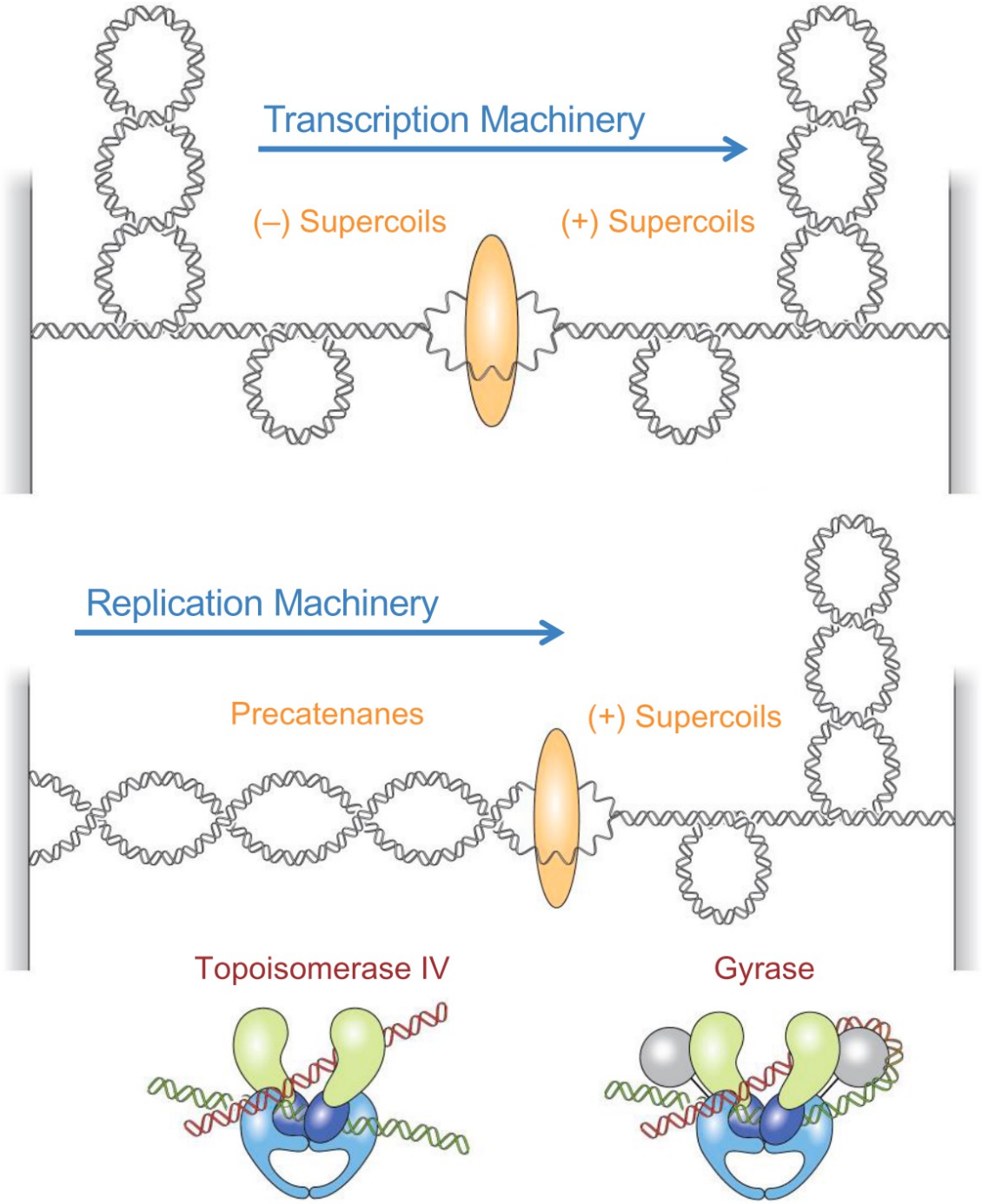

Figure 1.7. Cellular Functions of Type II Topoisomerases. Topoisomerase IV (bottom left) utilizes a canonical strand passage mechanism that allows the enzyme to easily accommodate separate molecules at a DNA crossover. Although the enzyme can relax supercoiling, it appears to function primarily as a decatenase in cells, removing precatenanes (middle). Gyrase instead utilizes a wrapping mechanism that enables it to rapidly remove (+)SCs ahead of transcription (top) and replication (middle) complexes. It can also actively introduce (-)SCs to modulate the superhelicity of the genome. Artwork by Ethan Tyler, NIH Medical Arts.

amino acid sequences to GyrA and GyrB, respectively.[71] Subsequent activity studies demonstrated that ParC and ParE could relax supercoils and compensate for the loss of topoisomerase I.

Without an ability to wrap DNA, topoisomerase IV cannot introduce (-)SCs on its own. However, the mechanism does allow the enzyme to more easily accommodate two separate DNA molecules at a crossover for decatenation (an intermolecular reaction).[124, 125] Topoisomerase IV catalyzes decatenation two orders of magnitude faster than gyrase can.[126] It also decatenates faster than it relaxes (+)SCs.[115, 120, 127, 128] Topoisomerase IV therefore tends to work behind the replication fork to remove knots and tangles following replication and recombination.[41, 95, 120, 129]

Type II Topoisomerases as Drug Targets

The type II topoisomerases are essential for regulating DNA topology; usefully, this function can also be harnessed for therapeutic treatment. A careful balance must be maintained between cut DNA in the cleavage complex and ligated DNA. (Figure 1.8)[12, 37, 62, 64] The equilibrium strongly favors ligated DNA as it is intrinsically more stable. Therefore, cleavage complexes are short-lived under normal circumstances. A number of different anticancer and antibacterial compounds target the human and bacterial type II topoisomerases by perturbing the system.[12, 37, 40, 42, 48, 62-64, 111]

Too much DNA cleavage can cause multiple problems in the cell.[12, 37, 62, 64, 130, 131] If the DNA break is encountered by a DNA tracking system and the system attempts to traverse the break, the normally transient DNA break can be made permanent. As such, the covalently bound protein is rendered incapable of resealing the DNA break, though the exact mechanism preventing ligation has not been determined. It is thought to be a result of direct protein interactions between DNA tracking systems and the type II topoisomerases or extreme overwinding of the DNA.[37, 131-133] Repair and/or recombination enzymes are then recruited which can subsequently induce apoptosis in human cells and the SOS response in bacteria.[37, 131-134] This can ultimately lead to mutagenesis and cell death. Therefore, compounds that stabilize covalent

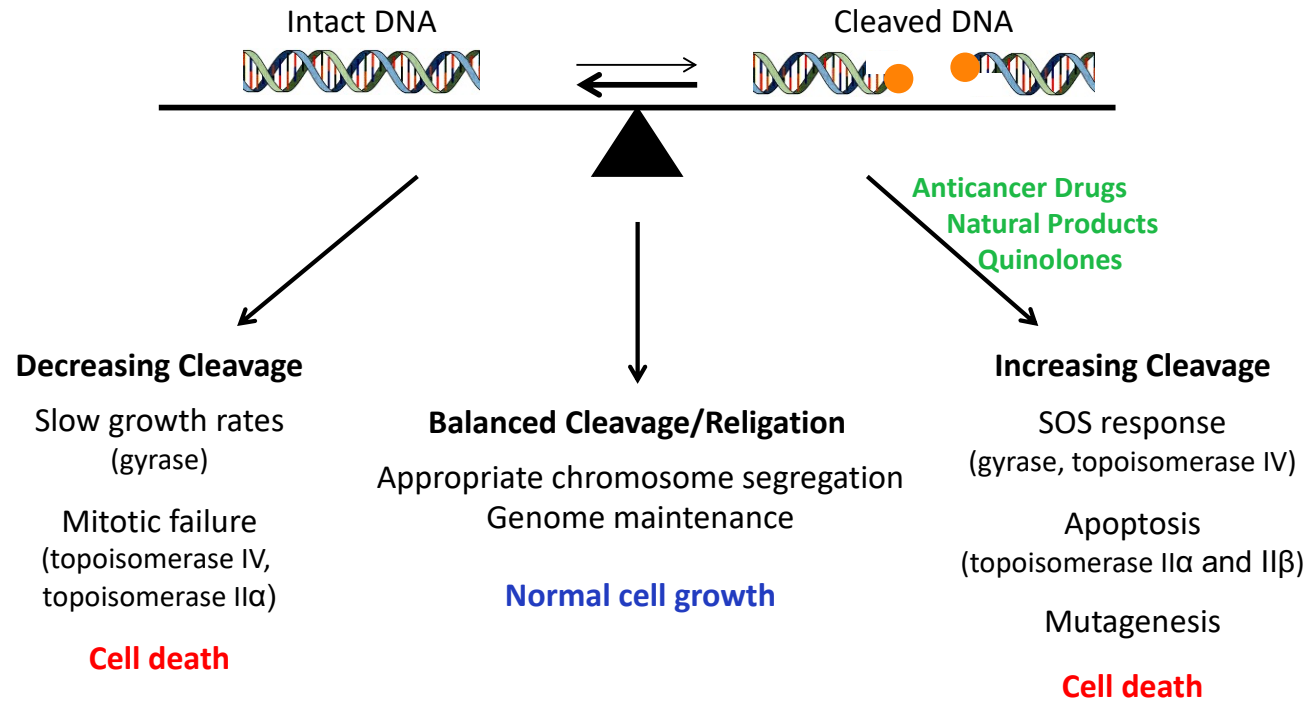

Figure 1.8. Critical Balance of DNA Cleavage and Religation. Although essential enzymes, the type II topoisomerases can be dangerous enzymes. Maintaining balanced cleavage and ligation, with the latter being favored, allows DNA transactions to occur normally and cells grow without issue. Too little cleavage can result in slow growth rates and mitotic failure. Conversely, too much cleavage can result in activation of DNA damage repair pathways, mutagenesis, and SOS or apoptotic signaling. Anticancer and antibacterial compounds perturb this and can lead ultimately to cell death.

cleavage complexes have deleterious effects. These compounds are called "poisons" because they effectively increase cleavage complex levels, converting type II topoisomerases into lethal toxins that fragment the genome.[37, 62, 89, 133]

Similarly, too little cleavage can be detrimental to cells.[12, 13] If type II topoisomerases cannot cleave the DNA, they cannot relieve the cell of DNA torsional and axial stress. DNA processes such as replication and transcription stall, daughter chromosomes are not untangled after replication, and cell growth slows. Proper chromosome segregation is compromised, ultimately leading to mitotic failure and cell death. Therefore, compounds that decrease the catalytic activity of type II topoisomerases (called catalytic inhibitors) work by robbing cells of the critical topology maintenance provided by these enzymes.[82, 133, 135, 136]

Cancer Therapeutics: Targeting Human Type II Topoisomerases

Both type II topoisomerase catalytic inhibitors and poisons have been used as anticancer therapeutics in the clinic.[37, 62, 133, 137-139] Most of the clinically relevant type II topoisomerase targeted compounds are poisons, including the anthracyclines (daunorubicin and doxorubicin), demethylepipodophylotoxins (etoposide and teniposide), anthracenedinones (mitoxantrone), and amsacrine (Figure 1.9).[37, 62, 133, 137, 139] The anthracyclines and demethyl-epipodophyllotoxins are used to treat solid tumors and systemic cancers alike, including leukemias, lymphomas, sarcomas, breast cancers, lung cancers, neuroblastomas, and germ-cell malignancies.13,15,17,18,54 In addition, mitoxantrone is used to treat breast cancer, acute myeloid leukemia (AML), non-Hodgkin lymphoma, and multiple sclerosis.[64, 140-143]

These drugs are *interfacial* poisons, meaning that they interact at the topoisomerase-DNA interface.[62, 63, 139] They are bifunctional and must interact with both the protein and the DNA to increase levels of DNA scission. Interfacial poisons insert between the ends of the double helix at the cut scissile bonds on the G-segment.[37, 62, 63, 133, 139] They distort the active site within the cleavage complex

demethyl-epipodophyllotoxins		
	R_1	R_2
Etoposide	OH	CH_3
Etoposide Phosphate	OPO_3H_2	CH_3
Teniposide	OH	

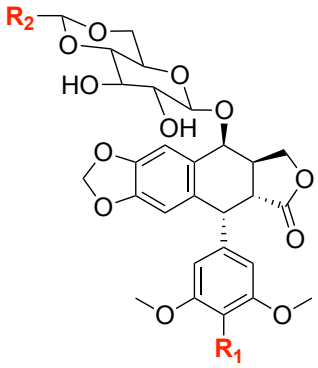

Demethyl-epipodophyllotoxins

anthracyclines		
	R_1	R_2
Doxorubicin	CH_2OH	OCH_3
Daunorubicin	CH_2	OCH_3
Idarubicin	CH_2OH	H

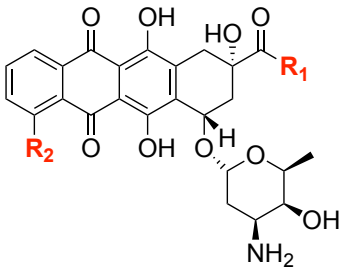

Anthracyclines

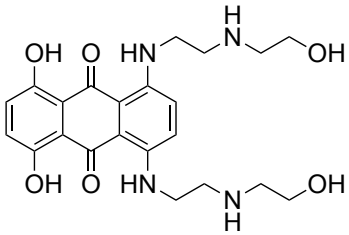

Mitoxantrone

Figure 1.9. Clinical Topoisomerase II Poisons. The demethyl-epipodophyllotoxins (etoposide, etoposide phosphate, and teniposide), the anthracyclines (doxorubicin, daunorubicin, and idarubicin), and the anthracenedione mitoxantrone target topoisomerase II and are approved for clinical use in the United States. Adapted from Vann et al.[42]

and appear to detach one of the catalytic magnesium ions from the phosphotyrosyl moiety.[144] In this ternary enzyme-drug-DNA complex, the drug acts as a physical barrier to prevent the enzyme from ligating the DNA, thereby increasing levels of enzyme-mediated DNA breaks.[37, 133, 145] To stabilize double-stranded breaks, two molecules (one at each scissile bond) must be present in the active site of the type II enzyme.

Etoposide is a classic, well-characterized and widely prescribed example of an interfacial topoisomerase II poison.[37, 62-65, 133, 146, 147] It was one of the first such compounds used clinically, and its parent compound podophyllotoxin has been used in alternative and traditional medicines for centuries. Podophyllotoxin, from the mayapple or American mandrake, prevents tubulin dimerization.[148] In so doing, the natural product inhibits microtubule formation and stops cells from proceeding through metaphase. Etoposide, a semi-synthetic derivative of podophyllotoxin, instead targets hTIIα and hTIIβ.[145-147, 149] The drug utilizes key interactions with the proteins to enter the binary enzyme-DNA complex and inhibit topoisomerase II-mediated DNA ligation.[137, 150-153]

Despite the importance of etoposide and other interfacial poisons as therapeutic agents for the treatment of cancer, these drugs are associated with very serious side effects.[64, 132, 143, 154-156] Among the most dramatic of these are the generation of treatment-related acute myelogenous leukemias (AMLs) that involve rearrangements of the mixed lineage leukemia (*MLL*) gene at chromosomal band 11q23.[64, 132, 143, 154-156] Approximately 2-3% of patients treated with etoposide or doxorubicin go on to develop these AMLs.[64, 132, 142, 143, 147, 156] Additionally, treatment of breast cancers and multiple sclerosis with mitoxantrone is associated with the development of acute promyelocytic leukemia (APL) characterized by chromosome 15:17 translocation of the promyelocytic leukemia gene (PML) and the retinoic acid receptor α (RARA) gene.[64, 140-143] In all cases, chromosomal breakpoints are located in close proximity to sites of topoisomerase II-mediated DNA cleavage. Approximately 60% of the breakpoints sequenced from APL patients reside within an 8-bp region of a topoisomerase II−DNA cleavage site induced by mitoxantrone.[64, 140-143]

Although topoisomerase IIα and IIβ are both targeted by these anticancer drugs, the contributions of the two enzyme isoforms to the therapeutic and leukemogenic properties of the drugs are not clear. Circumstantial evidence suggests that topoisomerase IIα may play a more prominent role in killing cancer cells, whereas topoisomerase IIβ may be more important in the induction of leukemic chromosomal translocations.[64, 133, 155-157] This hypothesis is supported by three main pieces of evidence. First, a skin-specific top2β-knockout mouse model had far fewer secondary leukemias develop and the cellular models required topoisomerase IIβ for DNA cleavage and rearrangement.[154] Second, translocation models show that genes are expressed in transcription factories. These factories are formed by the looping of long chromosomal regions that bring multiple chromosomes and transcription machineries into close proximity.[158, 159] *MLL* and its two most common translocation partners are found in the same transcription factory in multiple human cell lines[155, 156, 160, 161] and most etoposide-induced *MLL* breaks in these factories are dependent on the β isoform.[155] In addition, the genotoxic effects of etoposide in these cells appear to be mediated primarily by topoisomerase IIβ.[155] Finally, the differential expression patterns of topoisomerase IIα and IIβ may also play a role in the β-associated toxicities.[64, 97] The β isoform is proliferation-independent and exists in both differentiated and undifferentiated tissues. The α isoform, however, is primarily found in proliferating tissues. Therefore, in fully differentiated heart muscle, for instance, topoisomerase IIβ is essentially the only isoform expressed.[64, 97] Thus, some of the off-target toxicities of topoisomerase II-targeted drugs, including cardiomyopathy, are attributed (at least in part) to the β isoform.[64, 155, 157, 162] As topoisomerase IIα is highly expressed in proliferating cells, a classic status of many cancer cell types, the potential development of a drug that displays specificity for the α isoform is promising. Such novel agents include NK314 and ARN-21934.[64, 163, 164]

Some catalytic inhibitors of the human type II topoisomerases have also found clinical use, especially the bisdioxopiperazines.[133, 138] This small molecule class includes ICRF-159, ICRF-187, and MST-16.[133] ICRF-187, also known as dexrazoxane, is a potent inhibitor of DNA relaxation by hTIIα (IC_{50}

= 1.9 μM) and hTIIβ (IC_{50} = 2.3 μM).[165] Inhibition with dexrazoxane is ATP-dependent as it acts as a non-competitive ATPase inhibitor,[165] binding to the closed-clamp form of the topoisomerase-DNA complex.[166] In so doing, dexrazoxane allows strand passage but inhibits the hydrolysis of the second ATP molecule needed to release the G-segment and restart the catalytic cycle.[133, 157, 167] The compound has been used for its protective effects against the cardiotoxicity induced by anthracyclines like doxorubicin.[133, 138] While previous studies suggested that the cardioprotective effect was a result of dexrazoxane functioning as a type II topoisomerase inhibitor itself, recent work suggests that at least some of the effect stems from its ability to promote proteasomal degradation of hTIIβ in myocytes or its ability to act as a free-radical scavenger.[157, 167]

Antibacterials: Targeting Bacterial Type II Topoisomerases

In addition to their essential cellular functions,[5, 9, 34, 41, 95, 120, 126-129] the bacterial type II topoisomerases, gyrase and topoisomerase IV, have long been the targets of an important class of antibacterials, namely the fluoroquinolones.[48, 63, 111, 168-171] These broad-spectrum drugs are among the most widely prescribed antibacterials worldwide.[111, 169, 170, 172, 173] These drugs can be used to treat Gram-positive infections, caused by bacteria that have only a thick sugar-protein coat called the peptidoglycan layer protecting them. Bacteria classified as Gram-positive include *streptococci*, *staphylococci*, and *bacilli*. Importantly, the fluoroquinolones can also kill Gram-negative bacteria that have a thin peptidoglycan layer as well as an outer membrane that can make it hard for antibacterials to access the cell. Gram-negative bacteria include *acinetobacter*, enterobacteria, and *neisseria*.

Quinolone-based antibacterials have been used since 1962 when the first quinolone, nalidixic acid (Figure 1.10), was identified as an impurity in the synthesis of the antimalarial chloroquine.[174] Nalidixic acid had limited use and was primarily used to treat Gram-negative urinary tract infections (UTIs).[48, 63, 111] Introduction of a fluorine atom at C6 turned the quinolone scaffold into a fluoroquinolone. This second

1st Generation
(Quinolone)

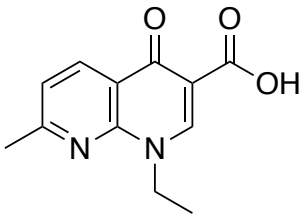

Nalidixic Acid

2nd Generation
(Fluoroquinolones)

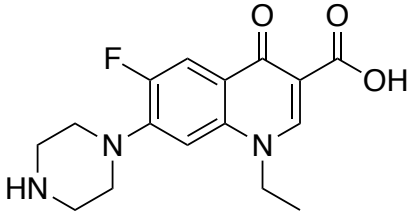

Norfloxacin

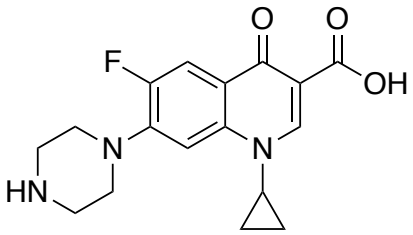

Ciprofloxacin

3rd Generation

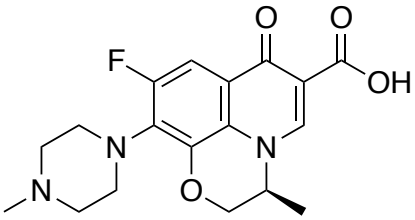

Levofloxacin

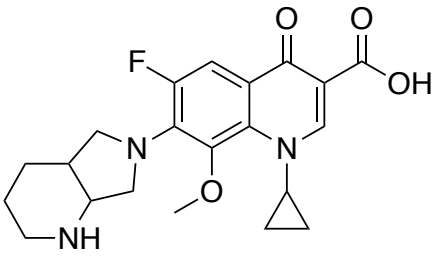

Moxifloxacin

4th Generation

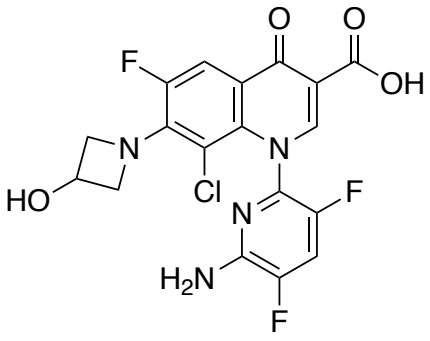

Delafloxacin

Figure 1.10. Fluoroquinolones. Structures of the widely-prescribed fluoroquinolone antibacterials are shown. The first of these drugs, nalidixic acid, is a quinolone. Introduction of a fluorine at C6 turned these compounds into fluoroquinolones. One of the newest members of the class, delafloxacin, is shown at the bottom.

generation of drugs, including norfloxacin and later ciprofloxacin, significantly expanded the use of the antibacterial class. The addition of the fluorine improved tissue penetration, and allowed norfloxacin to be used for UTI treatment as well as the treatment of sexually transmitted diseases. It was not until the introduction of ciprofloxacin in 1987[175] that fluoroquinolones had adequate tissue penetration, efficacy against Gram-positive species, and blood serum concentrations to be used outside of the urinary tract.[48, 111] Future alterations of the fluoroquinolone core iteratively improved the potency and efficacy of these compounds. Significant increases in the longevity of the compounds in the body (half-life) and activity against more Gram-positive pathogens has also enhanced the clinical utility of these drugs.

The fluoroquinolones act as interfacial poisons of bacterial type II topoisomerases.[110, 168-170, 173, 176-178] Much like the human type II topoisomerase poisons, two fluoroquinolones bind after DNA cleavage mediated by gyrase or topoisomerase IV – one in each active site of the protein. They make contacts with both the DNA, through intercalative π-stacking interactions,[179, 180] and the A subunit of the enzymes. In this way, the fluoroquinolones prevent enzyme-mediated ligation of the DNA and stabilize the cleavage complex.[180] Clinically relevant fluoroquinolones interact with gyrase and topoisomerase IV through a water−metal ion bridge (Figure 1.11).[48, 59, 111, 179-181] The bridge forms through chelation of a divalent metal ion by the C3/C4 ketoacid of the fluoroquinolone skeleton. As Mg^{2+} ions generally have an octahedral coordination sphere, the metal ion also interacts with four water molecules. Two of these water molecules interact with a highly conserved serine and an acidic residue that is located four amino acids upstream in the GyrA or GrlA/ParC subunits of gyrase or topoisomerase IV (Gram-positive/Gram-negative), respectively.[48]

In addition to the fluoroquinolones, a class of antibacterials that function as gyrase/topoisomerase IV inhibitors also exists. The aminocoumarins, including coumermycin A1 and novobiocin, act as competitive inhibitors of ATP binding and inhibit the ATP hydrolysis of these enzymes.[182] Recent interest in this compound class stems from the finding that these compounds can bind other ATP-hydrolyzing enzymes, such as eukaryotic heat shock protein Hsp90. The crystal structure of coumermycin A1 with *E.*

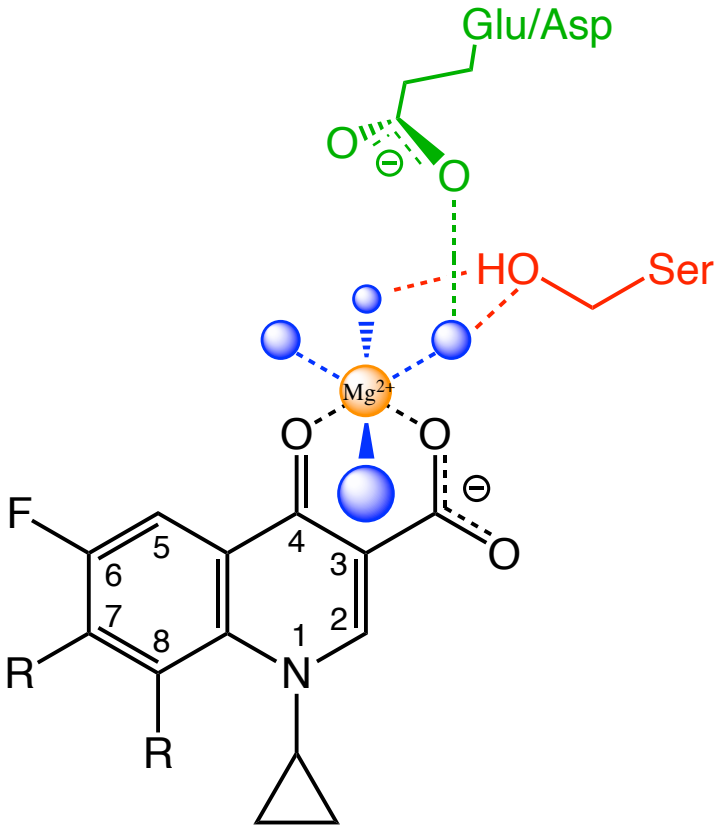

Figure 1.11. Water-metal Ion Bridge. The water-metal ion bridge mediates interactions between fluoroquinolones and gyrase and topoisomerase IV. A general drug structure is shown chelating a metal ion (Mg^{2+}, orange) through the C3/C4 ketoacid. Coordinating water molecules are blue and the serine and acidic residues are red and green, respectively. Adapted from Wohlkonig et al.[180]

coli and *Thermus thermophilus* gyrase from the Lamour laboratory will be useful in developing this class as both antibacterial and anticancer candidates.[182]

Fluoroquinolones can inhibit the overall catalytic cycle of bacterial type II topoisomerases as well.[48, 111] As such, it is difficult to distinguish between DNA cleavage enhancement and enzymatic inhibition to define the mode through which these compounds exert bactericidal effects. Do they work by stabilizing DNA cleavage, thereby killing cells through genomic fragmentation, or do they kill bacteria by preventing the crucial DNA topology maintenance of these enzymes?

Fluoroquinolone Resistance

Despite the importance of fluoroquinolones to the treatment of bacterial infections, their overuse has contributed to a rise in resistance that spans their entire spectrum of clinical usage.[48, 110, 169, 170, 173, 183-185] Bacteria are remarkably adaptable and resistance to nalidixic acid developed by 1969, just seven years after its introduction into the clinic.[183] Similarly, ciprofloxacin resistance arose as early as 1989 (2 years after its FDA approval)[186] and levofloxacin in 1996 (the same year it was released).[187]

Resistance to antibacterials comes in four major forms: antibacterial inactivation, limitation of drug uptake, increase in drug removal, or modification of the target.[48, 188] In the case of fluoroquinolones, plasmid-encoded acetylases can modify the C7 substituent of fluoroquinolones to inactivate the drugs or plasmid-encoded proteins can block fluoroquinolone binding.[189-191] A decrease in the chromosomal expression of porins, channels through which fluoroquinolones can enter the bacterial cell, limits the number of fluoroquinolone molecules that enter the cell in the first place. Furthermore, either chromosome- or plasmid-encoded efflux pumps can be used to remove fluoroquinolones and lower their concentration in the cell.[185, 189, 192] While bacteria have evolved all of these mechanisms for evading fluoroquinolones, clinically-associated resistance to this class is primarily target-mediated.[48, 168, 184] Mutations in either gyrase, topoisomerase IV, or both are associated with initiation of resistance. In fact, a 2010 study showed that in clinical isolates of *E. coli* resistant to fluoroquinolones, ~97% had a mutation

in gyrase and ~90% also had a mutation in topoisomerase.[188] Genetic studies have determined the primary targeting of various fluoroquinolones – targeting is both drug and species dependent. To come to this conclusion, stepwise resistance selection assays were performed with the idea that the first target to develop resistance is likely the one key to fluoroquinolone cell kill.[169] Mutation in the primary target confers the highest levels of resistance, followed by levels conferred by the secondary target. Mutation of both targets causes high levels of resistance.

Alteration of one or both of the two amino acid residues that anchor the water−metal ion bridge, located in what is termed the quinolone resistance determining region (QRDR) of gyrase and topoisomerase IV, results in this target-mediated fluoroquinolone resistance.[193-196] Approximately 90% of these mutations are in the conserved serine (Ser83) in the GyrA subunit of *E. coli* where the mutations were first discovered.[193-195, 197] The majority of the other mutations are in the aspartic or glutamic acid residue (Glu87 in *E. coli*) four amino acids downstream of the serine. The corresponding mutations in ParC of topoisomerase IV also confer high levels of resistance – on the order of 10-fold resistance.

Aside from inducing fluoroquinolone resistance, mutation of the conserved serine has no other phenotype.[48, 111] It has been proposed that this residue has been conserved through natural selection to provide resistance to the naturally occurring compound nybomycin.[48] The aspartic/glutamic acid residue, however, does seem to have a catalytic role – when mutated, overall enzymatic activity of gyrase or topoisomerase IV is decreased.[48, 111, 198, 199] Thus, the higher proportion of serine mutations in response to fluoroquinolones may be a product of the serine being non-essential while the acidic residue plays a part in enzyme catalysis.

Mediation of fluoroquinolone - type II topoisomerase interactions by the water-metal ion bridge

Although mutation of the serine and/or acidic residue have been associated with fluoroquinolone resistance for decades, recent studies have elucidated their role in mediating fluoroquinolone-type II topoisomerase interactions. The first data came from structural studies of *Streptococcus pneumoniae*

topoisomerase IV in a cleavage complex with moxifloxacin.[179] This 4 Å resolution structure showed two molecules of moxifloxacin intercalated 4 base pairs apart between the -1 and +1 positions at each cut site. In this structure, moxifloxacin is oriented such that the N1 substituent is closest to the serine and acidic residues implicated in fluoroquinolone resistance. In this orientation, the ketoacid of the drug does not make contact with either residue. A higher resolution (3.27 Å) structure of *Acinetobacter baumannii* topoisomerase IV bound to moxifloxacin similarly showed the drug situated in the gate segment.[180] However, this structure differed in two important ways: first, it showed an alternative orientation for the drug in which the keto acid points toward the serine and acidic residues and secondly, it is of high enough resolution to reveal the presence of a magnesium ion and its coordination sphere. With this information, the authors suggested that moxifloxacin, and likely other fluoroquinolones, bind through this magnesium and its coordinated water molecules.

Studies from the Osheroff laboratory were the first to confirm this binding mode using biochemical assays in conjunction with *Bacillus anthracis* topoisomerase IV.[199-201] Data with both wild-type (WT) and fluoroquinolone-resistant enzymes with mutations in the serine (Ser81) or glutamate (Glu85) support the hypothesis that a water-metal ion bridge mediates the interactions between these two residues and fluoroquinolones. Furthermore, these initial studies suggest that mutation of either Ser81 or Glu85 lead to fluoroquinolone resistance in *B. anthracis* topoisomerase IV through restriction of metal ion usage and decreased metal ion affinity. Functional studies with *E. coli* topoisomerase IV and gyrase from *B. anthracis* and *M. tuberculosis* as well as subsequent structural data have all provided further evidence to support this water-metal ion binding mode for fluoroquinolones.[79, 181, 202-204] Importantly, although the bridge mediates enzyme-drug interactions in a number of species, the precise utilization of the bridge differs between species. Specifically, the water-metal ion bridge appears to support binding in *B. anthracis* gyrase and topoisomerase IV as well as *M. tuberculosis* gyrase. However, the bridge may be more important for fluoroquinolone positioning in *E. coli* topoisomerase IV.[202]

This fluoroquinolone binding mode has two important implications. First, the fact that the C3/C4 ketoacid is utilized for enzyme interactions suggests that other substituents, namely at the N1, C5, C7, and C8 positions can be exchanged without compromising fluoroquinolone-topoisomerase interactions. Alteration of these positions can be used to alter minor interactions or enhance specificity of the core drug for different species. Additionally, interaction of the water-metal ion bridge through the conserved serine and acidic residues in bacterial type II topoisomerase lessens the likelihood for cross reactivity with the human enzymes, as hTIIα and hTIIβ have methionine residues in the corresponding region.[111] One caveat is that a set of quinolones containing a 3′- (aminomethyl)pyrrolidinyl [3′-(AM)P] group at C7 has been described with effects against both the bacterial and human type II topoisomerases.[205] This substituent allows the compounds containing this modification to overcome fluoroquinolone resistance mutations by mediating different interactions with the bacterial enzymes. Therefore, compounds in this series could be exploited for anticancer drug development.

Overcoming fluoroquinolone resistance

Fluoroquinolone resistance in context

Current estimates indicate that antibiotic-resistant infections cause 36,000 deaths per annum in the US alone[206] and 25,000 per annum in Europe.[207] Globally, that number is estimated to be upwards of 3.57 million deaths from resistant bacterial infections caused by just six of the leading pathogens in 2019.[208] As if these numbers were not concerning enough, predictions for the future are still more dire. If antimicrobial resistance is not curbed, deaths due to antimicrobial resistance may rise to 10 million per year according to The Review on Antimicrobial Resistance.[209] This number outpaces the current number of deaths due to cancer (8.2 million). The lack of new antibacterial candidates makes this prediction a very real and a very serious possibility.[210] Antibacterial new drug application approvals have dropped from just under 20 from 1980-1984 to 1 from 2010-2012.[187] A recent 2019 Pew Research Center analysis showed

that of the 42 drugs in the so-called antibiotic pipeline, only 1 in 4 is novel in any way.[206] For this reason, many researchers suggest that we are entering a post-antibacterial era wherein diseases that were once treated easily will now be life-threatening.

As an example, both the Centers for Disease Control (CDC) and the World Health Organization (WHO) maintain watch lists for antimicrobial resistance. Among the most urgent threats (the highest level listed by the CDC includes only 5 microbial species) is drug-resistant *Neisseria gonorrhoeae,* the causative agent of gonorrheal infections.[206, 211] Gonorrhea infections alone account for an estimated 87 million bacterial infections each year in persons aged 15-49;[212] 550,000 of which occur in the United States.[206] Interestingly, the disease affects the United States population disproportionately. In 2016, the highest rates of gonorrheal infection per 100,000 people were in African Americans (500), followed by American Indian/Native American (200), Native Hawaiian/Other Pacific Islander (150), and Hispanic populations (80).[213] This is as compared to a rate of ~58 cases per 100,000 White persons. In terms of age, the CDC reports that the highest rates of gonorrheal infection were observed in the age range 20–24 years (702.6 versus 720.9 cases per 100,000 females versus males, respectively) in 2018.[214]

Previously, fluoroquinolones were the recommended treatment for gonorrheal infections. However, mutations in the quinolone-resistance determining region (QRDR) of *N. gonorrhoeae* gyrase and topoisomerase IV have led to a decline in the efficacy of these drugs. The ease with which gonorrheal infections were cured in the past has undermined the gravity of the resistance problem.[215] If left untreated, infection with gonorrhea can cause pelvic inflammatory disease, infertility, and disseminated gonorrhea infection (DGI) which can lead to death.[211, 215] Additionally, there is evidence that transmission of HIV is increased in individuals already infected with gonorrhea.[216] Since their introduction, the fluoroquinolone class of antibacterials has been widely prescribed and was considered a first-line therapeutic for gonococcal infections from 1993-2006. Until 2007, ciprofloxacin, a second-generation quinolone, was part of the recommended treatment regimen for gonorrhea infection. Ciprofloxacin resistance rates rose

to 13.8% by the close of 2006 and the CDC changed its recommendations regarding the use of ciprofloxacin in early 2007.[217]

Strategies for antibacterial development

Antibacterial resistance is inevitable. Given the broad clinical applications of fluoroquinolones, it is critical to discover new drugs that can supplement their use in the clinic.[218-220] How, then, can we keep pace with and get ahead of this threat of target-mediated resistance? Three main strategies exist: 1) discover new targets, 2) design more drugs within existing classes that have better pharmacokinetic and resistance profiles, or 3) develop new drug class that work against validated targets but interact with different amino acid residues. This dissertation focuses primarily on the latter approach which has led to the development of two antibacterial classes, known as "novel bacterial topoisomerase inhibitors" (NBTIs)[181, 221, 222] and spiropyrimidinetriones (SPTs).[223-225]

Novel Bacterial Topoisomerase Inhibitors (NBTIs)

The novel bacterial topoisomerase inhibitors (NBTIs) are a promising class of antibacterials that were first identified as potent inhibitors of bacterial growth.[226] Subsequent analysis of the DNA gyrase and topoisomerase IV inhibition in *Escherichia coli*, S*taphylococcus. aureus*, and *Streptococcus pneumoniae* showed that these compounds work against the bacterial type II topoisomerases.[227] A number of different structural classes of NBTIs have been shown to inhibit the DNA supercoiling and DNA decatenation activities of gyrase and topoisomerase IV, respectively, and to enhance DNA cleavage mediated by the type II enzymes.[181, 221, 228-235] Recent data has shown that compounds in the NBTI class can overcome some bacterial resistance mutations associated with the widely-prescribed fluoroquinolones.[234, 235] These various structural classes have three common features: 1) an aromatic left-hand side (LHS) that is involved in DNA intercalation, 2) connected by a cyclic (or bicyclic) linker to 3) the aromatic right-hand side (RHS) that makes enzyme contacts.[236]

In contrast to fluoroquinolones, a single NBTI molecule binds in the 2-fold axis of gyrase or topoisomerase IV.[181, 234-236] The planar LHS mediates the base-stacking interactions with the bent G-segment DNA and binds between the two A subunit active sites and seems to stabilize the binary enzyme-DNA complex before cleavage.[181, 236] This binding mode leads to the other notable difference from fluoroquinolones: NBTIs enhance primarily single-stranded as opposed to double-stranded DNA breaks mediated by the enzyme.[234, 235, 236] LHS intercalation is thought to distort the DNA in such a way that once the first strand of DNA is cut, the scissile phosphate of the second strand is not in the right orientation for nucleophilic attack.[236]

The RHS makes hydrophobic contacts with the enzyme, also in the 2-fold axis of the A subunit.[236] The recent crystal structure of *S. aureus* gyrase in complex with the first-in-class NBTI, gepotidacin (GSK2140944), has further elucidated the role of the basic amine of the linker.[79, 235, 236] In this study, the amine makes an important contact with Asp83 of *S. aureus* gyrase. Contact is made with this residue in both A subunits, one directly and one indirectly through a water molecule. The importance of this contact seems to be in anchoring gepotidacin while providing enough flexibility for correct positioning of the LHS and RHS.[79, 236]

The most clinically advanced NBTI is gepotidacin (Figure 1.12). The compound is currently in Phase III clinical trials for the treatment of UTIs and uncomplicated urogenital gonorrhea. See Chapter VI for the characterization of gepotidacin against the two indications for which it is in clinical trials.

Mycobacterium Gyrase Inhibitors

Several NBTIs display activity against clinically relevant bacterial species.[181, 221, 228-235] However, most show poor activity against *M. tuberculosis*.[237] GSK126 (Figure 1.12), which is a naphthyridone/aminopiperidine-based NBTI, was identified in a screen as having moderate activity against the bacterium.[237] This discovery led to a subset of NBTIs that were derived from GSK126 and displayed high activity against *M. tuberculosis* in culture and in mouse infection models.

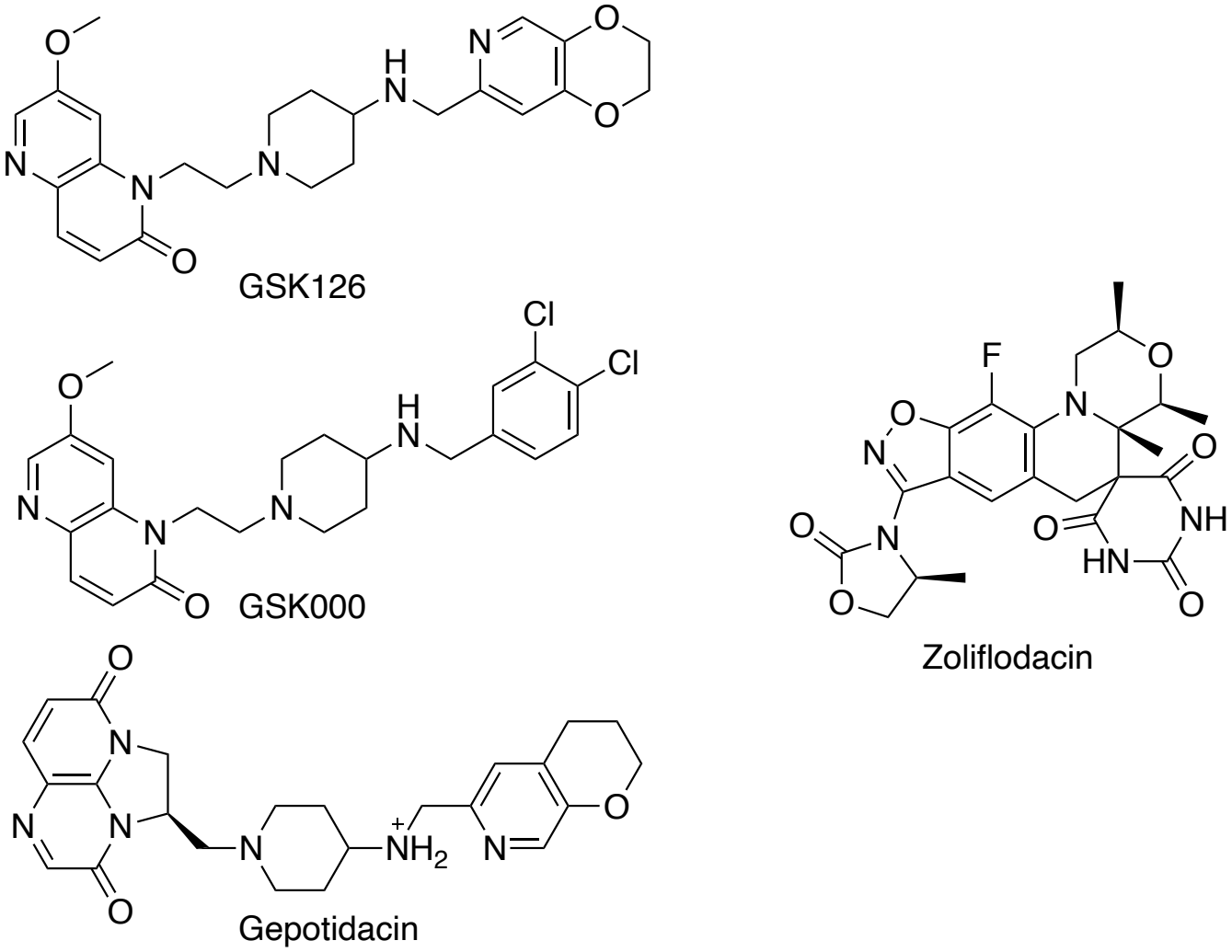

Figure 1.12. NBTI and SPT Structures. Left: Structures of three NBTIs are shown. GSK126 is the parent compounds to the MGI subclass, of which GSK000 is a member. Gepotidacin, a first-in-class triazaacenaphthylene, is in Phase III clinical trials. Right: Zoliflodacin is the first SPT progressing as a clinical candidate and is also in Phase III.

Compounds in this subclass are known as *M. tuberculosis* gyrase inhibitors (MGIs). A recent study characterized the mechanistic basis for the actions of MGIs against M. tuberculosis gyrase.[234] The MGIs GSK000 and GSK325 were specific for *M. tuberculosis* gyrase and enhanced only single-stranded breaks. These compounds also suppressed the generation of double-stranded breaks. Importantly, both GSK000 and GSK325 maintained activity against the most common fluoroquinolone resistance mutations identified clinically.

Relatively little is known about the actions of the parent NBTI class against gyrase and topoisomerase IV.[234, 235, 238] To address this important issue, the actions of GSK126 against a variety of bacterial type II topoisomerases, including gyrase from *M. tuberculosis* and gyrase and topoisomerase IV from *B. anthracis* and *E. coli* are reported in Chapter IV.

Spiropyrimidinetriones (SPTs)

Zoliflodacin (ETX0914/AZD0914) (Figure 1.12) is the most advanced clinical spiropyrimidinetrione (SPT).[223, 224] The compound is currently in Phase III clinical trials for the treatment of uncomplicated gonorrhea.[239] Similar to fluoroquinolones, the SPTs enhance double-stranded DNA scission mediated by gyrase and topoisomerase IV. Usefully, zoliflodacin has been shown to overcome some fluoroquinolone resistance mutations in *Pseudomonas aeruginosa*.[223, 224]

Scope of the Dissertation

The disparate fields of cancer therapy and bacterial infection eradication are brought together by a common feature: both cancer cells and bacterial cells (and, indeed, all living cells) encode the essential type II topoisomerases. While the field of chemotherapy is plagued by off-target effects that kill "healthy" cells, rising rates of antimicrobial resistance are threatening the clinical use of all antibacterial classes, including the fluoroquinolones. The broad clinical utilization of type II topoisomerase poisons for cancer

treatment and antibacterial treatment necessitates a deeper understanding of how these compounds interact with their targets. The goals of this dissertation are to characterize derivatives of the widely-prescribed anticancer agent etoposide, to define the actions of NBTIs against bacterial type II topoisomerases, and to determine the ability of NBTIs to overcome fluoroquinolone-associated resistance mutations.

Chapter I introduced DNA topology, the need for topoisomerases, the anticancer targeting of human type II topoisomerases, fluoroquinolone targeting of bacterial type II topoisomerases, and the problems and potential solutions to off-target anticancer therapeutic effects and fluoroquinolone resistance. Sections of this background material were taken from our recently published review [Vann, K. R., Oviatt, A. A., and Osheroff, N. (2021) Topoisomerase II Poisons: Converting Essential Enzymes into Molecular Scissors, *Biochemistry 60*, 1630-1641.].[42] The materials and methods used to accomplish the goals of this dissertation are detailed in Chapter II.

Chapter III describes the use of two-dimensional gel electrophoresis methods to separate DNA topoisomers. Generally, the products of reactions that monitor the interconversion of DNA between negatively supercoiled and relaxed DNA or positively supercoiled and relaxed DNA can be resolved by one-dimensional gel electrophoresis. However, in more complex reactions that contain both positively and negatively supercoiled DNA, one-dimensional resolution is insufficient. In these cases, a second dimension of gel electrophoresis is necessary. This chapter describes the technique of two-dimensional agarose gel electrophoresis and how it can be used to resolve a spectrum of DNA topoisomers. This work has been published [Gibson, E. G., Oviatt, A. A., and Osheroff, N. (2020) Two-Dimensional Gel Electrophoresis to Resolve DNA Topoisomers, *Methods Mol. Biol. 2119*, 15-24.].[240]

Chapter IV examines the effects of polyamine-etoposide hybrids on human topoisomerase IIα and IIβ. All of the compounds displayed an ability to induce enzyme-mediated DNA cleavage that was comparable to or higher than that of etoposide. Relative to the parent drug, the hybrid compounds displayed substantially higher activity toward topoisomerase IIβ than IIα. Modeling studies performed by our collaborators suggest that the enhanced specificity may result from interactions with Gln778 in

topoisomerase IIβ. The corresponding residue in the α isoform is a methionine. The results of this study have been published [Oviatt, A. A., Kuriappan, J. A., Minniti, E., Vann, K. R., Onuorah, P., Minarini, A., De Vivo, M., and Osheroff, N. (2018) Polyamine-containing etoposide derivatives as poisons of human type II topoisomerases: Differential effects on topoisomerase IIalpha and IIbeta, *Bioorg. Med. Chem. Lett. 28*, 2961-2968.].[241]

Chapter V reports the characterization of the NBTI GSK126 and its effects against bacterial type II topoisomerases from three Gram-negative and Gram-positive species. Our results suggest that NBTIs elicit their antibacterial effects by two different mechanisms: inhibition of gyrase/topoisomerase IV catalytic activity and enhancement of enzyme-mediated DNA cleavage. Furthermore, the relative importance of these two mechanisms may differ from species to species. Therefore, we propose that the mechanistic basis for the antibacterial properties of NBTIs is bimodal in nature. Additionally, we show that GSK126 can overcome some fluoroquinolone resistance mutations in the species utilized. This work has been published [Gibson, E. G., Oviatt, A. A., Cacho, M., Neuman, K. C., Chan, P. F., and Osheroff, N. (2019) Bimodal Actions of a Naphthyridone/Aminopiperidine-Based Antibacterial That Targets Gyrase and Topoisomerase IV, *Biochemistry 58*, 4447-4455.].[242]

Chapter VI investigates the interactions of gepotidacin with the type II topoisomerases from *E. coli* both in cells and *in vitro*. We show that gepotidacin has a well-balanced dual-targeting of gyrase and topoisomerase IV in this species and inhibits catalytic activity and enhances single-stranded DNA cleavage with both enzymes. Gepotidacin has a variable ability to overcome fluoroquinolone or NBTI resistance mutations *in vitro* but maintains activity against the corresponding engineered *E. coli* cells. Similarly, the compound has high activity against the bacterial type II topoisomerases from *N. gonorrhoeae*.

Conclusions and implications of the studies described herein as well as potential future studies are presented in Chapter VII.

CHAPTER II

METHODS

Materials

DNA Substrates

Negatively supercoiled pBR322 DNA was prepared from E. coli using a Plasmid Mega Kit (Qiagen) as described by the manufacturer. Calf thymus topoisomerase I (Invitrogen) treatment of negatively supercoiled pBR322 was used to prepare relaxed plasmid DNA. The relaxed pBR322 plasmid was purified as described previously.[202] Kinetoplast DNA (kDNA) was isolated from *Crithidia fasciculata* as described by Englund.[243]

Drugs and other

Etoposide was purchased from Sigma. Etoposide-polyamine hybrids (compounds **2-7**) were synthesized as described by Palermo *et al*.[244] Compound 2 previously has been described as F14512.[245] Etoposide and the etoposide-polyamine hybrids were stored at 4 °C as 20 mM stock solutions in 100% DMSO.

The NBTI GSK126 was synthesized as described previously by Blanco et al.[237] In their work, GSK126 was identified as compound 1. The NBTI was stored at 4 °C as a 1−2 mM stock solution in 10% dimethyl sulfoxide. Ciprofloxacin was obtained from Sigma-Aldrich and stored at 4 as 40 mM aliquots in 0.1 N NaOH. Gepotidacin was provided by GlaxoSmithKline and stored at 4 as 20 mM aliquots in 100% dimethyl sulfoxide. All other chemicals were analytical reagent grade.

Human Type II Topoisomerases

Enzymes

Recombinant human topoisomerase IIα and topoisomerase IIβ were expressed in *Saccharomyces cerevisiae* and purified as described previously.[246, 247] The enzyme was stored at -80 °C as a 1.5 mg/mL stock in 50 mM Tris-HCl, pH 7.9, 0.1 mM NaEDTA, 750 mM KCl, and 40% glycerol.

DNA Cleavage

DNA cleavage reactions with human topoisomerase IIα and topoisomerase IIβ were performed using the procedure of Fortune and Osheroff.[248] Reaction mixtures contained 220 nM human topoisomerase IIα or 208 nM topoisomerase IIβ and 10 nM negatively supercoiled pBR322 in a total of 20 μL of DNA cleavage buffer [10 mM Tris-HCl, pH 7.9, 5 mM $MgCl_2$, 100 mM KCl, 0.1 mM NaEDTA, and 2.5% (v/v) glycerol]. Assays were carried out in the absence of compounds or in the presence of 0–50 μM etoposide or compounds **2**-**7**. Mixtures were incubated for 6 min at 37 °C and enzyme-DNA cleavage complexes were trapped by the addition of 2 μL of 5% SDS followed by 2 μL of 250 mM Na_2EDTA, pH 8.0. Proteinase K (2 μL of a 0.8 mg/mL solution) was added, and samples were incubated at 45 °C for 30 min to digest the enzyme. Samples were mixed with 2 μL of 60% sucrose, 10 mM Tris-HCl, pH 7.9, 0.5% bromophenol blue; and 0.5% xylene cyanol FF, heated at 45 °C for 5 min, and subjected to electrophoresis in 1% agarose gels in 40 mM Tris-acetate, pH 8.3, and 2 mM EDTA containing 0.5 μg/mL ethidium bromide. DNA bands were visualized with ultraviolet light and quantified using an Alpha Innotech digital imaging system. DNA cleavage was monitored by the conversion of supercoiled plasmid DNA to linear (double-stranded break) and nicked (single-stranded break) molecules.

DNA Ligation

DNA ligation mediated by topoisomerase IIα or topoisomerase IIβ was monitored according to the procedure of Byl *et al*.[249] Reaction mixtures contained 220 nM human topoisomerase IIα (or 440 nM for

reactions performed in the absence of drug) or 208 nM human topoisomerase IIβ in a total of 20 μL of DNA cleavage buffer. In reactions that contained no drug, 5 mM $MgCl_2$ was replaced by 5 mM $CaCl_2$ to increase levels of baseline DNA scission. DNA cleavage/ligation equilibria were established for 6 min at 37 °C as described above in the absence or presence of 100 μM (α isoform) or 25 μM (β isoform) etoposide or 25 μM compounds **2-7**. Ligation was initiated by shifting samples from 37 to 0 °C. Reactions were stopped at time points ranging from 0-30 s by the addition of 2 μL of 5% SDS followed by 2 μL of 250 mM Na_2EDTA, pH 8.0. Samples were processed and analyzed as described under plasmid DNA cleavage. Linear DNA cleavage product at time zero was set to 1.0 to allow direct comparisons between the different compounds and DNA ligation was monitored by the loss of linear DNA.

Persistence of Topoisomerase II-DNA Cleavage Complexes

The persistence of topoisomerase II-DNA cleavage complexes was determined using a modification of the procedure of Gentry *et al*.[250] Initial reactions contained 55 nM DNA, 440 nM topoisomerase IIα or 415 nM topoisomerase IIβ, and 100 μM (α isoform) or 50 μM (β isoform) etoposide or 25 μM compounds **2-7** in a total of 20 μL of DNA cleavage buffer. Reactions were incubated for 10 min (α isoform) or 6 min (β isoform) at 37 ºC and then diluted 20-fold with DNA cleavage buffer at 37 ºC. Samples (20 μL) were removed at times ranging from 0-150 min, and DNA cleavage was stopped with 2 μL of 5% SDS followed by 2 μL of 250 mM Na_2EDTA, pH 8.0. Samples were mixed with 2 μL of agarose gel loading buffer and processed and analyzed as described under plasmid DNA cleavage. Levels of DNA cleavage were set to 1.0 at time zero, and the persistence of cleavage complexes was determined by the decay of linear reaction product over time.

Molecular Modeling

The crystal structures of DNA cleavage complexes formed with the α and β isoforms of human topoisomerase II in the presence of etoposide, PDBid 5GWK[251] and PDBid 3QX3[145], respectively, were obtained from the RCSB PDB repository. Compounds **2**-**7**[244] were all included in the docking studies. Models with both enzyme isoforms were generated with the Protein Preparation Wizard in the Schrödinger 2017 suite.[252]

Structures for compounds **2**-**7** were prepared with Ligprep for molecular docking, using the OPLS2005 force field and charges. For each ligand, all possible protonation and ionization states were generated at a pH of 7.4. Stereoisomers were generated for the six structures, with a limit of 32 stereoisomers per ligand. To address protein flexibility in molecular docking, we initially performed standard docking and moved onto fully flexible active site docking.

Docking Calculations

The receptor grid for each target was prepared using the OPLS2005 force field. We specified the area surrounding the co-crystallized ligand (*i.e.*, etoposide) as the receptor-binding pocket. The grid center was set to be the centroid of the bound etoposide. The cubic grid had a side length of 20 Å. Core constraints were used in the receptor grids based on the assumption that all the ligands exhibit an etoposide-like binding mode for the conserved epipodophyllotoxin core.[244] After grid preparation, ligands were first docked into the generated receptor grids using Glide SP (Standard Precision) docking.[253] Flexible ligand sampling was considered in the docking procedure. All poses were subjected to post-docking minimization.

Induced Fit Docking

We used the Glide results from the standard docking procedure for subsequent induced fit docking calculations, as available within Schrödinger, to model the conformational changes in the active site induced by the ligand binding.[254, 255] A maximum of 20 poses were saved per ligand. All residues within

5.0 Å of the bound ligand were refined using the Prime molecular dynamics module to allow for binding domain flexibility.

Bacterial Type II Topoisomerases

Enzymes

Bacillus anthracis

Full-length wild-type *B. anthracis* gyrase subunits (GyrA and GyrB), wild-type topoisomerase IV subunits (GrlA and GrlB), the GyrA mutant ($GyrA^{S85L}$), as well as the GrlA mutant ($GrlA^{S81F}$), were expressed and purified as described by Dong et al.[256]

Escherichia coli

Wild- type *E. coli* gyrase subunits (GyrA and GyrB) were expressed and purified as described by Maxwell et al.[257] Mutant *E. coli* $GyrA^{S83L}$ was expressed and purified as described by Dong et al.[256] Mutant *E. coli* $GyrA^{P35L}$ was provided by Pan Chan at GlaxoSmithKline.

Wild-type *E. coli* topoisomerase IV (ParC and ParE) and the ParC mutant ($ParC^{S80L}$) were expressed and purified as described by Peng and Marians[258] or by a minor modification of Corbett et al.[259] The *E. coli* ParC mutant ($ParC^{D79N}$) was provided by Pan Chan at GlaxoSmithKline.

Mycobacterium tuberculosis

Wild-type *M. tuberculosis* gyrase subunits (GyrA and GyrB) and the GyrA mutant ($GyrA^{A90V}$) were expressed and purified as described by Blower et al.[260] and modified by Aldred et al.[203]

Neisseria gonorrhoeae

Wild-type *N. gonorrhoeae* gyrase subunits (GyrA and GyrB) and topoisomerase IV subunits (ParC and ParE), *N. gonorrhoeae* GyrA mutants ($GyrA^{S91F}$, $GyrA^{A92T}$) and ParC mutant ($ParC^{D86N}$) were provided by Pan Chan at GlaxoSmithKline. *N. gonorrhoeae* gyrase and topoisomerase IV mutants ($GyrA^{D95G}$, $ParC^{S87N}$, $ParC^{S87R}$, and $ParC^{E91A}$) were expressed and purified as described by Dong et al.[256]

	B. anthracis	*E. coli*	*M. tuberculosis*	*N. gonorrhoeae*
Gyrase (FQ_R)	S85L	S83L	A90V	S91F;D95G
Gyrase ($NBTI_R$)		P35L		A92T
Topoisomerase IV (FQ_R)	S81F	S80L		S87N; S87R; E91A
Topoisomerase IV ($NBTI_R$)		D79N		D86N

Table 2.1. Mutant Bacterial Type II Topoisomerases. The mutant enzymes utilized for the studies presented in this dissertation are shown. Included are fluoroquinolone-resistant (FQ_R) and NBTI-resistant ($NBTI_R$) gyrase and topoisomerase IV from four species. Data with underlined mutants are presented. Future work will address the mutants listed under *N. gonorrhoeae* that are not underlined.

Gyrase-Catalyzed DNA Supercoiling

DNA supercoiling assays were based on previously published protocols.[200, 203] Assays contained 200 nM B. anthracis wild-type or mutant ($GyrA^{S85L}$) gyrase (1:2 GyrA:GyrB ratio), 10 nM E. coli wild-type or mutant ($GyrA^{S83L}$) gyrase (1:1 GyrA:GyrB ratio), or 75 nM M. tuberculosis wild-type or mutant ($GyrA^{A90V}$) gyrase (1.5:1 GyrA:GyrB ratio), 5 nM relaxed pBR322, and 1.5 mM ATP in a total volume of 20 µL of 50 mM Tris-HCl, pH 7.5, 5 mM $MgCl_2$, 175 mM KGlu, and 50 µg/mL BSA for all enzymes except M. tuberculosis gyrase or 10 mM Tris-HCl, pH 7.5, 40 mM KCl, 6 mM $MgCl_2$, 0.1 mg/mL BSA, and 10% glycerol for M. tuberculosis gyrase. Stated enzyme concentrations reflect those of the holoenzyme (A_2B_2) calculated on the basis of the limiting subunit. In reactions with gyrase from B. anthracis and M. tuberculosis, 5 and 2 mM DTT, respectively, were included. Reaction mixtures were incubated at 37 °C for 30 min, which represents the minimum time required to completely supercoil the DNA in the absence of the drug. Reaction mixtures were stopped by the addition of 3 µL of a mixture of 0.77% SDS and 77.5 mM Na_2EDTA. Samples were mixed with 2 µL of loading buffer and incubated at 45 °C for 2 min before being loaded onto 1% agarose gels in 100 mM Tris- borate, pH 8.3 and 2 mM EDTA. Gels were stained with 1 µg/mL ethidium bromide for 30 min. DNA bands were visualized and quantified as described above. IC_{50} values were determined using Prism and represent the concentration of GSK126 that decreased activity by 50%.

Topoisomerase IV-Catalyzed DNA Decatenation

DNA decatenation assays were based on previously published protocols.[203, 261] Assays contained 25 nM B. anthracis wild-type or mutant ($GrlA^{S81F}$) topoisomerase IV (1:2 GrlA:GrlB ratio) or 10 nM E. coli wild-type or mutant ($ParC^{S80L}$) topoisomerase IV (1:1 ParC:ParE ratio), 5 nM kDNA, and 1.5 mM ATP in 20 µL of 40 mM HEPES, pH 7.6, 100 mM KGlu, 10 mM $Mg(OAc)_2$, and 25 mM NaCl. Stated enzyme concentrations reflect those of the holoenzyme (A_2B_2) calculated on the basis of the limiting subunit. Reaction mixtures were incubated at 37 °C for 30 min, which represents the minimum time

required to completely decatenate the DNA in the absence of the drug. Reactions were stopped by the addition of 3 μL of a mixture of 0.77% SDS and 77.5 mM Na_2EDTA. Samples were mixed with 2 μL of loading buffer and incubated at 45 °C for 2 min before being loaded onto 1% agarose gels in 100 mM Tris-borate, pH 8.3, and 2 mM EDTA. Gels were stained with 1 μg/mL ethidium bromide for 30 min. DNA bands were visualized and quantified as described above. IC_{50} values were determined using Prism and represent the concentration of GSK126 that decreased activity by 50%.

DNA Cleavage

DNA cleavage assays with bacterial gyrase and topoisomerase IV were based on the procedure of Aldred et al.[203] Reactions were carried out in the absence of compound or in the presence of increasing concentrations of ciprofloxacin or an NBTI, and unless stated otherwise, the mixtures contained 500 nM B. anthracis wild-type or mutant ($GyrA^{S85L}$) gyrase (1:2 GyrA:GyrB ratio), 150 nM B. anthracis wild-type or 125 nM mutant ($GrlA^{S81F}$) topoisomerase IV (1:2 GrlA:GrlB ratio), 50 nM E. coli wild-type or mutant ($GyrA^{S83L}$) gyrase (1:1 GyrA:GyrB ratio), 20 nM E. coli wild-type or 10 nM mutant ($ParC^{S80L}$) topoisomerase IV (1:1 ParC:ParE ratio), or 100 nM M. tuberculosis wild-type or mutant ($GyrA^{A90V}$) gyrase (1.5:1 or 1:1 GyrA:GyrB ratio, respectively). Stated enzyme concentrations reflect those of the holoenzyme (A_2B_2) calculated on the basis of the limiting subunit. The subunit ratios that were employed represent the minimal amount of protein required to generate maximal cleavage at 37 °C.

Assays contained 10 nM negatively supercoiled pBR322 in a total volume of 20 μL of reaction buffer: 50 mM Tris-HCL, pH 7.5, 100 mM KGlu, 5 mM $MgCl_2$, 1 mM dithiothreitol (DTT), and 50 μg/mL BSA for B. anthracis gyrase; 10 mM Tris-HCl, pH 7.5, 40 mM KCl, 6 mM $MgCl_2$, 0.1 mg/mL bovine serum albumin, and 10% glycerol for M. tuberculosis gyrase; and 40 mM Tris-HCl, pH 7.9, 50 mM NaCl, 10 mM $MgCl_2$, and 12.5% glycerol for all other enzymes. In some cases, $MgCl_2$ in reaction buffers was replaced with an equivalent concentration of 5 mM $CaCl_2$ or 1.5 mM ATP was included in reaction mixtures. Unless stated otherwise, reaction mixtures were incubated at 37 °C for 30 min with B. anthracis

gyrase and for 10 min with all other enzymes. Enzyme−DNA cleavage complexes were trapped by adding 2 μL of 5% sodium dodecyl sulfate (SDS) followed by 2 μL of 250 mM Na2EDTA and 2 μL of 0.8 mg/mL Proteinase K (Sigma-Aldrich). Reaction mixtures were incubated at 45 °C for 30 min to digest the enzyme. Samples were mixed with 2 μL of loading buffer [60% sucrose, 10 mM Tris-HCl, pH 7.9, 0.5% bromophenol blue, and 0.5% xylene cyanol FF] and incubated at 45 °C for 2 min before being loaded onto 1% agarose gels. Reaction products were subjected to electrophoresis in 40 mM Tris-acetate, pH 8.3, and 2 mM EDTA containing 0.5 μg/mL ethidium bromide. DNA bands were visualized with medium-range ultraviolet light and quantified by scanning densitometry using a Protein Simple AlphaImager HP digital imaging system. DNA single- or double-stranded cleavage was monitored by the conversion of supercoiled plasmid to nicked or linear molecules, respectively, and quantified in comparison to a control reaction in which an equal amount of DNA was digested by EcoRI (New England BioLabs). EC_{50} values were determined using Prism and represent the concentration of GSK126 at which 50% maximal single-stranded DNA cleavage was observed.

CHAPTER III

TWO-DIMENSIONAL GEL ELECTROPHORESIS TO RESOLVE DNA TOPOISOMERS

Introduction

The superhelicity of DNA can have a profound effect on a number of DNA processes including replication, transcription, and recombination.[3, 5, 11, 12, 14, 39, 61] Therefore, it is important to be able to distinguish DNA molecules that are underwound (negatively supercoiled), contain no torsional stress (relaxed), and overwound (positively supercoiled). The easiest way to resolve supercoiled and relaxed DNA topoisomers is by agarose gel electrophoresis. To maintain the topological state of DNA during electrophoresis, the molecules must be in a "closed" system (i.e., the ends cannot have free-rotation). Therefore, this method applies primarily to circular DNA molecules.

Because the charges on DNA come from the phosphate groups in the DNA backbone, all DNA molecules have the same charge-to-mass ratio. Thus, in a vacuum, DNA topoisomers would all migrate at the same rate. However, when subjected to electrophoresis through a gel matrix, smaller or more compact molecules migrate more readily through the medium than a molecule that has more volume. When DNA is in a "relaxed" state, in which there is no torsional stress on the molecule, it maintains a more open structure (Figure 3.1). Thus, it has a wide diameter. However, when torsional stress is applied to the molecule by increasing or decreasing the number of turns of the double helix, free DNA converts ~75% of the torsional stress to axial stress,[3] which is manifested by the double helix wrapping around itself to form "superhelical twists." As seen in Figure 3.1, superhelical twisting leads to a more compact structure of DNA; the greater the superhelical twisting (or supercoiling), the more compact the structure. Therefore, the more supercoiled the DNA molecule, the faster it will migrate through an agarose gel toward the cathode. Superhelical twists occur in discrete units (i.e., molecules will have 1, 2, 3, ... etc.

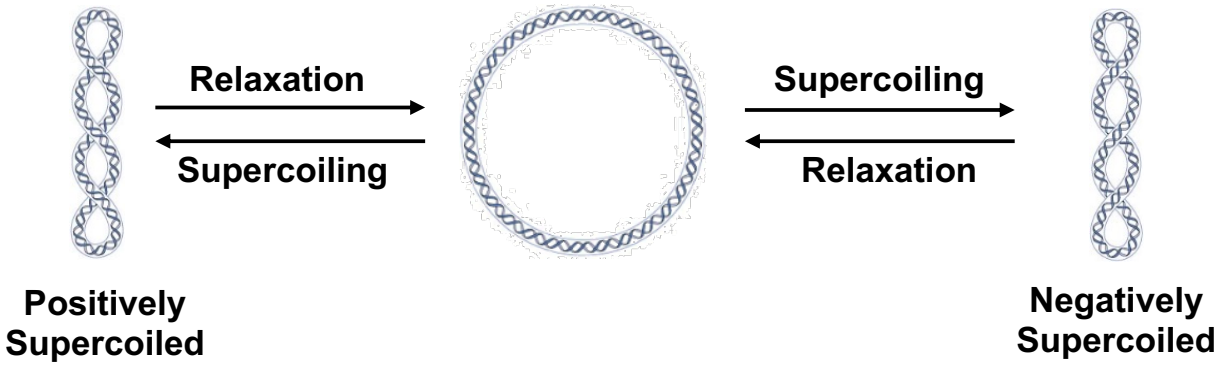

Fig. 3.1: Interconversion of DNA topoisomers. DNA that is not under torsional stress is referred to as "relaxed" (center), while over- and under-winding results in DNA that is positively (left) or negatively (right) supercoiled, respectively. The term "supercoiled" is derived from the fact that when under torsional stress, some of the stress is alleviated by the DNA forming superhelical twists about itself.

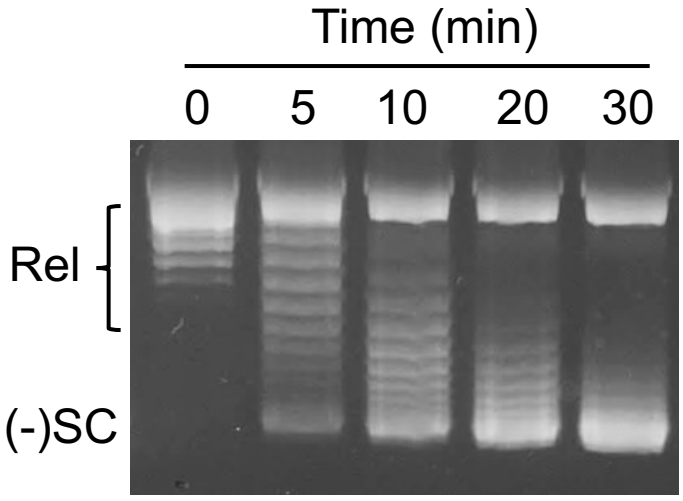

Fig. 3.2: One-dimensional resolution of relaxed and negatively supercoiled DNA topoisomers. A time course for the conversion of relaxed plasmid to negatively supercoiled molecules by S. aureus gyrase is shown. Reaction products were resolved by one-dimensional agarose gel electrophoresis and DNA bands were visualized by mid-range ultraviolet light following staining with ethidium bromide. The positions of relaxed (Rel) and negatively supercoiled [(-)SC] DNA are indicated on the gel.

DNA nodes or crossovers). Individual DNA topoisomers (i.e., plasmids with a specific number of DNA nodes or superhelical twists) will run as distinct bands.

Results and Discussion

When monitoring reactions in which a DNA molecule is being converted from relaxed to negatively or positively supercoiled, or from supercoiled to relaxed, one-dimensional electrophoresis is generally sufficient to resolve topoisomers (Figure 3.2). In these cases, all of the intermediate DNA topoisomers will contain a number of supercoils ranging from that of the substrate to that of the product. In the example shown in Figure 3.2, the time course follows a reaction in which a relaxed plasmid is converted to a negatively supercoiled molecule by an enzyme known as DNA gyrase.[12, 39, 68] Hence, all of the individual DNA bands that are visualized contain either no supercoils (relaxed) or some number of negative supercoils.

In contrast to the reaction shown in Figure 3.2, some reactions are more complex. For example, Figure 3.3 shows a time course for the conversion of positively to negatively supercoiled DNA by gyrase.[117, 235, 262] In this case, positive supercoils are removed to produce relaxed DNA followed by the introduction of negative supercoils. Positively supercoiled DNA is slightly more compact[3] than its negatively supercoiled counterpart and therefore migrates slightly further on an agarose gel.[263] However, one-dimensional electrophoresis is insufficient to determine whether the intermediate bands are positively or negatively supercoiled. Thus, it is necessary to use two-dimensional electrophoresis to resolve this issue.

The first dimension in two-dimensional gel electrophoresis separates DNA topoisomers as described above. To distinguish positive from negative intermediate topoisomers, the gel is then soaked in chloroquine, a DNA intercalative agent. DNA intercalators locally unwind the double helix. Because

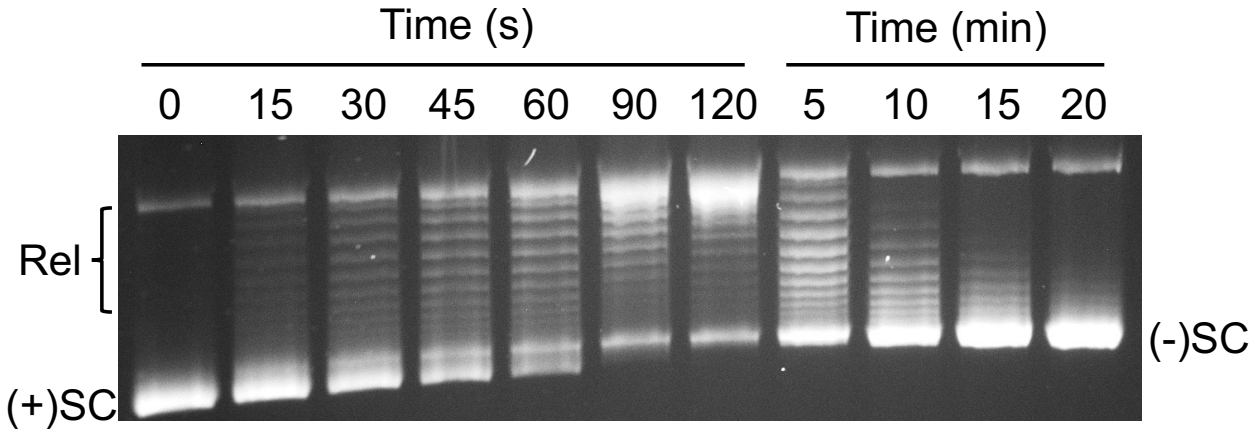

Fig. 3.3: One-dimensional resolution of negatively and positively supercoiled DNA topoisomers. A time course for the conversion of positively supercoiled plasmid to negatively supercoiled molecules by *S. aureus* gyrase is shown. Reaction products were resolved by one-dimensional agarose gel electrophoresis and DNA bands were visualized by mid-range ultraviolet light following staining with ethidium bromide. The positions of relaxed (Rel), positively supercoiled [(+)SC], and negatively supercoiled [(-)SC] DNA are indicated on the gel.

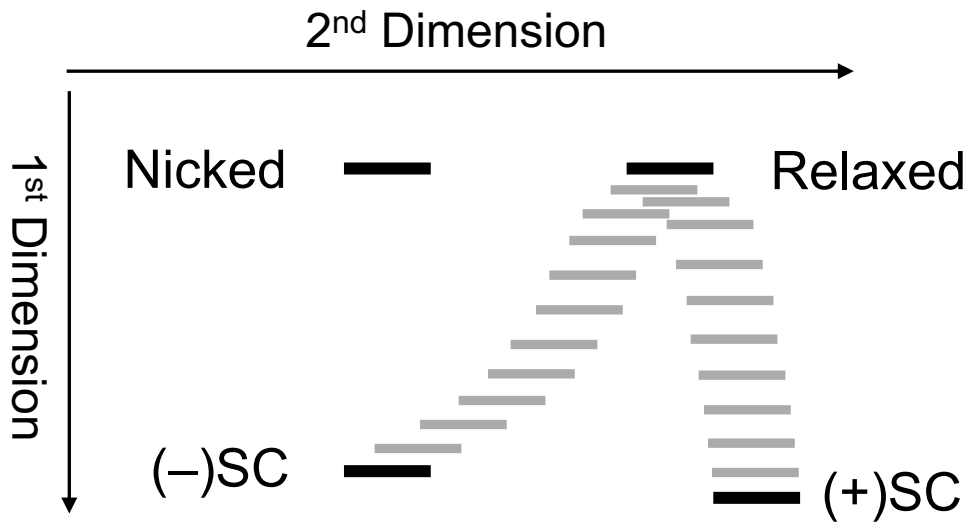

Fig. 3.4: Migration of DNA topoisomerases following two-dimensional agarose gel electrophoresis. The positions of nicked, relaxed, negatively supercoiled [(-)SC], and positively supercoiled [(+)SC] DNA are shown as black bands. Gray bands represent DNA topoisomers of intermediate supercoiling. Partially negatively supercoiled molecules migrate as the arc between relaxed and (-)SC DNA and partially positively supercoiled molecules migrate as the arc between (+)SC and relaxed DNA.

the number of turns of the double helix is invariant in a closed circular system,[3, 11] the local underwinding (which is constrained by the presence of the intercalator) is compensated by a global overwinding.[249, 264, 265] Hence, negatively supercoiled molecules will tend to look less negatively supercoiled (or even fully relaxed) in the presence of an intercalator and relaxed DNA will tend to look positively supercoiled. Because molecules that already contain a high level of positive superhelical twists cannot absorb very much intercalator, positively supercoiled DNA changes very little in the presence of a DNA intercalator.[249, 263] Similarly, the migration of nicked DNA changes relatively little in the presence of an intercalator. This is because the presence of the nick opens the topological system and the absorption of an intercalator does not lead to compensatory overwinding. In the example described below, the amount of chloroquine that is added is sufficient to make negatively supercoiled DNA appear to be fully relaxed and relaxed DNA to be fully positively supercoiled. Once the gel is soaked in chloroquine, it is turned 90 " clockwise and is subjected to electrophoresis once again (Figure 3.4). Fully relaxed DNA, which comigrates with nicked DNA in the first dimension, migrates considerably further in the second dimension, as it appears to be positively supercoiled. Conversely, the migration of negatively supercoiled DNA (which now appears to be relaxed) in the second dimension is greatly retarded compared to positively supercoiled DNA. The addition of the second dimension allows positively and negatively supercoiled topoisomers to be readily resolved from one another; intermediate positively supercoiled molecules run in an arc between fully positively supercoiled DNA and the apex band of relaxed DNA, whereas intermediately negatively supercoiled DNA runs on an arc between relaxed and fully negatively supercoiled molecules (Figure 3.4).

Conclusions

When samples that correspond to those shown in the one-dimensional gel in Figure 3.3 are subjected to two-dimensional gel electrophoresis (Figure 3.5), it becomes obvious that all of the

intermediate bands observed at 30 s are positively supercoiled, that a mixed population is seen at 90 s, and that all of the intermediate bands observed at 5 min are negatively supercoiled topoisomers. Therefore, two-dimensional electrophoresis is a useful method for discerning differences in supercoil state. This can be applied to the analysis of reactions such as gyrase relaxation of positive supercoiling and introduction of negative supercoils.

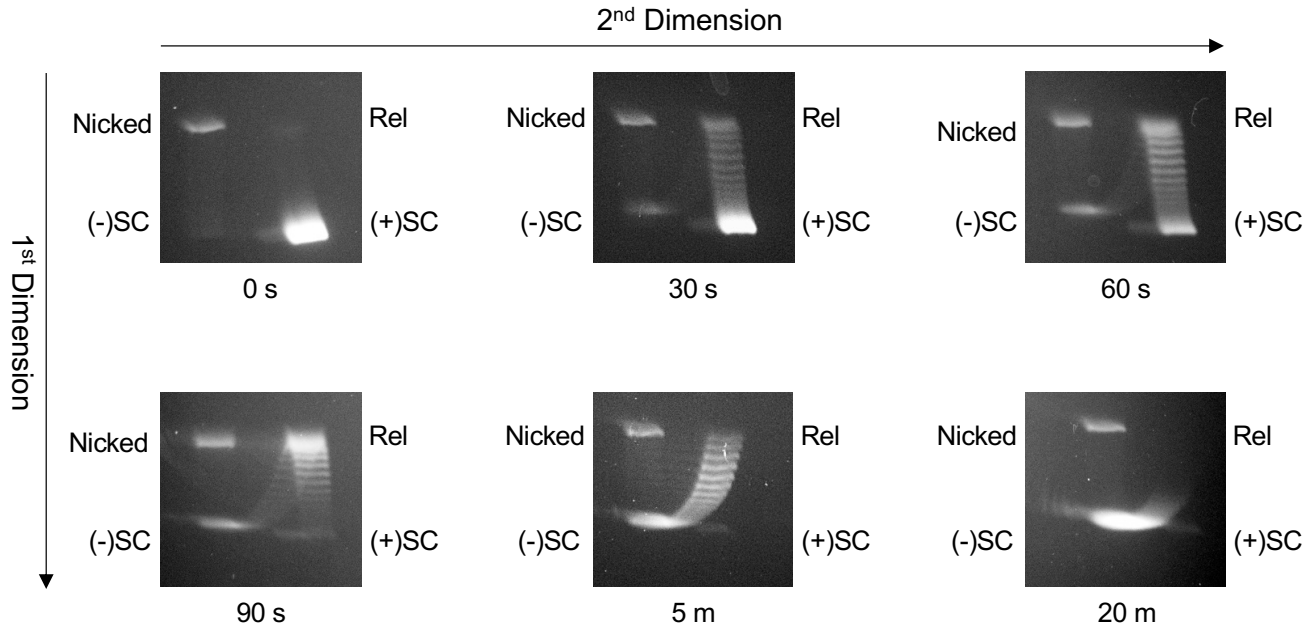

Fig. 3.5 Two-dimensional resolution of negatively and positively supercoiled DNA topoisomers. A time course for the conversion of positively supercoiled plasmid to negatively supercoiled molecules by *S. aureus* gyrase is shown. Reaction products were resolved by two-dimensional agarose gel electrophoresis and DNA bands were visualized by mid-range ultraviolet light following staining with ethidium bromide. Samples at the reaction times shown are from the time course depicted in Fig. 3. The positions of nicked, relaxed (Rel), positively [(+)SC], and negatively supercoiled [(-)SC] DNA are indicated on the gel and methods are described below.

CHAPTER IV

POLYAMINE-CONTAINING ETOPOSIDE DERIVATIVES AS POISONS OF HUMAN TYPE II TOPOISOMERASES: DIFFERENTIAL EFFECTS ON IIα AND IIβ

Introduction

As described in the introduction, etoposide is one of the most widely prescribed anticancer drugs in the world and acts as an interfacial "poison" against human topoisomerase IIα and topoisomerase IIβ. [63, 133, 147 137, 145, 151] The stabilization of cleavage complexes, which ultimately generates un-ligatable DNA ends that need to be repaired by recombination pathways,[11, 12, 37, 63, 64, 133] can overwhelm cells and triggers cell death pathways. [11, 12, 37, 63, 64, 133]

Despite the importance of etoposide as a therapeutic agent for the treatment of cancer, the drug is associated with very serious side effects.[64, 132, 143, 154-156] Among the most dramatic of these are the generation of treatment-related acute myelogenous leukemias (AMLs) that involve rearrangements of the *mixed lineage leukemia* gene at chromosomal band 11q23.[64, 132, 143, 154-156] Although etoposide targets topoisomerase IIα and IIβ, the contributions of the two enzyme isoforms to the therapeutic and leukemogenic properties of the drug are not clear. Circumstantial evidence suggests that topoisomerase IIα may play a more prominent role in killing cancer cells, whereas topoisomerase IIβ may be more important in the induction of leukemic chromosomal translocations.[64, 132, 143, 154-156]

In an effort to minimize off-target effects, the etoposide derivative F14512 was developed (Figure 4.1).[245] This drug, which was in clinical trials for human refractory/relapsing AMLs[266] and canine lymphomas,[267] replaces the C4 sugar moiety of etoposide with a spermine substituent.[245] F14512 (compound **2**) was designed to be taken up preferentially by cancer cells with active polyamine transport, thereby lessening off-target effects in non-cancer cells.[245, 268] Unexpectedly, F14512 turned out to be a much stronger topoisomerase II poison than etoposide.[245, 250] At least in part, this enhanced activity was

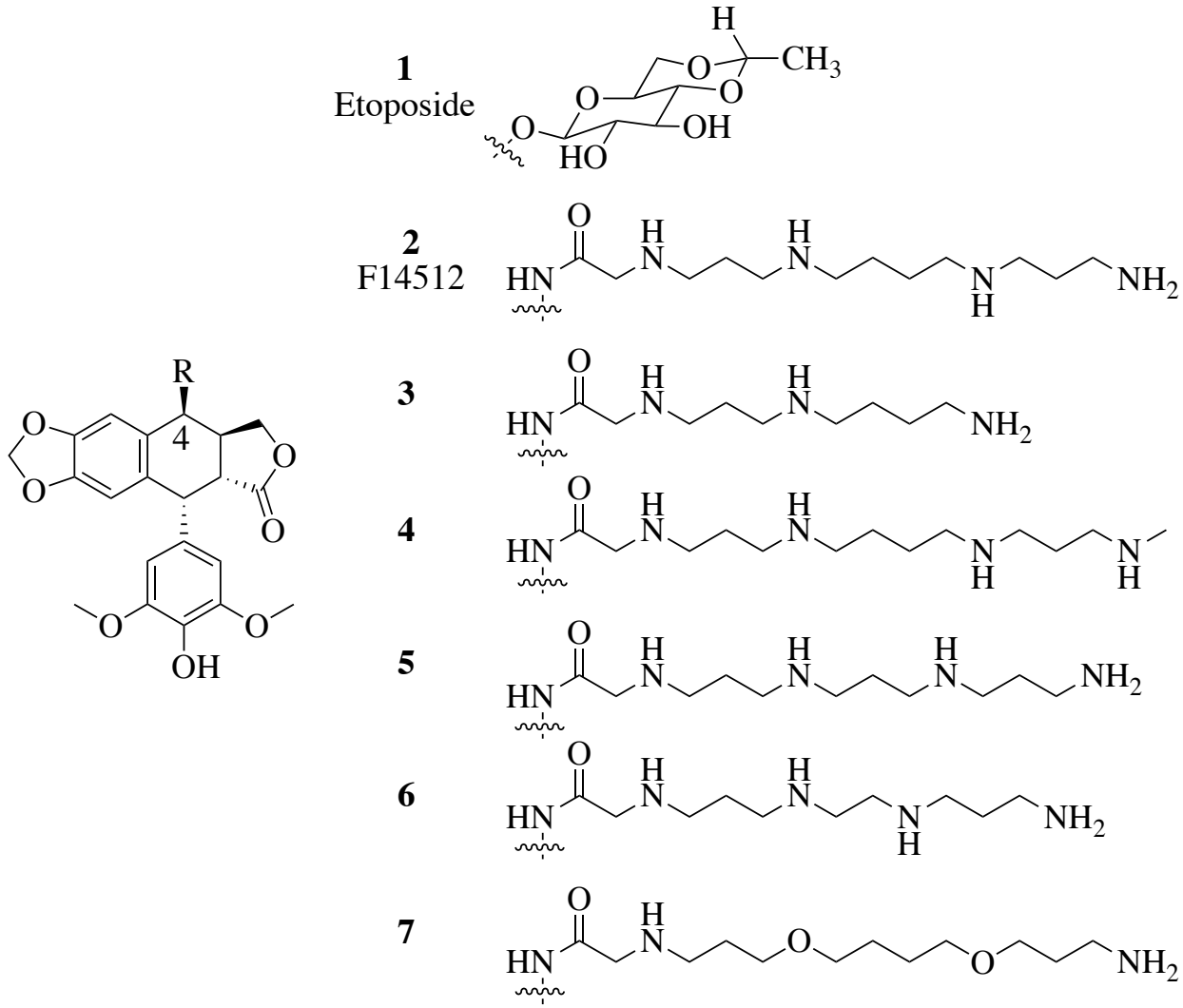

Figure 4.1. Structures of etoposide (1) and etoposide-polyamine hybrids (2-7). Etoposide has a sugar moiety attached to the C4 position of the demethyl-epipodophyllotoxin core, while the hybrids have polyamine substituents at this position.

believed to reflect the fact that the spermine moiety of F14512 interacts with DNA,[245] whereas the parent drug does not.[250, 269, 270] The linkage between the etoposide core and spermine is critical for the enhanced potency and efficacy of F14512.[250] Thus, the increased activity is not due to the additive effects of a topoisomerase II poison and a separate DNA binding agent.

To assess the role of the polyamine moiety in promoting drug activity against type II topoisomerases, Palermo *et al*. synthesized a series of etoposide derivatives with varying C4 polyamine substituents (Figure 4.1).[244] In contrast to NMR studies carried out with F14512 and topoisomerase IIα, which indicated no interactions between the spermine substituent and the enzyme in the binary complex (enzyme•drug),[250] modeling studies suggest that there are important polyamine-topoisomerase II contacts in the ternary complex (*i.e.* enzyme•DNA•drug).[244] Furthermore, based on correlations with activity studies, the authors proposed that these polyamine-enzyme interactions in the ternary cleavage complex contributed to the enhanced ability of the etoposide-polyamine chimeras to poison topoisomerase IIα.[244]

In vitro, F14512 is more potent against topoisomerase IIβ than the α isoform.[245, 250] In contrast, at least in A549 lung cancer cells, it has been suggested that topoisomerase IIα is the primary cytotoxic target of the drug.[271] However, the level of topoisomerase IIα in the A549 cells used in the study were considerably higher than that of topoisomerase IIβ.[271] Consequently, the relative roles of the two enzyme isoforms in the actions of F14512, in lung and other cancer cells, remain an open question.

Results and Discussion

To understand further how hybrid etoposide-polyamine drugs interact with type II topoisomerases and discriminate between the two enzyme isoforms, the abilities of compounds **2**-**7** (Figure 4.1) to enhance DNA cleavage mediated by human topoisomerase IIα and IIβ were assessed and compared to those of etoposide. As seen in Figure 4.2, all of the polyamine-based compounds displayed activities against topoisomerase IIα or IIβ that were equal to or greater than that of etoposide. The ability

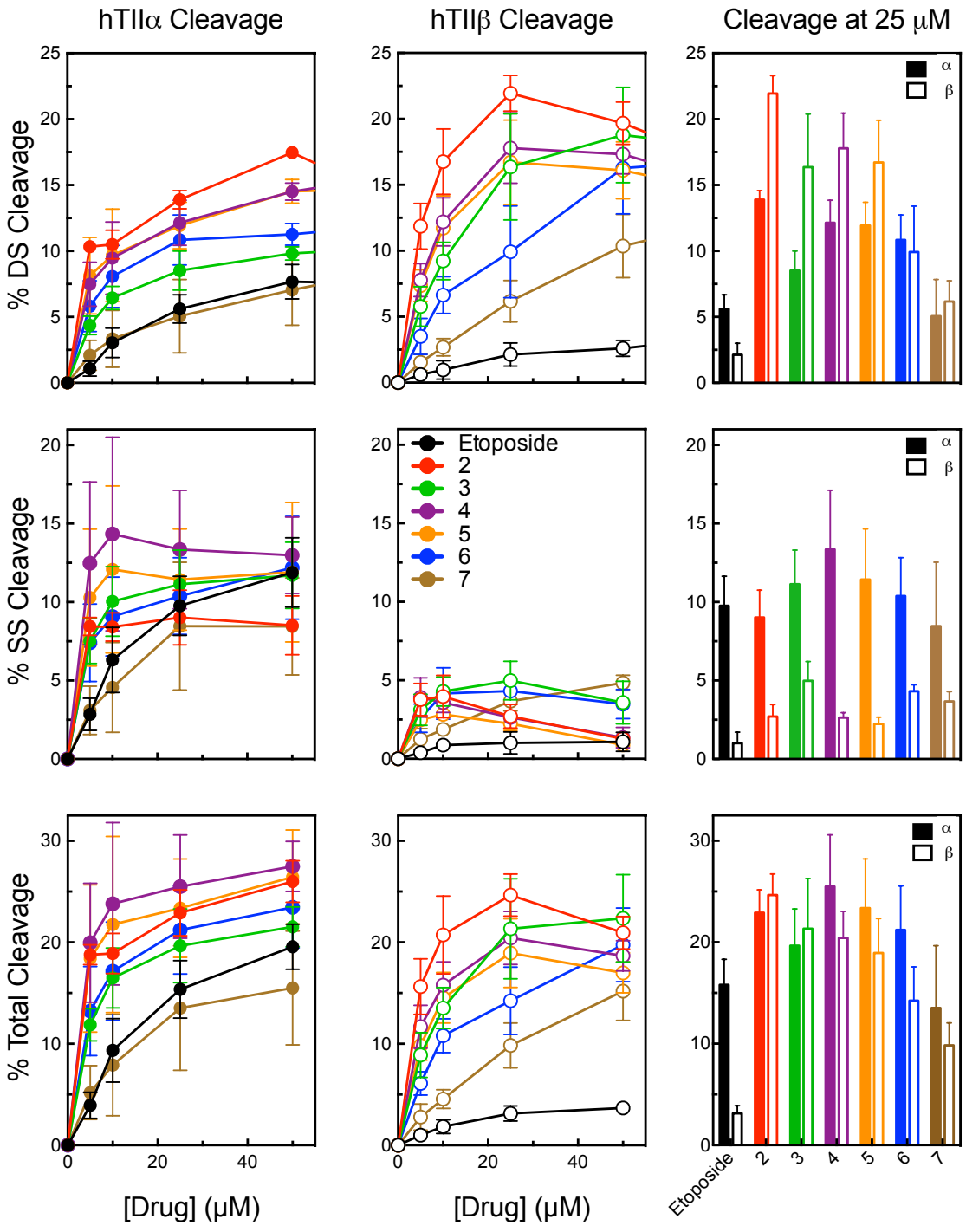

Figure 4.2. Etoposide-polyamine hybrids enhance double- and single-stranded DNA cleavage mediated by human type II topoisomerases. The effect of compounds on DNA cleavage mediated by topoisomerase IIα (hTIIα, closed circles, left panels) and topoisomerase IIβ (hTIIβ, open circles, middle panels) are shown. The percentage of double-stranded (DS, top row), single-stranded (SS, middle row), and total cleavage complexes (DS+SS cleavage, bottom row) is shown for each compound. DNA cleavage levels were calculated relative to a linearized DNA standard and baseline cleavage from reactions with no drug was removed. Bar graphs comparing hTIIα (closed bars) and hTIIβ (open bars) cleavage at 25 μM (right panels) are shown. Error bars represent standard deviations for at least 3 independent experiments.

of compound **2** (F14512), which has the tetramine spermine side-chain, to induce double-stranded breaks was higher than the other derivatives examined, as described previously for topoisomerase IIα.[245, 244, 250] The compounds displayed a modest decrease in their ability to induce enzyme-mediated DNA cleavage when the side-chain was substituted by the triamine spermidine (**3**), or by spermine that was methylated on the terminal amine (**4**) or that contained shortened methylene linkers between the inner amino groups (**5** or **6**). The lowest activity was seen with compound **7**, in which the second and third amino groups were replaced with oxygens. Thus, the number of amines and their spacing all appear to contribute to the activity of this series of etoposide-polyamine hybrids.

Furthermore, as reported with compound **2**,[244, 250] the etoposide-polyamine hybrids generally displayed a greater ability to induce double-stranded DNA breaks with topoisomerase IIβ than topoisomerase IIα (Figure 4.2, top row). This is despite the fact that the parent drug etoposide induces higher levels of double-stranded breaks with the α isoform.[244, 250] To aid comparisons between the two enzyme isoforms, the bar graph (Figure 4.2, top row, right) shows the induction of double-stranded DNA cleavage at 25 μM drug. This is the maximum concentration of compounds at which multiple cleavage events per plasmid were not observed. Similar effects were seen for the relative potencies of etoposide-polyamine hybrids as determined by levels required to induce 10% enzyme-mediated double-stranded DNA breaks (Table 4.1). All the compounds were considerably more potent than etoposide and, in general, were more potent against topoisomerase IIβ than IIα.

In contrast to results with double-stranded DNA cleavage, etoposide and the derivatives all induced considerably higher levels of single-stranded DNA breaks with topoisomerase IIα than with IIβ (Figure 4.2 middle row). In general, the etoposide-polyamine hybrids induced levels of single-stranded breaks that were similar to or higher than that of the parent drug. However, with the exception of compound **7**, all of the hybrid molecules maintained lower single-stranded to double-stranded ratios (*i.e.,* they induced higher

Compound	Concentration (μM) Required to Induce 10% Cleavage	
	Topoisomerase IIα	Topoisomerase IIβ
Etoposide	>100	>100
2	4.8	4.3
3	54.1	11
4	13.2	7.5
5	12.2	8.1
6	20.5	25.3
7	98.9	49.9

Table 4.1. Relative potencies of etoposide-polyamine hybrids. Values are reported for both hTIIα and hTIIβ.

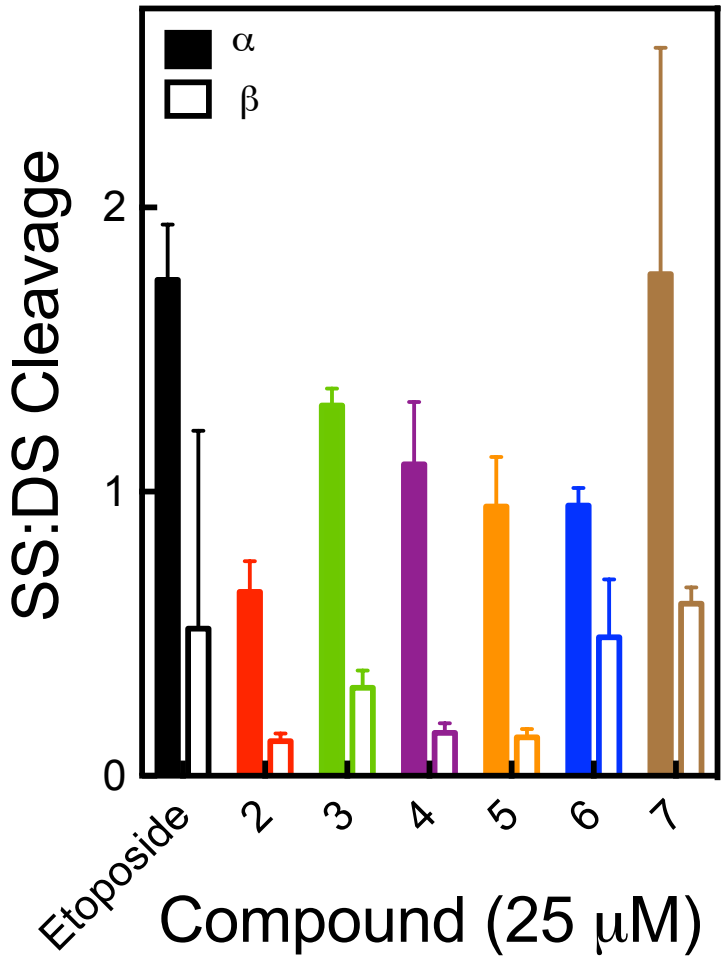

Figure 4.3. Ratio of single-stranded to double-stranded DNA cleavage induced by etoposide-polyamine hybrids. The ratio of single-stranded (SS) to double-stranded (DS) cleavage at 25 μM drug was calculated for human topoisomerase IIα (hTIIα, closed bars) and topoisomerase IIβ (hTIIβ, open bars). Error bars represent standard deviations for at least 3 independent experiments.

levels of double- as compared to single-stranded DNA breaks) than etoposide with both of the topoisomerase II isoforms (Figure 4.3).

Taking both double- and single-stranded cleavage into account, the total percentage of the DNA molecules that are in cleavage complexes induced by the etoposide-polyamine hybrids were similar or higher than that seen for etoposide with topoisomerase IIα and considerably higher for topoisomerase IIβ (Figure 4.2 bottom row).

Effects of etoposide-polyamine hybrids on DNA cleavage complex stability

Etoposide and F14512 increase topoisomerase II-mediated DNA scission by stabilizing cleavage complexes. This is reflected as an inhibition of the ability of the enzyme to religate cleaved DNA[137, 250] and an enhanced persistence of DNA cleavage complexes.[250, 272] This was also the case for all of the etoposide-polyamine hybrids examined. As seen in Figure 4.4, they inhibited religation to an extent similar to that of etoposide. Furthermore, most of the cleavage complexes formed in the presence of the etoposide-polyamine hybrids persisted to a similar extent as etoposide following dilution with drug-free buffer (Figure 4.5). As documented previously,[250] cleavage complexes formed with topoisomerase IIα were more stable than those formed with the β isoform.

The abilities of etoposide-polyamine hybrids to induce DNA cleavage were generally greater than that of etoposide with topoisomerase IIα. However, the activities of these compounds against topoisomerase IIβ were dramatically higher than that of the parent compound (Table 4.2). Whereas the total levels of DNA cleavage for the hybrid compounds ranged from ~0.9 to 1.7 times that generated by etoposide with topoisomerase IIα, these cleavage ratios were ~3-8 times higher with topoisomerase IIβ (Table 4.2).

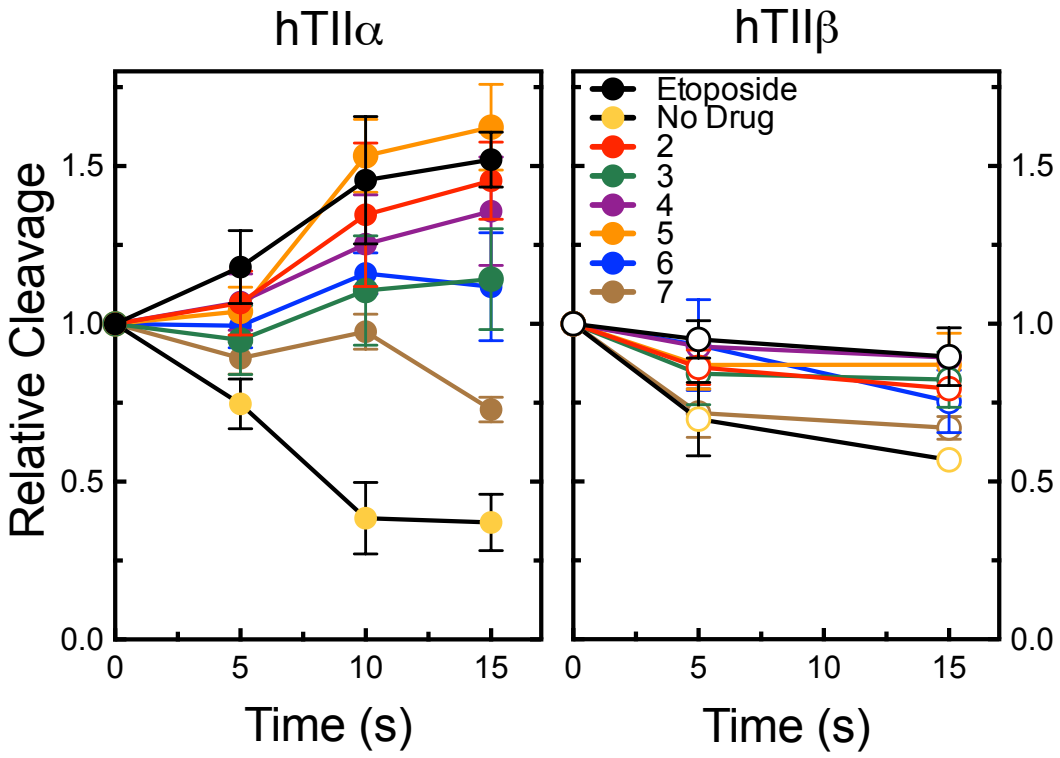

Figure 4.4. Effects of etoposide-polyamine hybrids on DNA religation mediated by human topoisomerase IIα (hTIIα, left panel, closed circles) and IIβ (hTIIβ, right panel, open circles). Reactions were performed in the absence of drug (yellow) or in the presence of 100 μM etoposide with topoisomerase IIα, 25 μM etoposide with topoisomerase IIβ , or compounds **2**-**7** (25 μM) with either isoform. The level of DNA cleavage was set to 1.0 at time zero to facilitate direct comparisons and religation is expressed as the loss of double-stranded breaks. Error bars represent the standard deviations of at least 3 independent experiments.

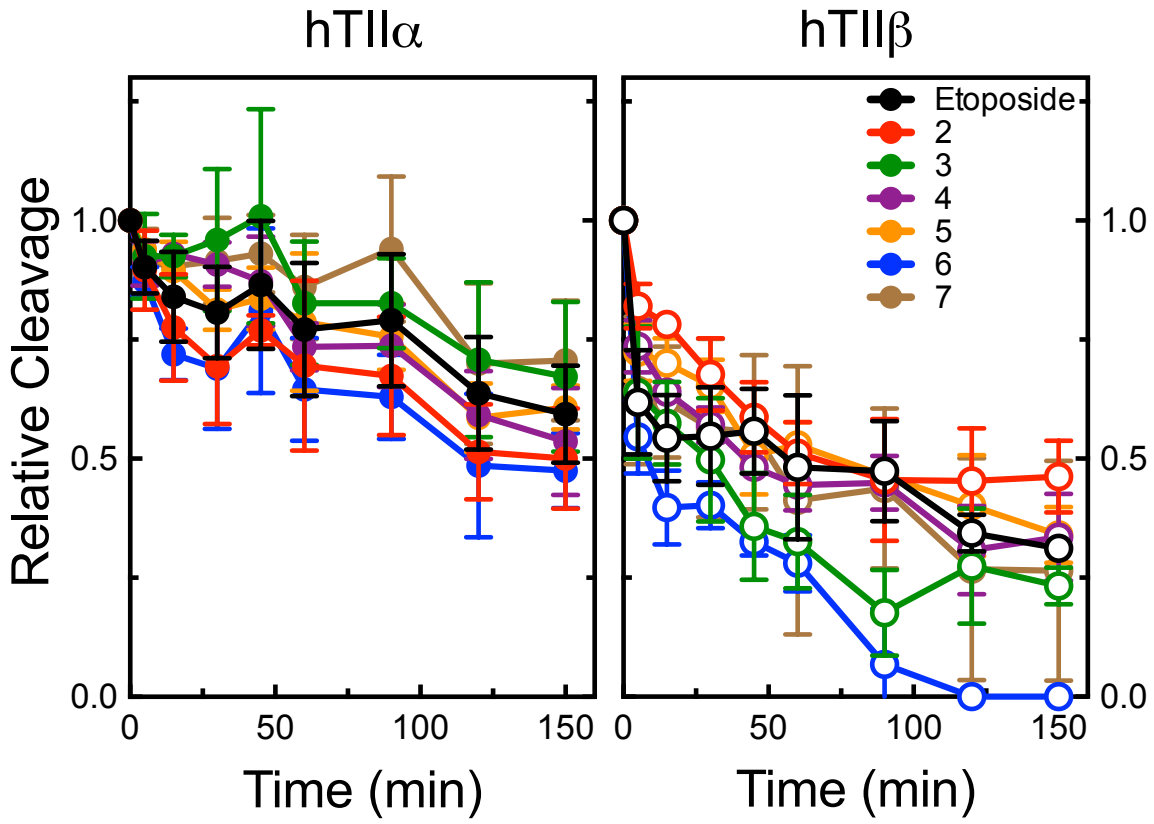

Figure 4.5. Persistence of DNA cleavage complexes formed in the presence of etoposide-polyamine hybrids. Results are shown for human topoisomerase IIα (hTIIα, left panel, closed circles) and IIβ (hTIIβ, right panel, open circles). Reactions were performed in the presence of 100 μM etoposide with topoisomerase IIα, 50 μM etoposide with topoisomerase IIβ , or compounds **2**-**7** (25 μM) with either isoform. Cleavage at time zero was set to 1.0 to facilitate direct comparisons. Reactions were allowed to reach cleavage-ligation equilibrium, diluted, and persistence was measured by assessing the loss of double-stranded breaks following dilution with drug-free reaction buffer. Error bars represent the standard deviations of at least 3 independent experiments.

	Topoisomerase IIα			Topoisomerase IIβ		
	DS Cleavage	SS Cleavage	Total Cleavage	DS Cleavage	SS Cleavage	Total Cleavage
Etoposide	1.00	1.00	1.00	1.00	1.00	1.00
2	2.48	0.92	1.49	10.31	2.68	7.85
3	1.52	1.14	1.28	7.69	4.92	6.80
4	2.16	1.37	1.66	8.36	2.61	6.51
5	2.13	1.17	1.52	7.85	2.21	6.03
6	1.93	1.06	1.38	4.66	4.27	4.54
7	0.90	0.87	0.88	2.90	3.63	3.13

Table 4.2. Relative activities of etoposide-polyamine hybrids compared to etoposide. The fold enhancement of human topoisomerase IIα- and topoisomerase IIβ-mediated cleavage by each drug at 25 μM was calculated. The percentage of double-stranded (DS), single-stranded (SS), or total cleavage induced by the derivative was divided by that induced upon etoposide treatment. Fold enhancement was compared to the parent drug and the enhancement value for etoposide was therefore set to 1.0. Results are indicative of at least 3 independent experiments.

Modeling of the etoposide-polyamine hybrid interactions with human topoisomerase IIα and IIβ

To provide potential insight into the major differences in drug activity against the enzyme isoforms, the etoposide-polyamine hybrids were modeled into the DNA cleavage/ligation active sites of topoisomerase IIα and IIβ. Crystal structures obtained from the Protein Data Bank for the α (5GWK) and β (3QX3) isoforms were employed for these docking studies.[145, 251]

Whereas the sugar moiety of etoposide is surrounded by a hydrophobic pocket comprised of three methionine residues in topoisomerase IIα, one of these amino acids (proximal to the C6 of the sugar) is a polar glutamine (Gln778) residue in the β isoform.[145, 251] On the basis of genetic studies, alterations in this amino acid affect biological sensitivity to etoposide.[273] In the original data coordinates of the topoisomerase IIβ structure, Gln778 adopts two different conformations. Specifically, the side chain of the residue can point toward either etoposide or the protein. In the latter case, Gln778 points away from the bound ligand. Based on the highest occupancy of Gln778 in the crystal structure, we selected a starting conformation for docking in which the side chain of Gln778 is flipped away from the drug core, thus forming no interactions with etoposide.

As seen in Figure 4.6, all of the etoposide-polyamine hybrids dock into the same active site pocket in the two enzyme isoforms. In our induced fit docking calculations with topoisomerase IIβ (Figure 4.7, bottom), Gln778 (which is a polar residue) regularly flips to form stabilizing interactions either with the carbonyl group of the polyamine chain (panel C, H-bond length from 1.7-2.6 Å), or with the D-ring ether oxygen of the epipodophyllotoxin core (panel D, H-bond length from 1.9-2.5 Å). This implies that Gln778 changes its starting conformation to form electrostatic interactions with the etoposide-polyamine hybrid. In contrast, the corresponding methionine (Met762) in topoisomerase IIα (which is a non-polar residue) is unable to form electrostatic interactions with the ligand (Figure 4.7, top). Although this methionine can adopt different conformations (compare panels A and B), Met762 never forms favorable interactions with the bound ligand. In our modeling studies, the methionine remained 3.5-9 Å away from the bound ligand.

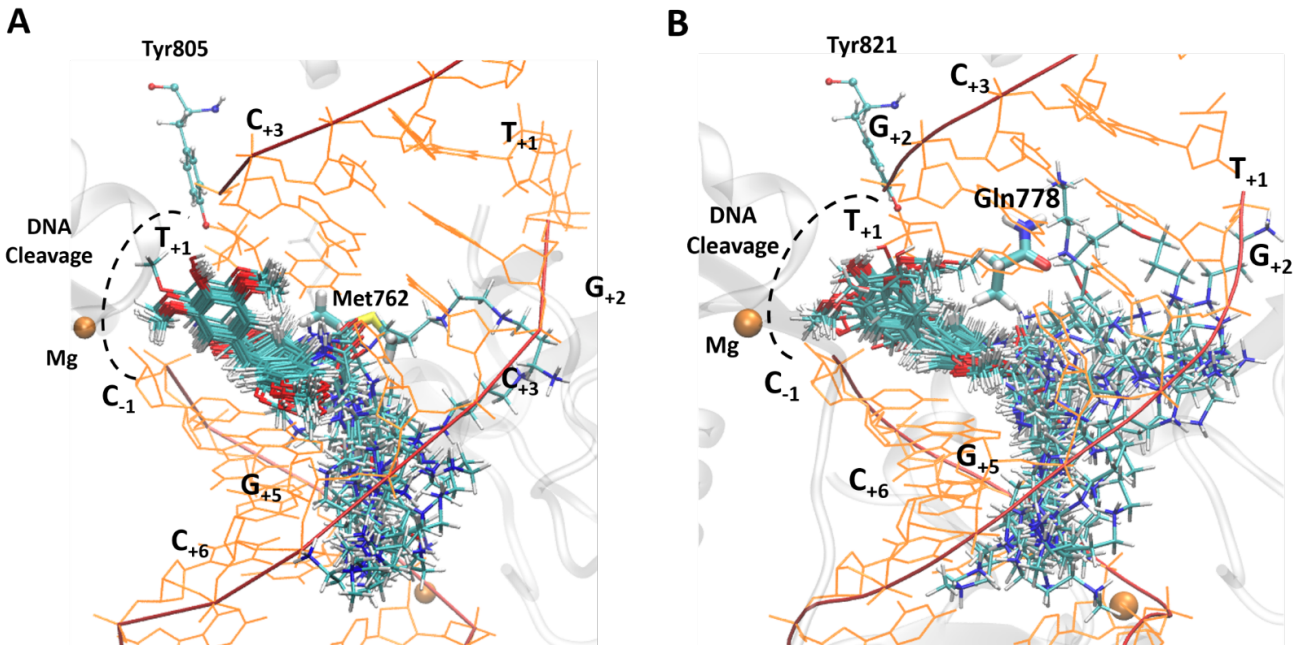

Figure 4.6. Superposition of all of the docking poses of F14512 (2) and of compounds 3–7 with topoisomerase IIα (panel A) and IIβ (panel B). The 4'-demethylepipodophyllotoxin core is docked in the same position as for etoposide, with the polyamine chains binding to the major groove of the DNA.

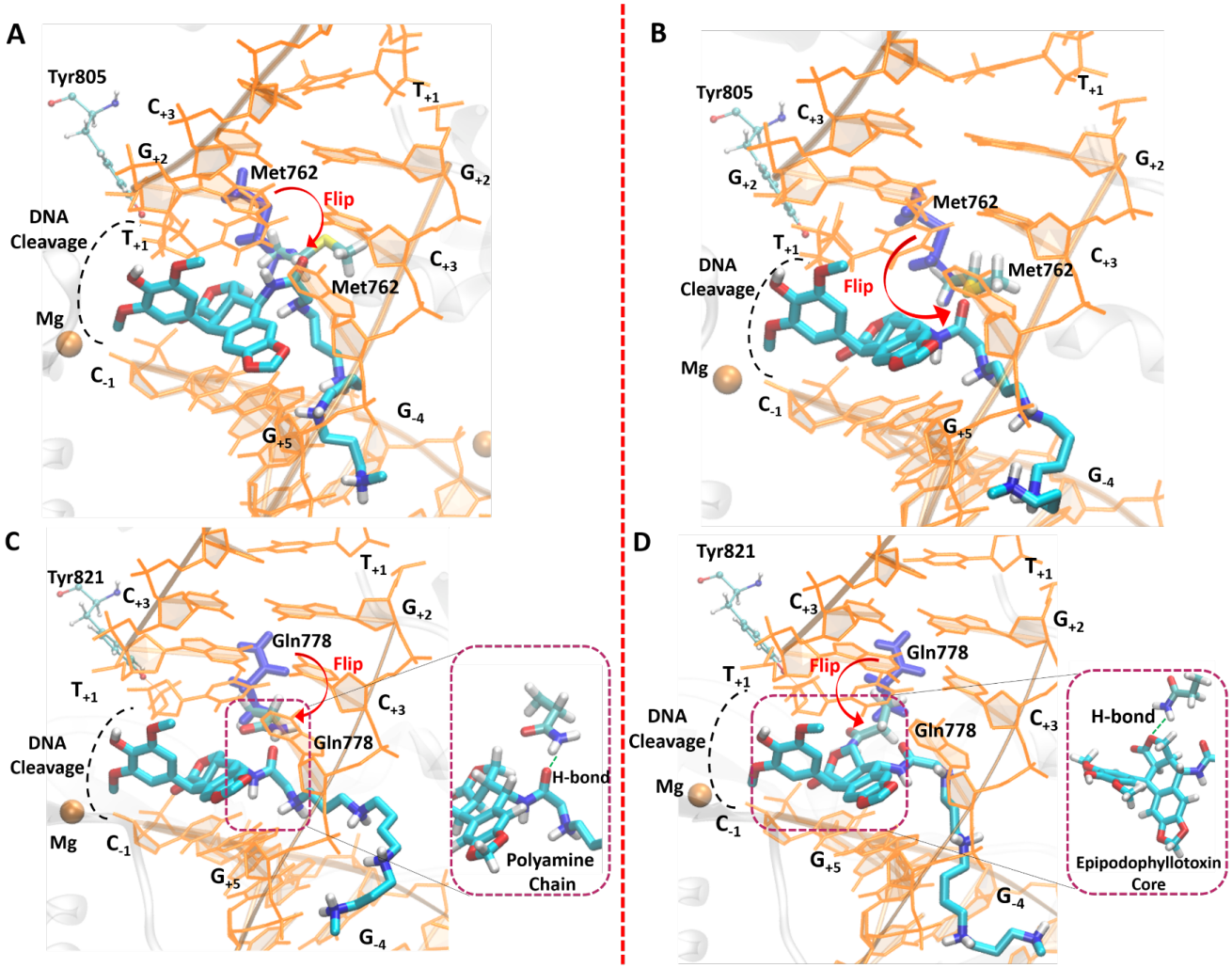

Figure 4.7. Molecular modeling of compound 4 in the DNA cleavage/religation active sites of topoisomerase IIα and IIβ. Compound **4** was chosen because it is potent and efficacious against both enzyme isoforms. It is shown in the active site of topoisomerase IIα (panels A and B) with the different conformations of Met762 and in the active site of topoisomerase IIβ (panels C and D) with the different conformations of Gln778. Interactions of the drug with Gln778 in topoisomerase IIβ are shown with the residue interacting with the carboxyl group of the polyamine tail of **4** (panel C) or with the ether oxygen of the epipodophyllotoxin core (panel D).

The differential effects of the glutamine versus methionine residue likely contribute to the fact that the etoposide-polyamine hybrids induce higher levels of DNA cleavage with the topoisomerase IIβ over the α isoform, especially when compared to the parent drug etoposide.

Finally, the amino groups of the polyamine conjugates of compounds **2**-**6** all appear to form stable hydrogen bonds with several DNA bases (Figure 4.8 A). However, modeling studies suggest that the oxygen atoms in the polyamine tail of compound **7** are unable to form comparable hydrogen bonds (Figure 4.8 B). This might explain the lower DNA cleavage activity observed with this compound (with both the α and β isoforms) and the fact that its DNA cleavage profile more closely resembles that of etoposide than the other polyamine hybrids.

Conclusions

In conclusion, etoposide derivatives in which the C4 sugar moiety is replaced with a variety of polyamine tails induce higher levels of DNA cleavage with human topoisomerase IIα and IIβ than does the parent drug. These etoposide-polyamine hybrids displayed higher levels of activity against the β isoform, especially when compared to etoposide. Molecular docking studies suggest that this enhanced specificity may result from interactions with a glutamine residue that is present in topoisomerase IIβ, but not in topoisomerase IIα. The results of our enzymology and modeling studies form the basis of a testable hypothesis for the design of future drugs[274] with enhanced specificity toward a single isoform of human topoisomerase II.

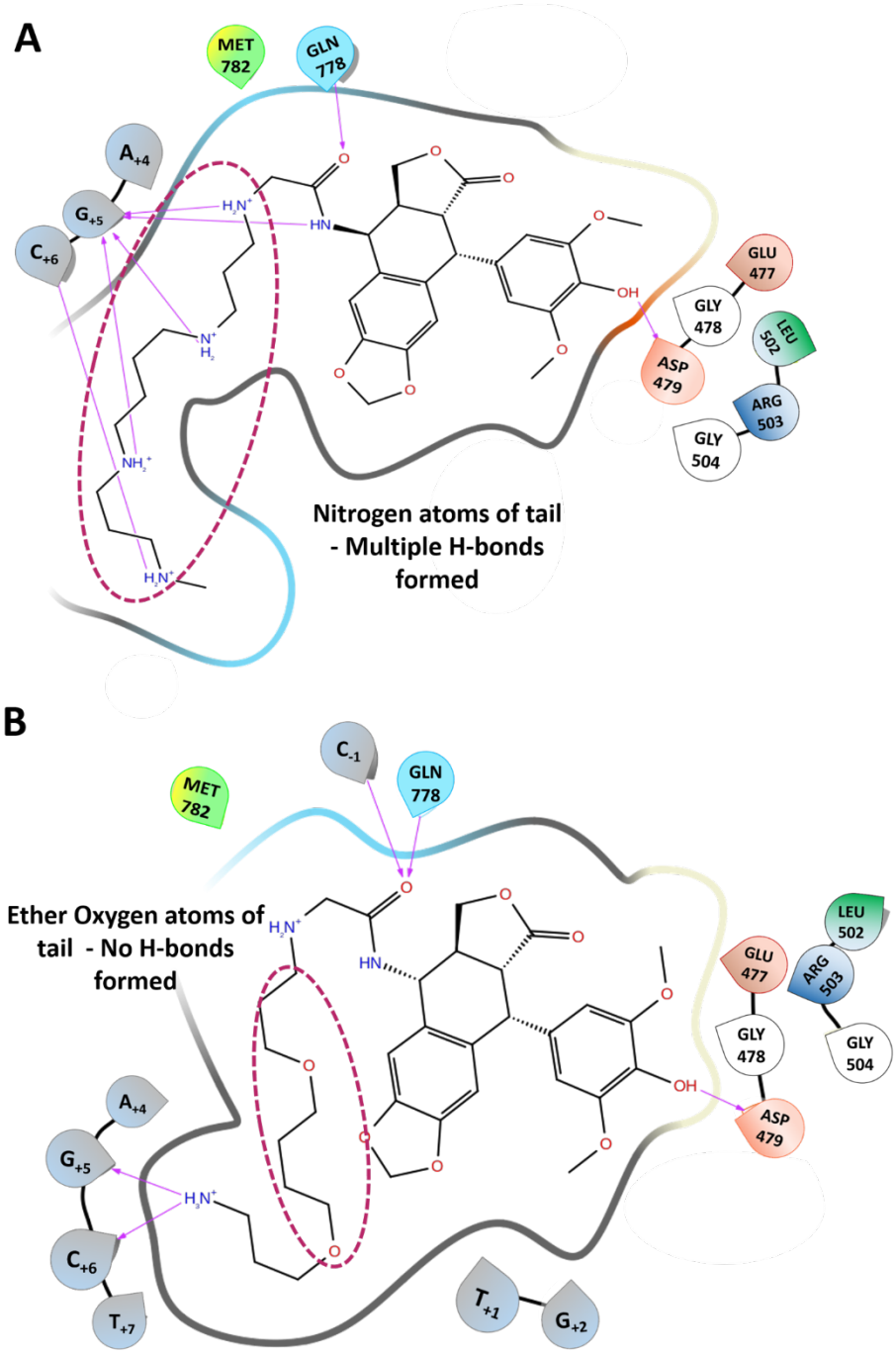

Figure 4.8. Ligand interaction diagrams for docking of etoposide-polyamine hybrids with topoisomerase IIβ. Panel A shows that the nitrogen atoms in the polyamine chain of compound **4** can form H-bonds with the indicated DNA bases (pink arrows). In contrast, panel B shows that the ether atoms of compound **7** are unable to form any favorable interactions with the DNA bases.

CHAPTER V

BIMODAL ACTIONS OF A NAPHTHYRIDONE/AMINOPIPERADINE-BASED ANTIBACTERIAL THAT TARGETS GYRASE AND TOPOISOMERASE IV

Introduction

In addition to their essential cellular functions,[9, 12, 95] the bacterial type II topoisomerases, gyrase and topoisomerase IV, are the targets for fluoroquinolone antibacterials.[39, 48, 111, 169, 170, 173, 222, 275] These broad-spectrum drugs are among the most widely prescribed antibacterials worldwide,[48, 169, 173, 177] and act by stabilizing covalent protein-cleaved DNA complexes that are generated during the catalytic cycles of the type II enzymes.[37, 39, 48, 110, 275] Clinically relevant fluoroquinolones interact with the bacterial type II topoisomerases through a water-metal ion bridge.[48, 180, 200, 202-204] The C3/C4 ketoacid of the fluoroquinolone skeleton chelates a divalent metal ion, which is coordinated by four water molecules. Two of these water molecules interact with a highly conserved serine and an acidic residue that is located four amino acids upstream in the GyrA or GrlA/ParC subunits of gyrase or topoisomerase IV (Gram-positive/Gram-negative), respectively.[180]

Despite the importance of fluoroquinolones in the treatment of bacterial infections, their overuse has contributed to a rise in resistance that spans their entire spectrum of clinical usage.[48, 111, 169, 170, 173] This resistance is most often associated with mutations in the two amino acid residues that anchor the water-metal ion bridge.[48, 111, 169, 170, 173] Given the broad clinical applications of fluoroquinolones, it is critical to discover new drug classes that can supplement their use in the clinic. One approach is to develop novel drugs that act on validated targets, such as gyrase and topoisomerase IV, but interact differently with the enzymes. This approach has led to the development of compounds known as “novel bacterial topoisomerase inhibitors” (NBTIs) (Figure 5.1).[111, 181, 226, 275]

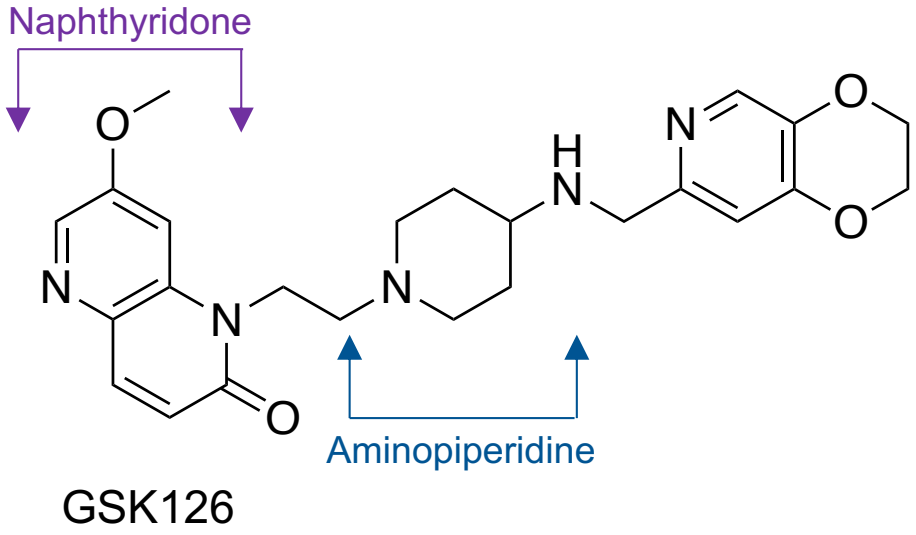

Figure 5.1. Structure of the NBTI GSK126. The naphthyridone (purple) and aminopiperidine (blue) moieties are indicated.

Several NBTIs display activity against clinically relevant bacterial species.[111, 181, 221, 222, 228-233] However, most show poor activity against *M. tuberculosis*.[237] GSK126 (Figure 5.1), which is a naphthyridone/aminopiperidine-based NBTI, was identified in a screen as having moderate activity against the bacterium.[237] This discovery led to a subset of NBTIs that were derived from GSK126 and displayed high activity against *M. tuberculosis* in culture and in mouse infection models.[237] Compounds in this subclass are known as *M. tuberculosis* gyrase inhibitors (MGIs). Whereas a recent study characterized the mechanistic basis for the actions of MGIs against *M. tuberculosis* gyrase,[234] relatively little is known about the actions of the parent NBTI class against gyrase and topoisomerase IV.[111, 222, 275]

In order to address this important issue, we analyzed the actions of GSK126 against a variety of bacterial type II topoisomerases, including gyrase from *M. tuberculosis*, and gyrase and topoisomerase IV from *B. anthracis* and *E. coli*. This NBTI was chosen for initial studies to afford direct comparisons with the MGIs. Results indicate that GSK126 has a broader spectrum of activity against gyrase and topoisomerase IV than the MGIs, but displays similar mechanistic characteristics. GSK126 acted in a bimodal fashion; it was a potent inhibitor of gyrase-catalyzed DNA supercoiling and topoisomerase IV-catalyzed decatenation and also induced single-stranded DNA cleavage (i.e., acted as a topoisomerase poison) with both enzymes. However, the relative importance of these two modes of NBTI action (inhibiting vs. poisoning) appears to differ among bacterial species. Thus, we propose that the mechanistic basis for the antibacterial properties of NBTIs is bimodal in nature.

Results and Discussion

MGIs are the best-characterized members of the naphthyridone/aminopiperidine-based NBTI drug class.[234, 237] However, their selection for activity against *M. tuberculosis* resulted in a group of compounds with narrow specificity.[234] This narrow specificity range raises questions regarding the spectrum of action

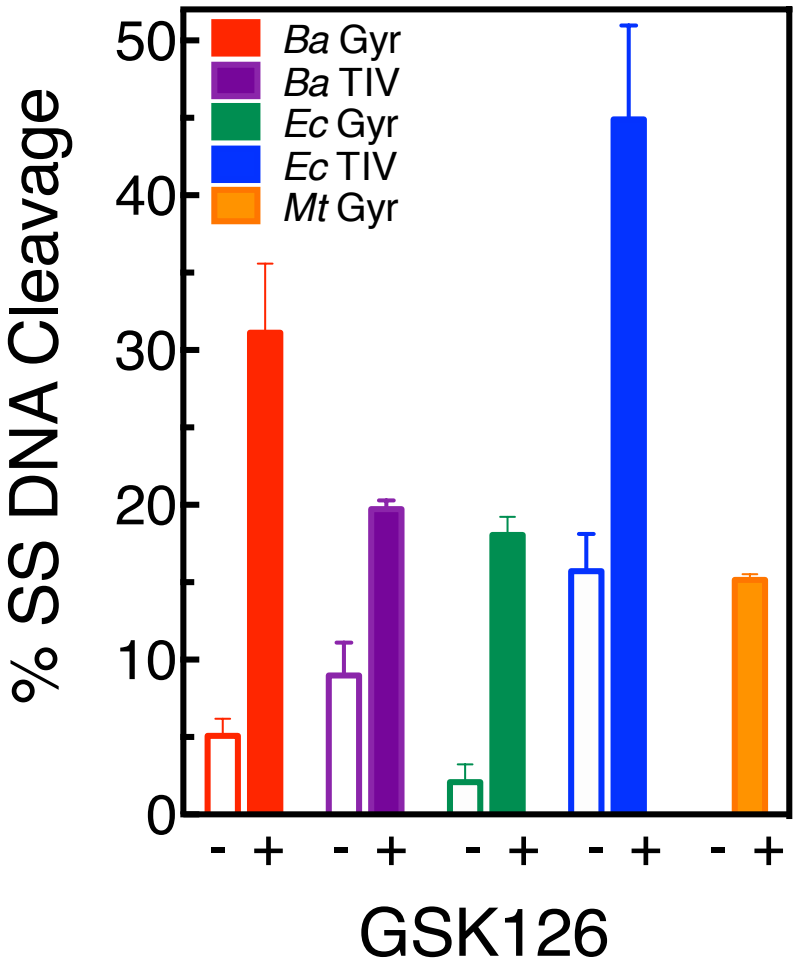

Figure 5.2. GSK126 displays a broad spectrum of DNA cleavage enhancement against gyrase and topoisomerase IV. The effects of GSK126 (solid bars) on single-stranded DNA cleavage mediated by gyrase and topoisomerase IV are shown for the NBTI concentration that generated the highest levels of single-stranded breaks (see Figures 4 and 9). Data are shown for *B. anthracis* gyrase (*Ba* Gyr, red, 0.5 μM GSK126) and topoisomerase IV (*Ba* TIV, purple, 0.5 μM), *E. coli* gyrase (*Ec* Gyr, green, 15 μM) and topoisomerase IV (*Ec* TIV, blue, 1 μM), and *M. tuberculosis* gyrase (*Mt* Gyr, orange, 10 μM) are shown. The corresponding single-stranded DNA cleavage in the absence of GSK126 is shown as empty bars. Error bars represent the SD (standard deviation) of at least three independent experiments.

of the parent NBTI series and whether the mechanism of the naphthyridone/aminopiperidine-based compounds are translatable across species.

Therefore, the ability of GSK126 (the parent compound of MGIs) to induce enzyme-mediated single-stranded breaks was examined against gyrase and topoisomerase IV from a variety of Gram-negative and Gram-positive bacteria (Figure 5.2). In contrast to MGIs, the NBTI displayed a much broader spectrum of activity. The compound showed activity against all the enzymes examined, including those from *B. anthracis, E. coli,* and *M. tuberculosis*. In order to assess the basis for the actions of GSK126 against bacterial type II topoisomerases, we characterized its activity against all the enzymes shown in Figure 5.2. This allowed us to characterize the actions of a NBTI against Gram-negative and Gram-positive gyrase and topoisomerase IV as well as *M. tuberculosis* gyrase (this species does not encode topoisomerase IV[276]) to afford direct comparisons to MGIs.

Effects of GSK126 on the DNA Supercoiling Activity of Wild-type and Fluoroquinolone-resistant Gyrase

NBTIs have been shown to inhibit the catalytic function of gyrase, but it is not known how enzyme inhibition vs. the ability of NBTIs to enhance DNA cleavage affects drug-induced cell death. Therefore, the effects of GSK126 on DNA supercoiling catalyzed by *B. anthracis*, *E. coli*, and *M. tuberculosis* gyrase were examined (Figure 5.3). The NBTI was a potent catalytic inhibitor of the *B. anthracis* and *E. coli* enzymes, but displayed lower activity against *M. tuberculosis* gyrase (IC_{50} ~ 0.4 μM and 2 μM compared to IC_{50} ~ 75 μM, respectively). In addition, GSK126 was able to decrease the activity of the latter enzyme by only 60%. Furthermore, the compound displayed a variable ability to overcome the effects of the common clinical fluoroquinolone resistance mutations (all are at corresponding serine residues) in *B. anthracis* ($GyrA^{S85L}$), *E. coli* ($GyrA^{S83L}$), and *M. tuberculosis* ($GyrA^{A90V}$) gyrase (Figure 5.3). Whereas GSK126 maintained activity against all three mutant enzymes, its potency dropped considerably against the *B. anthracis* and *M. tuberculosis* gyrase mutants (compared to the wild-type enzyme). In contrast, the

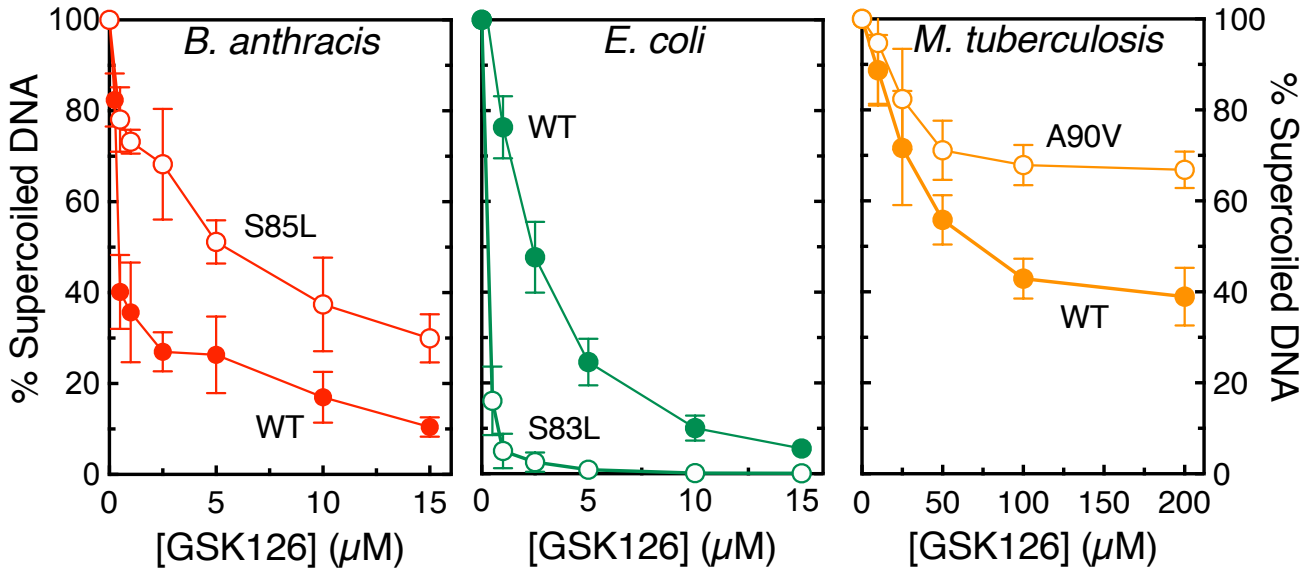

Species	WT IC_{50} (μM)	Mutant IC_{50} (μM)
B. anthracis	~0.4	~3.7 (S85L)
E. coli	~2.0	<0.5 (S83L)
M. tuberculosis	~75	>200 (A90V)

Figure 5.3. GSK126 inhibits DNA supercoiling catalyzed by wild-type (WT) and fluoroquinolone-resistant gyrase. The effects of GSK126 on the supercoiling of relaxed DNA by WT (filled circles) and fluoroquinolone-resistant (empty circles) *B. anthracis* WT and $GyrA^{S85L}$ (top left, red), *E. coli* WT and $GyrA^{S83L}$ (top middle, green), and *M. tuberculosis* WT and $GyrA^{A90V}$ (top left, orange) gyrase are shown. Error bars represent the SD of at least three independent experiments. The bottom panel shows a table of IC_{50} values.

compound was 5-10-fold more potent against the *E. coli* gyrase that harbored the fluoroquinolone resistance mutation.

Effects of GSK126 on the DNA Cleavage Activity of Wild-type and Fluoroquinolone-resistant Gyrase

In contrast to studies on the inhibition of gyrase supercoiling, [221, 228-230, 232, 233, 238, 277-279] relatively little is known about how NBTIs affect gyrase-mediated DNA cleavage. [181, 221, 228, 234, 235] Therefore, the effects of GSK126 on DNA cleavage mediated by wild-type gyrase from *B. anthracis, E. coli,* and *M. tuberculosis* was examined (Figure 5.4). Paralleling previous results for MGIs and other classes of NBTIs,[181, 221, 234, 235] GSK126 displayed a potent ability to induce single-stranded DNA breaks generated by all three enzymes [EC_{50} (concentration of GSK126 required to obtain 50% maximal cleavage) values ranged from sub-micromolar to ~1 μM], but displayed no ability to induce double-stranded breaks.

In contrast to the concentration dependence for the enhancement of single-stranded DNA breaks with *E. coli* and *M. tuberculosis* gyrase, GSK126 induced a sharp increase in DNA cleavage mediated by the *B. anthracis* enzyme (Figure 5.4). This presumably reflects a strong binding of the NBTI to the *B. anthracis* gyrase-DNA complex, which is consistent with the sharp decline in supercoiling rates with this enzyme in the presence of GSK126 (Figure 5.3).

Although NBTIs and fluoroquinolones both bind in the active site of gyrase in the cleavage complex, they do not interact with the same amino acid residues. However, very little is known about how the presence of common fluoroquinolone resistance mutations in gyrase affect the ability of NBTIs to induce enzyme-mediated DNA cleavage.[234] As shown in Figure 5.4, GSK126 was slightly more efficacious against *B. anthracis* $GyrA^{S85L}$ and induced substantially more single-stranded DNA cleavage against *M. tuberculosis* $GyrA^{A90V}$ gyrase than their wild-type counterparts. In contrast, GSK126 displayed no ability to enhance DNA cleavage mediated by *E. coli* $GyrA^{S83L}$ gyrase (control experiments carried out in the presence of Ca^{2+} demonstrate that $GyrA^{S83L}$ displays wild-type levels of baseline DNA cleavage, not

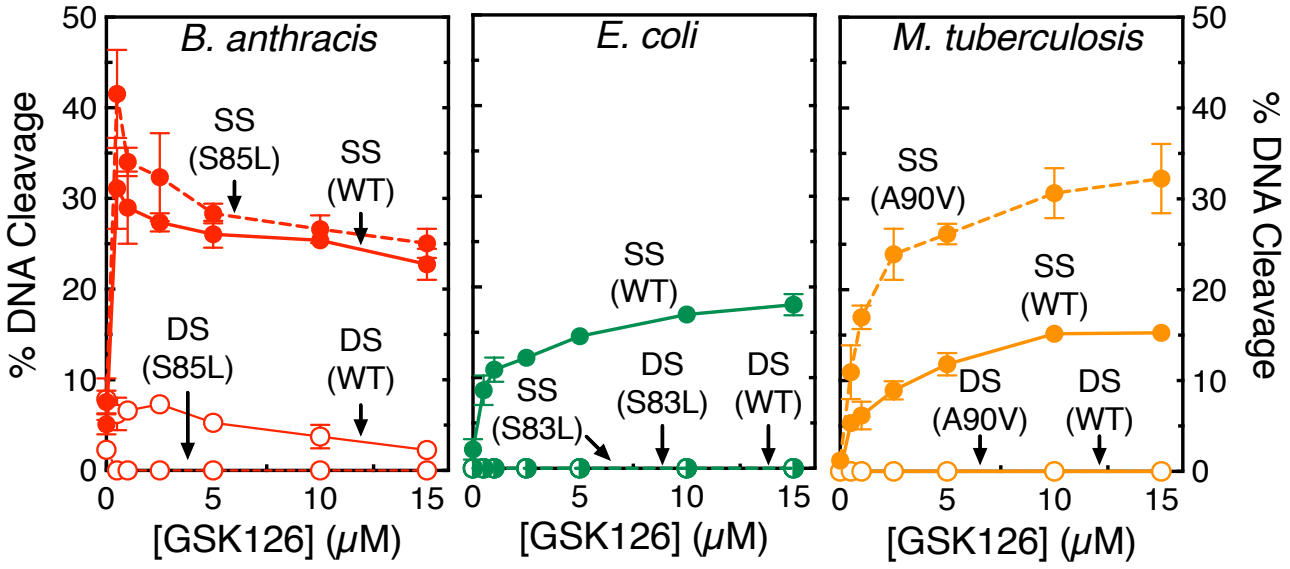

Figure 5.4. Effects of GSK126 on DNA cleavage mediated by wild-type (WT) and fluoroquinolone-resistant gyrase. The effects of GSK126 on single-stranded (SS, filled circles) and double-stranded (DS, empty circles) DNA cleavage mediated by WT (solid line) and fluoroquinolone-resistant (dashed line) *B. anthracis* WT and GyrA^{S85L} (left, red), *E. coli* WT and GyrA^{S83L} (middle, green), and *M. tuberculosis* WT and GyrA^{A90V} (right, orange) gyrase are shown. Some of the data shown for *M. tuberculosis* WT and GyrA^{A90V} gyrase are from Gibson et. al.[30] Error bars represent the SD of at least three independent experiments.

shown). This is the first reported instance in which DNA cleavage enhancement by a NBTI or related compound has failed to overcome resistance induced by a fluoroquinolone-resistant mutation in gyrase.

GSK126 Enhances only Single-stranded DNA Cleavage Mediated by Gyrase and Suppresses Enzyme-generated Double-stranded DNA Breaks

To further assess the ability of GSK126 to induce gyrase-mediated single- vs. double-stranded breaks with the wild-type enzyme, DNA cleavage reactions were carried out at NBTI concentrations as high as 200 μM and at reaction times up to six times longer than required to achieve DNA cleavage-ligation equilibrium. Under all conditions examined, only the enhancement of single-stranded breaks was observed (Figure 5.5). Furthermore, no enhancement of double-stranded breaks was seen in the presence of ATP, which is required for overall catalytic activity (Figure 5.6). However, it is notable that levels of single-stranded DNA cleavage generated by *E. coli* gyrase in the presence of ATP were considerably lower than those seen in the absence of the high energy cofactor (see Figure 5.4). This finding opens the possibility that under physiological conditions, GSK126 acts primarily as a catalytic inhibitor (as opposed to a poison) of *E. coli* gyrase. Conversely, the potent DNA cleavage enhancement with *M. tuberculosis* gyrase vs. the relatively weak inhibitory properties of GSK126 against this enzyme suggest that the opposite may be the case for GSK126 and *M. tuberculosis*.

The double-stranded cleavage of DNA by type II topoisomerases is carried out by two coordinated single-stranded cleavage events.[37, 82, 280] Thus, the generation of single-stranded DNA breaks that are observed in the presence of GSK126 can reflect multiple mechanisms. For example, the compound in any given cleavage complex may stabilize the break only at one of the scissile bonds. Alternatively, after cleavage at one scissile bond, the presence of GSK126 may alter the structure of the enzyme-DNA complex such that the second DNA strand cannot be cut. This latter mechanism is favored by structural studies that indicate distortion in the cleavage complex in the presence of NBTIs.[181, 235] To help elucidate the mechanisms by which GSK126 induces only single-stranded DNA breaks, the $MgCl_2$ in DNA

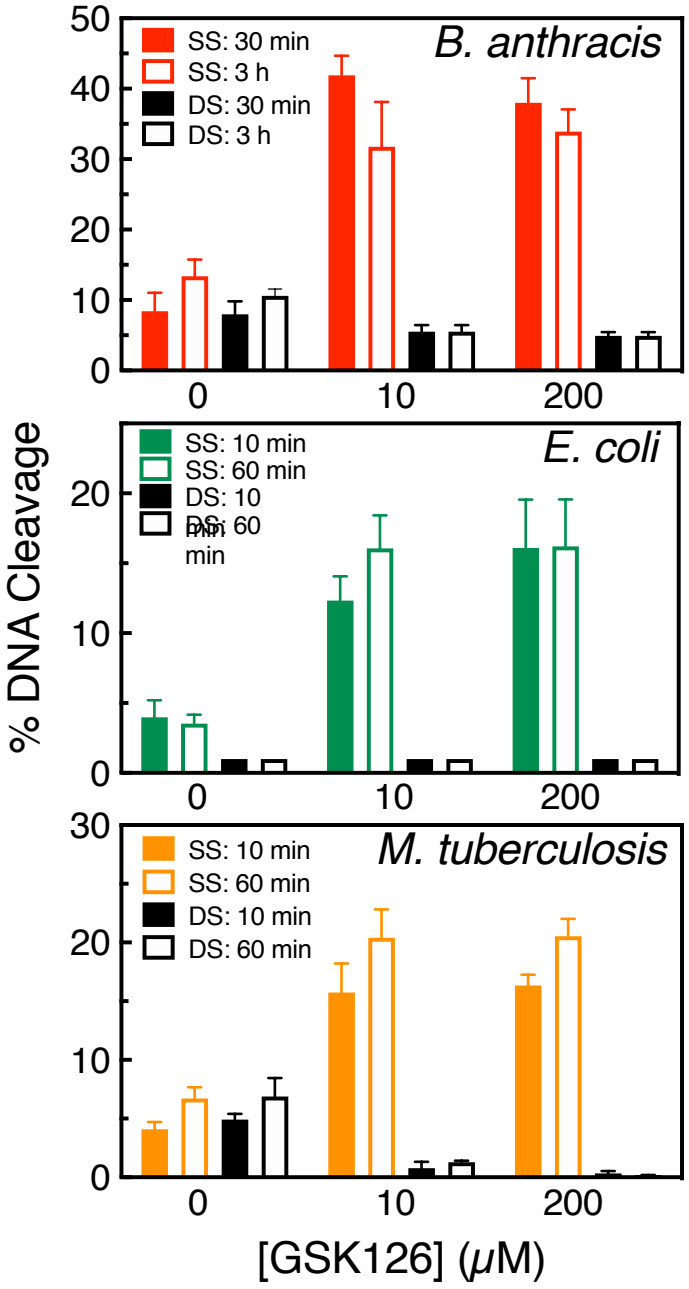

Figure 5.5. GSK126 enhances only single-stranded DNA breaks mediated by gyrase. The top panel shows the enhancement of *B. anthracis* gyrase-mediated single- (red) or double-stranded (black) DNA breaks at 30 min (filled bar) or 3 h (empty bar) in the absence or presence of 10 μM or 200 μM GSK126. The middle panel shows the enhancement of *E. coli* gyrase-mediated single- (green) or double-stranded (black) DNA breaks at 10 min (filled bar) or 60 min (empty bar) in the absence or presence of 10 μM or 200 μM GSK126. The bottom panel shows the enhancement of *M. tuberculosis* gyrase-mediated single- (orange) or double-stranded (black) DNA breaks at 10 min (filled bar) or 60 min (empty bar) in the absence or presence of 10 μM or 200 μM GSK126. Error bars represent the SD of at least 3 independent experiments.

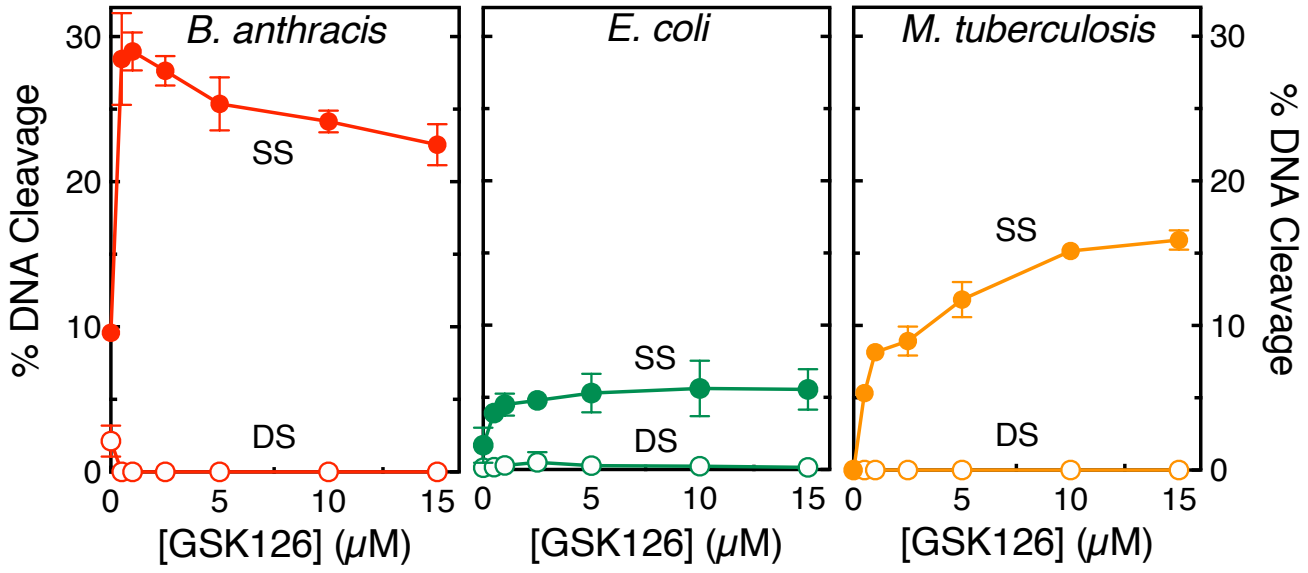

Figure 5.6. GSK126 enhances only single-stranded DNA breaks mediated by gyrase in the presence of ATP. The effects of GSK126 on single-stranded (SS, filled circles) and double-stranded (DS, empty circles) DNA cleavage mediated by *B. anthracis* (left, red), *E. coli* (middle, green), and *M. tuberculosis* (right, orange) gyrase in the presence of 1.5 mM ATP are shown. Error bars represent the SD of at least three independent experiments.

cleavage assays was replaced with $CaCl_2$. This latter divalent metal ion raises baseline levels of DNA cleavage with most type II topoisomerases, so that double-stranded breaks can be observed more easily even in the absence of drug (compare levels of double-stranded DNA breaks in the absence of GSK126 in Figure 5.4 with those in Figure 5.7). As seen in Figure 5.7 (or more clearly in Figures 5.4 and 5.6 with *B. anthracis* gyrase), the rise in single-stranded cleavage mediated by gyrase at increasing concentrations of GSK126 was accompanied by a coordinate decrease in double-stranded breaks. This finding suggests that cleavage of one scissile bond in the presence of GSK126 suppresses cleavage at the opposite scissile bond.

Taken together, the above data provide strong evidence that GSK126 (a naphthyridone/aminopiperidine-based NBTI), like the naphthyridone/aminopiperidine-based MGIs (GSK000 and GSK325)[234] and other structural classes of NBTIs (NBTI GSK299423, 5643, and gepotidacin),[181, 221, 235] induces only gyrase-mediated single-stranded DNA breaks across a variety of species.

Effects of GSK126 on the DNA Decatenation Activity of Wild-type and Fluoroquinolone-resistant Topoisomerase IV

Depending upon the bacterial species and the specific drug, the primary cellular target of fluoroquinolones may be gyrase, topoisomerase IV, or both enzymes.[48, 110, 111, 170] However, less is known about the targeting of NBTIs. Therefore, to be able to make direct comparisons with DNA gyrase, the ability of GSK126 to inhibit decatenation catalyzed by *B. anthracis* and *E. coli* topoisomerase IV was characterized.

Consistent with studies with other structural classes of NBTIs[181, 221, 228-230, 232-235, 238, 277-279, 281] and as seen with gyrase (Figure 5.3), GSK126 was a potent inhibitor of topoisomerase IV function (IC_{50} ~ 2.3 μM for *B. anthracis* and 1.4 μM for *E. coli,* respectively) (Figure 5.8). Furthermore, GSK126 maintained activity against the $ParC^{S80L}$ fluoroquinolone-resistant mutant of *E. coli* topoisomerase IV (IC_{50} ~ 1.4 μM)

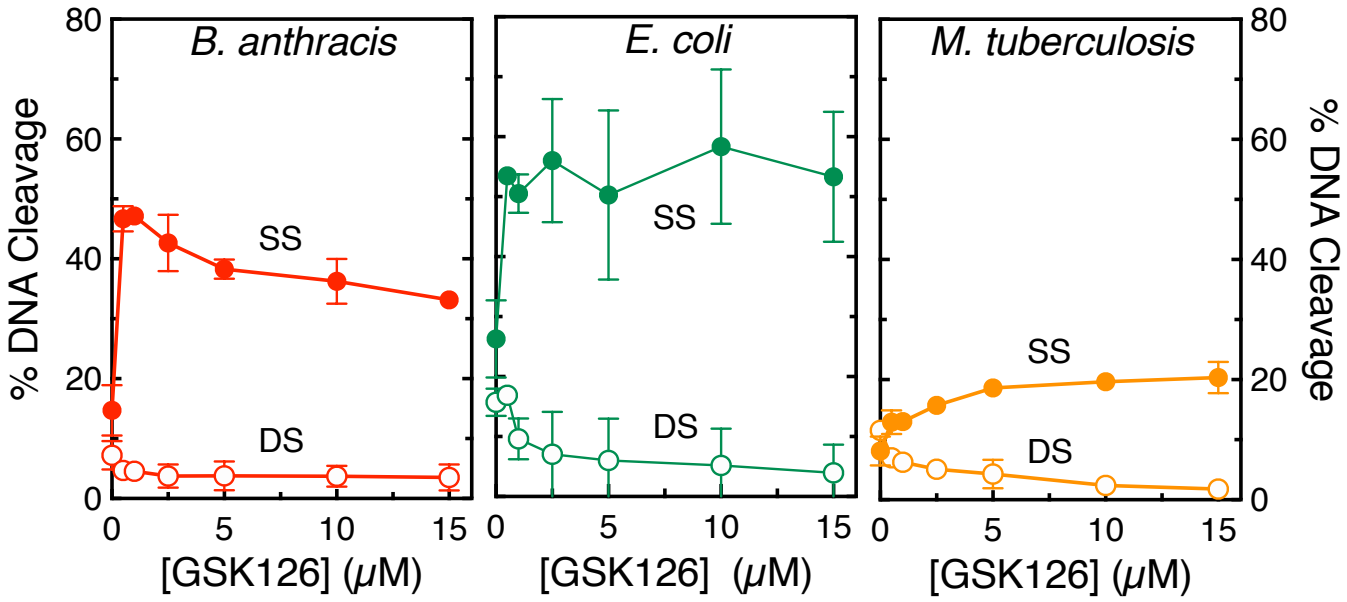

Figure 5.7. GSK126 suppresses double-stranded DNA breaks generated by gyrase. The effects of GSK126 on single-stranded (SS, filled circles) and double-stranded (DS, empty circles) DNA cleavage mediated by *B. anthracis* (left, red), *E. coli* (middle, green), and *M. tuberculosis* (right, orange) gyrase are shown. Reaction mixtures contained 5 mM $CaCl_2$ in place of $MgCl_2$ to increase baseline levels of DNA cleavage. Error bars represent the SD of at least three independent experiments.

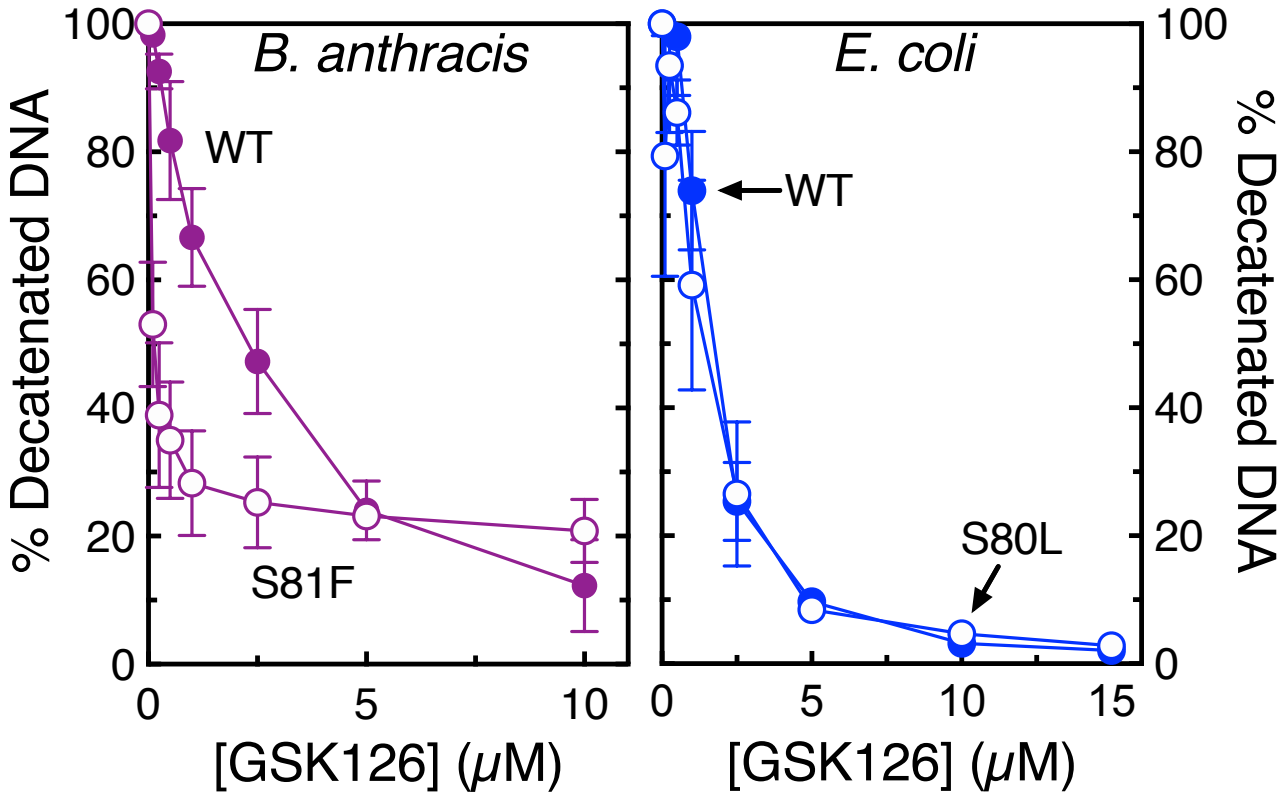

Species	WT IC_{50} (μM)	Mutant IC_{50} (μM)
B. anthracis	~2.3	~0.1 (S81F)
E. coli	~1.4	~1.4 (S80L)

Figure 5.8. GSK126 inhibits DNA decatenation catalyzed by wild-type (WT) and fluoroquinolone-resistant topoisomerase IV. The effects of GSK126 on DNA decatenation by WT (filled circles) and fluoroquinolone-resistant (empty circles) *B. anthracis* WT and $GrlA^{S81F}$ (top left, purple) and *E. coli* WT and $ParC^{S80L}$ (top right, blue) topoisomerase IV are shown. Error bars represent the SD of at least three independent experiments. The bottom panel shows a table of IC_{50} values.

and displayed even greater potency against the GrlA^{S81F} mutant of the *B. anthracis* enzyme (Figure 5.8). As above, these fluoroquinolone resistance mutations are at the corresponding serine residues.

Effects of GSK126 on the DNA Cleavage Activity of Wild-type and Fluoroquinolone-resistant Topoisomerase IV

Virtually nothing has been reported regarding the effects of NBTIs on DNA cleavage mediated by topoisomerase IV. Consequently, we examined the ability of GSK126 to enhance DNA cleavage mediated by the enzyme (Figure 5.9). The NBTI was a potent enhancer of single-stranded DNA cleavage with wild-type *B. anthracis* and *E. coli* topoisomerase IV (EC_{50} values for both enzymes were <0.5 μM). As seen with gyrase in Figure 5.4, no enhancement of double-stranded breaks was observed. Furthermore, in parallel with results with *B. anthracis* gyrase, there was a sharp increase in DNA cleavage mediated by *B. anthracis* topoisomerase IV in the presence of GSK126. Once again, this likely reflects a tight binding between the NBTI and the topoisomerase IV-DNA complex.

The effects of fluoroquinolone resistance mutations on the induction of topoisomerase IV-mediated DNA cleavage by GSK126 were also examined (Figure 5.9). Both the potency and efficacy of the NBTI against the *B. anthracis* GrlA^{S81F} mutant enzyme were similar to those observed for wild-type topoisomerase IV. In contrast, similar to results with *E. coli* gyrase (see Figure 5.4), GSK126 was ineffective at inducing DNA cleavage with the *E. coli* topoisomerase IV fluoroquinolone-resistant ParC^{S80L} mutant. This is despite the fact that the NBTI maintained the ability to inhibit overall catalytic activity.

GSK126 Enhances only Single-stranded DNA Cleavage Mediated by Topoisomerase IV and Suppresses Enzyme-generated Double-stranded DNA Breaks

As found with gyrase, GSK126 induced only single-stranded DNA breaks mediated by *B. anthracis* and *E. coli* topoisomerase IV. Even at high concentrations of GSK126 and longer reaction times, no

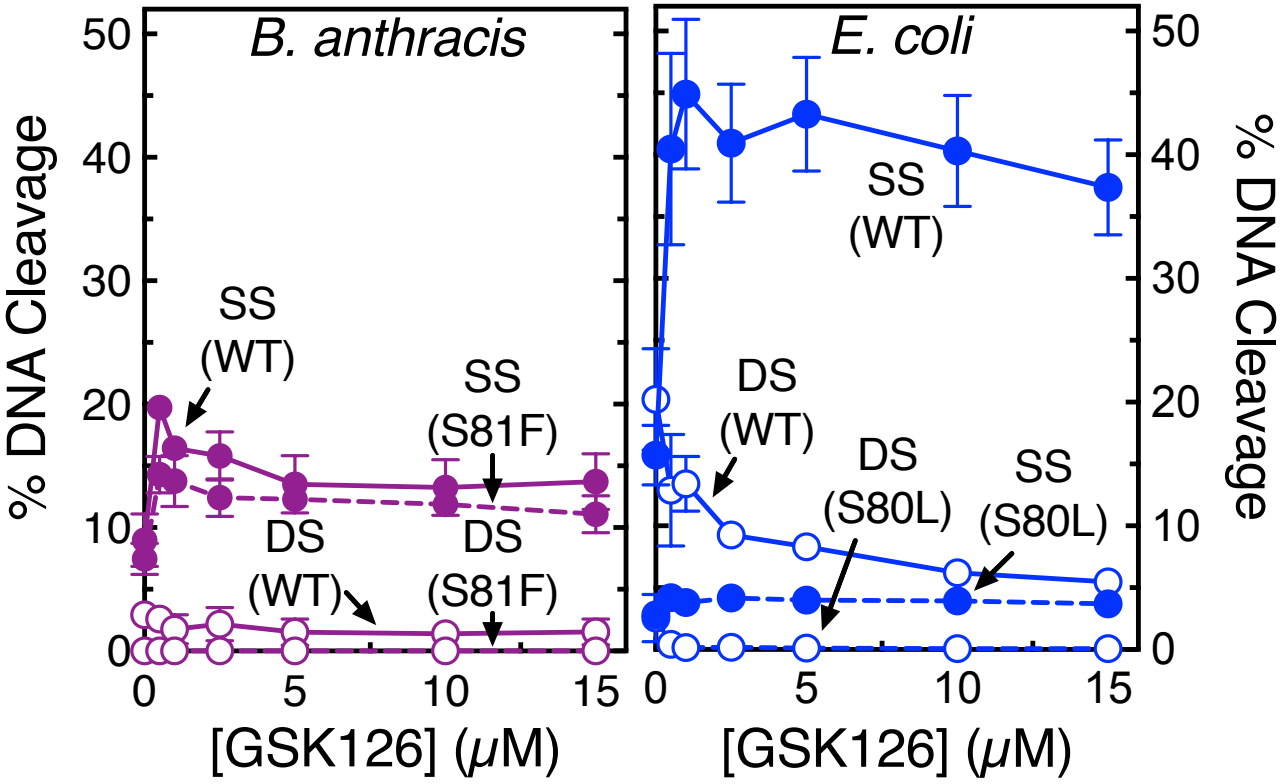

Figure 5.9. Effects of GSK126 on DNA cleavage mediated by wild-type (WT) and fluoroquinolone-resistant topoisomerase IV. The effects of GSK126 on single-stranded (SS, filled circles) and double-stranded (DS, empty circles) DNA cleavage mediated by WT (solid line) and fluoroquinolone-resistant (dashed line) *B. anthracis* WT and GrlA^{S81F} (left, purple) and *E. coli* WT and ParC^{S80L} (right, blue) topoisomerase IV are shown. Error bars represent the SD of at least three independent experiments.

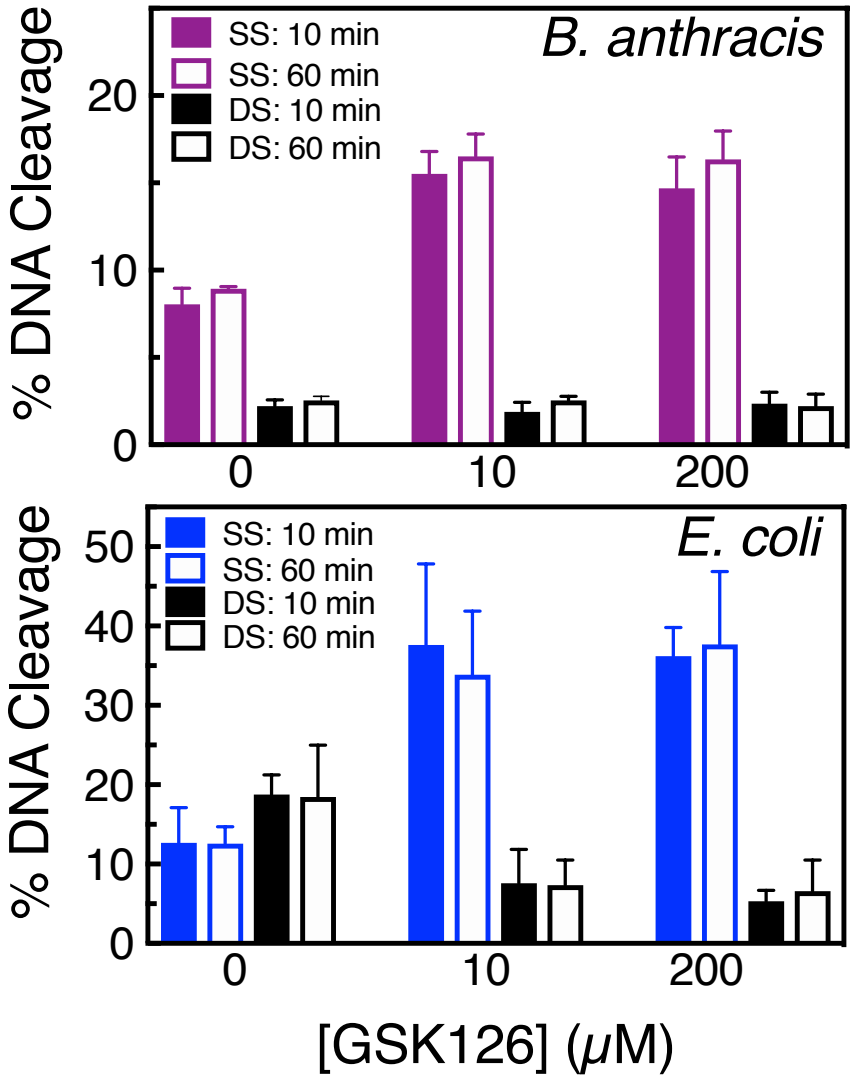

Figure 5.10. GSK126 enhances only single-stranded DNA breaks mediated by topoisomerase IV. The top panel shows the enhancement of *B. anthracis* topoisomerase IV-mediated single- (purple) or double-stranded (black) DNA breaks at 10 min (filled bar) or 60 min (empty bar) in the absence or presence of 10 μM or 200 μM GSK126. The bottom panel shows the enhancement of *E. coli* topoisomerase IV-mediated single- (blue) or double-stranded (black) DNA breaks at 10 min (filled bar) or 60 min (empty bar) in the absence or presence of 10 μM or 200 μM GSK126. Error bars represent the SD of at least 3 independent experiments.

enhancement of double-stranded breaks was observed (Figure 5.10). Furthermore, paralleling the results with gyrase, no double-stranded DNA breaks were observed in the presence of ATP (Figure 5.11). However, the ability of GSK126 to induce DNA cleavage with *E. coli* topoisomerase IV was marginal in the presence of the high energy cofactor. Thus, as was seen with *E. coli* gyrase (see Figure 5.6), this finding suggests that under physiological conditions, GSK126 acts primarily as a catalytic inhibitor of *E. coli* topoisomerase IV.

Because topoisomerase IV generally maintains higher levels of baseline DNA cleavage than gyrase, double-stranded DNA breaks can be monitored in Mg^{2+}-containing reactions. As seen in Figure 5.9 with *E. coli* topoisomerase IV and Figure 5.11 with *B. anthracis* topoisomerase IV, the increase in NBTI-induced single-stranded breaks was accompanied by a decrease in double-stranded DNA breaks. This suppression of double-stranded breaks becomes even more apparent for both species of topoisomerase IV in Ca^{2+}-containing reactions (Figure 5.12). Note that data with *E. coli* topoisomerase IV are shown using a lower ratio (1:1) of enzyme to DNA than in Mg^{2+}-containing reactions (2:1) because levels of double-stranded breaks are often so high with this enzyme in the presence of Ca^{2+} that baseline reactions contain multiply cleaved DNA products (not shown). Taken together, the above results indicate that GSK126 enhances single-stranded and suppresses double-stranded DNA breaks generated by bacterial type II topoisomerases.

Conclusions

Given the rise in fluoroquinolone resistance, there is a need to supplement or eventually replace these drugs. The NBTIs display promise to address this unmet medical need. However, there is a paucity of published data describing the mechanism of action of these compounds against their type II topoisomerase targets. Structural work with NBTIs has focused on the interaction of these compounds with gyrase.[181, 235, 282, 283] Whereas previous studies have reported the inhibition of DNA supercoiling by gyrase or

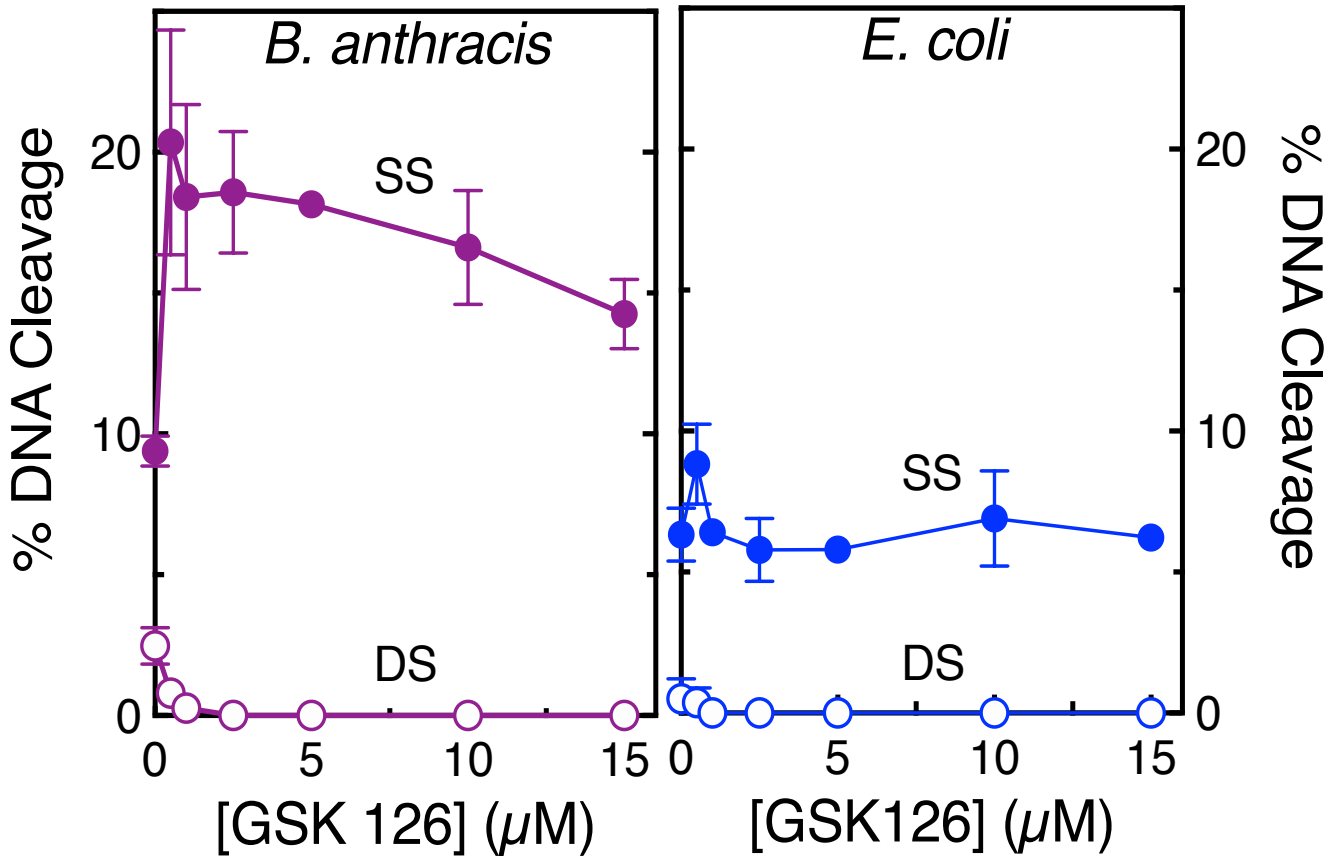

Figure 5.11. GSK126 enhances only single-stranded DNA breaks mediated by topoisomerase IV in the presence of ATP. The effects of GSK126 on single-stranded (SS, filled circles) and double-stranded (DS, empty circles) DNA cleavage mediated by *B. anthracis* (left, purple) and *E. coli* (right, blue) topoisomerase IV in the presence of 1.5 mM ATP are shown. Error bars represent the SD of at least three independent experiments.

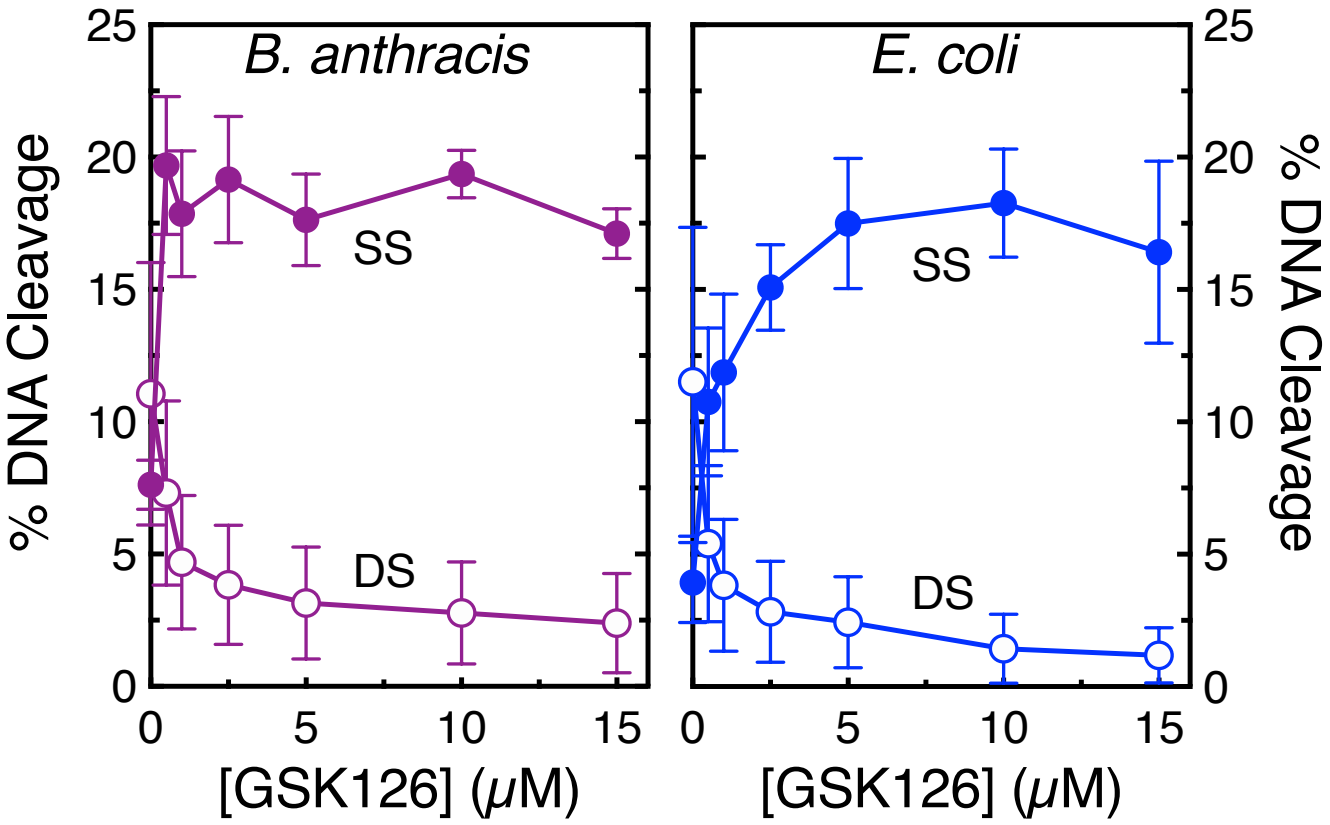

Figure 5.12. GSK126 suppresses double-stranded DNA breaks generated by topoisomerase IV. The effects of GSK126 on single-stranded (SS, filled circles) and double-stranded (DS, empty circles) DNA cleavage mediated by *B. anthracis* topoisomerase IV (left, purple) and *E. coli* (right, blue) topoisomerase IV are shown. Reaction mixtures contained 5 mM $CaCl_2$ in place of $MgCl_2$ to increase baseline levels of DNA cleavage. Note that data shown for *E. coli* topoisomerase IV were generated at a 1:1 enzyme:plasmid ratio to ensure that baseline reactions carried out in the absence of GSK126 did not include DNA molecules that contained multiple double-stranded breaks. Error bars represent the SD of at least three independent experiments.

decatenation or relaxation by topoisomerase IV,[181, 221, 228-230, 232-235, 238, 277-279] only a handful of studies have examined the effects of NBTIs on DNA cleavage.[181, 221, 228, 234, 235] Thus, it was not obvious that previous conclusions could be extended across bacterial species or from gyrase to topoisomerase IV. Consequently, we examined the effects of the NBTI GSK126 on the catalytic and DNA cleavage activities of wild-type and fluoroquinolone-resistant gyrase and topoisomerase IV from *B. anthracis* and *E. coli* and gyrase from *M. tuberculosis*.

NBTIs as bimodal agents that target bacterial type II topoisomerases

Results of the present work indicate that GSK126 is a potent catalytic inhibitor of gyrase and topoisomerase IV from a variety of gram-positive and gram-negative bacterial species. Furthermore, the NBTI enhances single-stranded DNA cleavage and suppresses double-stranded cleavage mediated by these enzymes. These findings make it likely that NBTIs (at least those that enhance DNA cleavage) display a similar bimodal mechanism of action against gyrase and topoisomerase IV across a spectrum of bacteria. However, the role that "inhibition of catalytic activity" vs. "enhancement of cleavage" plays in the antibacterial properties of NBTIs remains an enigma and may differ from species to species. To this point, results with *E. coli* gyrase and topoisomerase IV suggest that under physiological conditions (i.e., in the presence of ATP) GSK126 acts primarily as a catalytic inhibitor rather than a poison with these enzymes. This finding opens the possibility that the antibacterial activity of GSK126 against *E. coli* (Minimal Inhibitory Concentration = 0.26 μM)[234] may be more closely linked to its ability to inhibit the critical catalytic activities of gyrase and topoisomerase IV as opposed to its ability to enhance DNA strand breaks. Conversely, the potent DNA cleavage enhancement with *M. tuberculosis* gyrase vs. the relatively weak inhibitory properties of GSK126 against this enzyme suggest that DNA cleavage enhancement may be the more important mode of action in this species. Alternatively, the more balanced effects of GSK126 on the catalytic and DNA cleavage activities of the *B. anthracis* type II topoisomerases leave the door open for either mode of action (or a combination of both) to predominate in cells. Taken together, the

results of the present study suggest that NBTIs are antibacterial agents that act in a bimodal fashion. Despite the fact that they target the same enzymes across a wide range of bacterial species, the mechanism by which they manifest their antibacterial properties in distinct species may be fundamentally different.

At the present time, it is not possible to predict the actions of any NBTI against any given bacterial type II topoisomerase *a priori*. Eventually, mechanistic *in vitro* studies with wild-type and resistant enzymes will have to be coupled with parallel cellular studies to develop a set of "rules" that describe the actions of NBTIs. If this information can be generated, it should hasten the development of this potentially important class of compounds.

CHAPTER VI

ACTIONS OF AND RESISTANCE TO GEPOTIDACIN IN *E. COLI* AND *N. GONORRHOEAE* GYRASE AND TOPOISOMERASE IV

Introduction

NBTIs are an emerging class of gyrase/topoisomerase IV-targeted antibacterials. However, GSK126 (as described in the previous chapter) and related compounds are not under clinical development due to inhibition of the human ether-à-go-go-related gene (hERG) cardiac potassium channel. Therefore, newer members of the NBTI class with greater clinical potential have been developed with this deleterious effect in mind.

Gepotidacin is a first-in-class triazaacenaphthylene NBTI and is the most clinically advanced member of the class.[231, 284-286] The compound currently is in phase III clinical trials that are assessing the efficacy and safety of the drug against uncomplicated urinary tract infections (UTIs)[287] and uncomplicated urogenital gonorrhea.[288] Approximately 75-80% of UTIs are caused by *E. coli*; however, there have been no reports of the effects of gepotidacin on wild-type or resistant gyrase or topoisomerase IV from this species. Similarly, no studies on the interactions of gepotidacin with the type II enzymes from *N. gonorrhoeae* are in the literature. Therefore, this chapter investigates the interactions of gepotidacin with these type II topoisomerases both in cells and *in vitro*. The chapter also discusses the basis for target-mediated resistance to gepotidacin in *E. coli* gyrase and topoisomerase IV. Results strongly suggest that the NBTI is a "dual-targeting" compound that requires mutations in both type II enzymes for target-mediated resistance to occur in *E. coli.* Furthermore, resistance mutations in gyrase and topoisomerase IV lead to altered interactions between gyrase/topoisomerase IV and gepotidacin.

Results and Discussion

Gepotidacin has balanced targeting of gyrase and topoisomerase IV in cultured E. coli cells

Exposure of *E. coli* cells to gepotidacin is lethal and displays a minimum inhibitory concentration (MIC) of 0.125 μg/mL (Table 6.1). Although the drug is not as potent as the fluoroquinolone ciprofloxacin (MIC = 4 nM), it should be noted that the *E. coli* strain (TOP10) carries an efflux pump mutation that might differentially affect these two compounds.

Drugs that act against both gyrase and topoisomerase IV, such as fluoroquinolones, can differentially target these enzymes with regard to cytotoxicity. For example, depending on the bacterial strain and the drug employed, gyrase or topoisomerase IV can act as the primary lethal target of fluoroquinolones. Furthermore, in some cases, dual targeting, in which actions against both enzymes are required for lethality, have been observed. Drugs that equally target gyrase and topoisomerase IV have an obvious advantage in that target-mediated resistance is observed only when mutations in both enzymes occur. In *E. coli,* gyrase is the primary lethal target of the fluoroquinolone ciprofloxacin.

During clinical trials, mutations in gyrase ($GyrA^{P35L}$) and topoisomerase IV ($ParC^{D79N}$) were found in clinical isolates from patients that displayed resistance. To determine whether these mutations were responsible (at least in part) for the resistance observed clinically, and to define the primary lethal target of gepotidacin, these two mutations were introduced individually or in combination into the TOP10 strain, resulting in the creation of the isogenic strains TOP10-1 ($GyrA^{P35L}$), TOP10-2 ($ParC^{D79N}$), and TOP10-3 ($GyrA^{P35L}$, $ParC^{D79N}$) (Table 6.1). The MIC of gepotidacin for each of the strains carrying individual mutations in gyrase or topoisomerase IV were the same as seen with the wild-type TOP10 parent strain. However, the MIC value of the compound against the TOP10-3 strain that carried mutations in both enzymes was 128-fold higher. These data strongly support the conclusion that the $GyrA^{P35L}$ and $ParC^{D79N}$ mutations confer resistance to gepotidacin and that mutations in both enzymes are required for cellular resistance to the compound. Thus, it appears that gyrase and topoisomerase IV are dual targets for gepotidacin and that this compound targets both enzymes similarly (balanced targeting).

	Mutation		MIC (μg/mL)			
E. coli	GyrA	ParC	Gepotidacin	Fold	Ciprofloxacin	Fold
TOP10	WT	WT	0.125	NA	0.0015	NA
TOP10-1	P35L	WT	0.125	1	0.012	8
TOP10-2	WT	D79N	0.125	1	0.002	1
TOP10-3	**P35L**	**D79N**	**16**	**128**	**0.012**	**8**

Table 6.1. Gepotidacin MIC values against *E. coli* TOP10 NBTI target mutants. The MIC values of gepotidacin and ciprofloxacin against WT cells or cells with a presumed NBTI-resistance mutation in gyrase ($GyrA^{P35L}$), topoisomerase IV ($ParC^{D79N}$), or both ($GyrA^{P35L}$, $ParC^{D79N}$) were determined by broth dilution. The fold change from the WT strain TOP10 is given for comparison. Data are provided by our collaborator Dr. Pan Chan at GlaxoSmithKline. MIC values are the average of 2 independent determinations. NA = not applicable.

E. coli gyrase carrying the GyrA^{P35L} mutation appears to be cross-resistant to ciprofloxacin (Table 6.1). No cross-resistance was observed in the strain that carried the topoisomerase IV ParC^{D79N} mutation. It is not known whether this latter observation reflects a lack of resistance at the enzyme level or the fact that gyrase is the primary cytotoxic target of ciprofloxacin in *E. coli* cells.

In vitro effects of gepotidacin on E. coli gyrase and topoisomerase IV activity

Although the cellular studies provide strong evidence that gyrase and topoisomerase IV are targeted by gepotidacin, the effects of the compound on these enzymes have never been reported. Therefore, the following sections describe the effects of gepotidacin on the catalytic and DNA cleavage activities of WT and mutant *E. coli* gyrase and topoisomerase IV.

Effects of gepotidacin on the DNA supercoiling activities of WT and mutant E. coli gyrase

Gepotidacin inhibited DNA supercoiling catalyzed by *E. coli* gyrase at low concentrations (IC_{50} ≈ 0.1 μM) (Figure 6.1, left panel). The NBTI maintained high activity against the GyrA^{P35L} mutant enzyme, although the potency dropped ~5-fold (IC_{50} ≈ 0.5 μM). In contrast to DNA cleavage, gepotidacin maintained WT activity against fluoroquinolone-resistant mutant GyrA^{S83L} (IC_{50} ≈ 0.1 μM). These data once again suggest that mutations alter the positioning of the NBTI rather than its affinity for the active site of *E. coli* gyrase and that the presence of the compound in the vicinity of the DNA gate is sufficient to inhibit overall catalytic activity, even if it cannot stabilize cleavage complexes.

Ciprofloxacin inhibited DNA supercoiling with lower potency than did gepotidacin (IC_{50} ≈ 4 μM) (Figure 6.1, right panel). The fluoroquinolone displayed even lower activity against the well-characterized GyrA^{S83L} resistance mutation (IC_{50} ≈ 8 μM). Surprisingly, the activity of ciprofloxacin against the NBTI-resistant GyrA^{P35L} was increased substantially. The IC_{50} was less than 0.1 μM. This is in contrast to the slight resistance observed for the fluoroquinolone against this mutation in cultured cells.

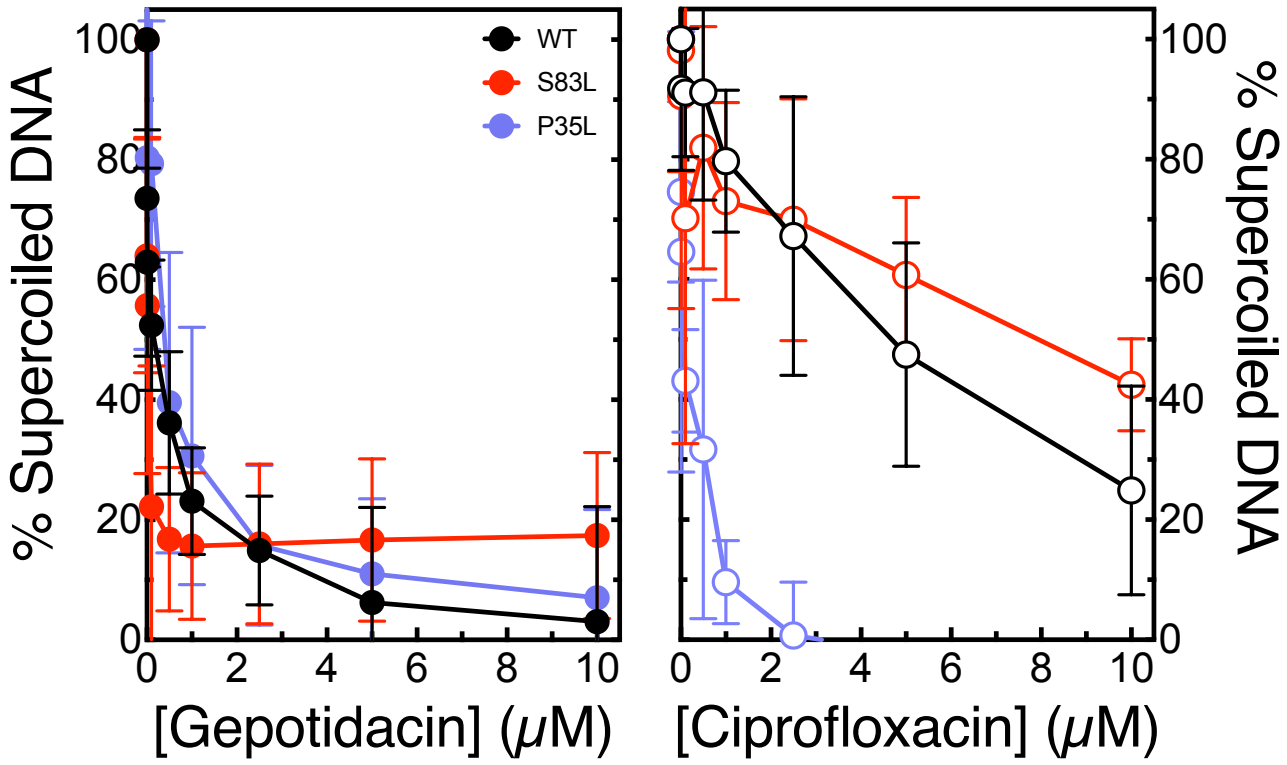

Figure 6.1. Gepotidacin inhibits DNA supercoiling catalyzed by wild-type (WT), fluoroquinolone-resistant, and NBTI-resistant *E. coli* gyrase. The effects of gepotidacin on the supercoiling of relaxed DNA by WT (black), fluoroquinolone-resistant GyrA^{S83L} (red), and NBTI-resistant GyrA^{P35L} (blue) are shown on the left. In comparison, the effects of ciprofloxacin on these enzymes are shown on the right. Error bars represent the SD of at least three independent experiments.

Effects of gepotidacin on the DNA cleavage activities of WT and mutant E. coli gyrase

As seen in Figure 6.2 (left panel), gepotidacin was a potent enhancer of DNA cleavage mediated by *E. coli* gyrase. Similar to other NBTIs, the compound induced only single-stranded DNA breaks. The CC_{50} (concentration at which 50% maximal DNA cleavage was observed) was approximately 2.5 μM. Virtually no double-stranded breaks were observed even at 100 μM gepotidacin, a concentration that was 40 times higher than the CC_{50} for single-stranded breaks. The CC_{50} for DNA cleavage is higher than the IC_{50} for inhibition of DNA supercoiling; however, this could be caused by differences in assay conditions and enzyme concentrations used for DNA supercoiling versus cleavage reactions.

In contrast to the NBTI, the fluoroquinolone ciprofloxacin induced primarily double-stranded breaks ($CC_{50} \approx 20$ μM) with maximal levels being similar to those observed for single-stranded breaks with gepotidacin (~27%) (Figure 6.2, right panel). However, an increase in single-stranded breaks ($CC_{50} \approx 2.75$ μM) was also observed with ciprofloxacin. There appears to be a "product-precursor" relationship between single- and double-stranded breaks with the former being generated at lower concentrations. This finding suggests that the affinity of the second ciprofloxacin molecule to enter the active site of the gyrase is lower than that of the first.

The effects of gepotidacin on the DNA cleavage activity of gyrase harboring the mutation $GyrA^{P35L}$ is shown in Figure 6.3 (left panel, blue). Because the compound did not induce any double-stranded breaks, only the data for single-stranded breaks are shown. Although the potency of gepotidacin against gyrase $GyrA^{P35L}$ was still high, the efficacy of the compound was reduced considerably from a maximal cleavage of ~26.75% (WT, black) to ~3.6% (P35L, blue). This finding confirms that $GyrA^{P35L}$, which has been linked to gepotidacin resistance in clinical samples and cultured *E. coli* cells, confers resistance at the enzyme level. Furthermore, the high potency and low efficacy of gepotidacin against $GyrA^{P35L}$ suggests that the mutation does not cause resistance by reducing the affinity of the compound for the enzyme. Rather, it may result from an altered positioning of the compound in the cleavage complex, as has been seen previously for a fluoroquinolone resistance mutation in *E. coli* topoisomerase IV.

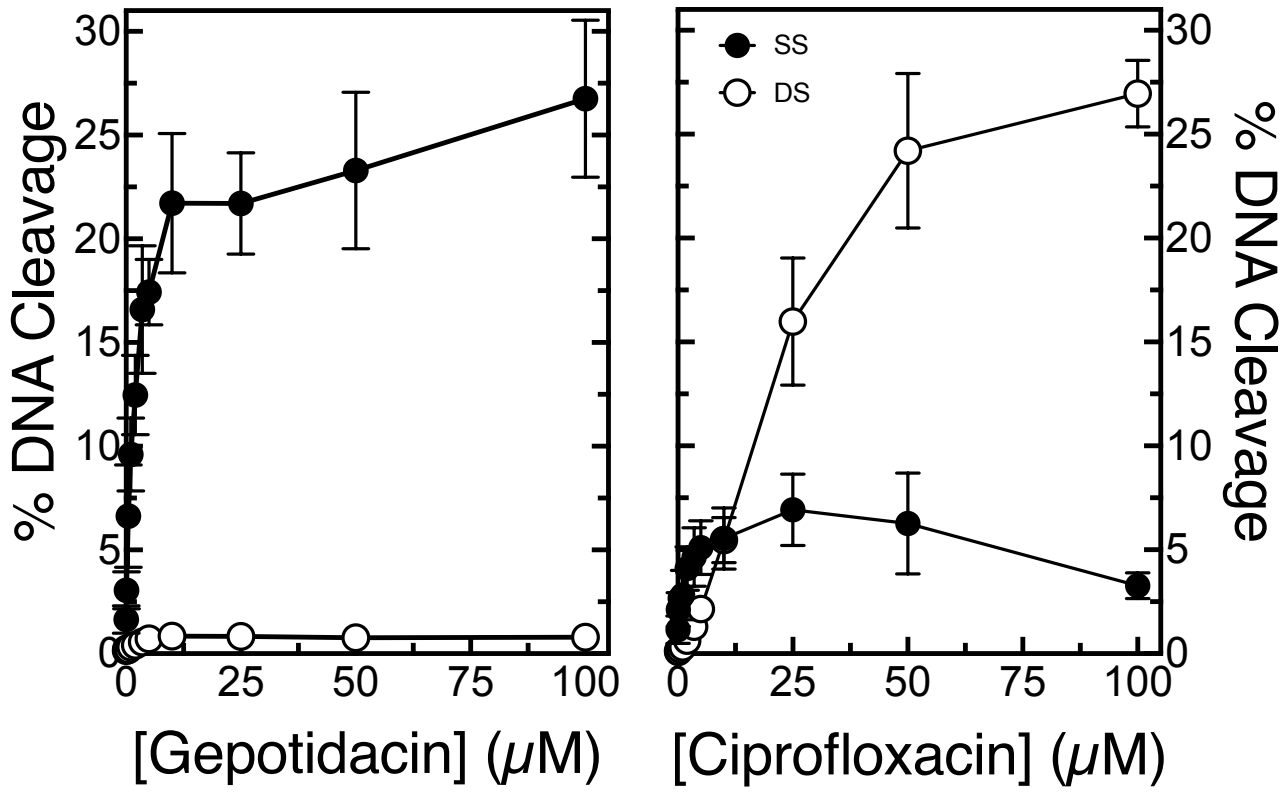

Figure 6.2. Effects of gepotidacin on DNA cleavage mediated by WT *E. coli* gyrase. The effects of gepotidacin on single-stranded (SS, filled circles) and double-stranded (DS, empty circles) DNA cleavage mediated by WT *E. coli* gyrase are shown on the left. Corresponding data with ciprofloxacin is on the right. Error bars represent the SD of at least three independent experiments.

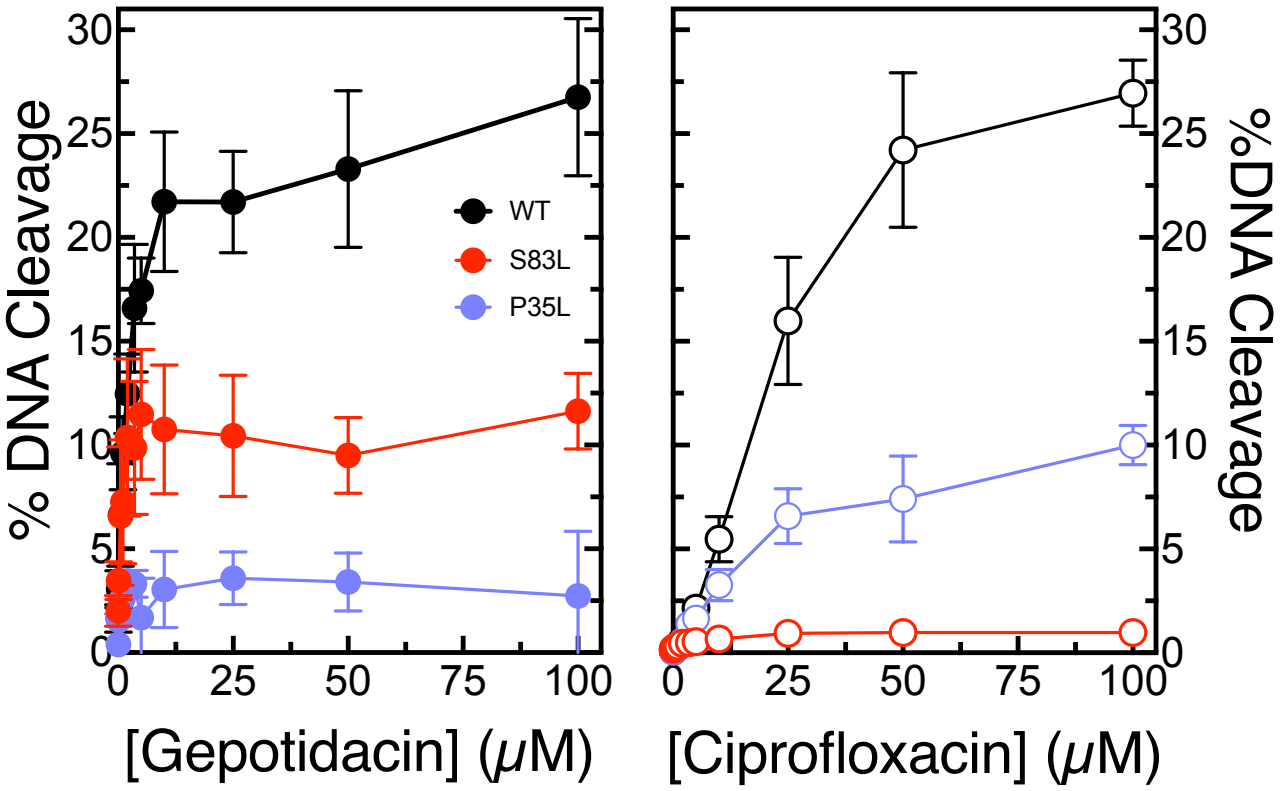

Figure 6.3. Effects of gepotidacin on DNA cleavage mediated by WT, fluoroquinolone-resistant, and NBTI-resistant *E. coli* gyrase. The effects of gepotidacin on single-stranded (SS, filled circles, left) and ciprofloxacin on double-stranded (DS, empty circles, right) DNA cleavage mediated by WT (black), fluoroquinolone-resistant $GyrA^{S83L}$ (red), and NBTI-resistant $GyrA^{P35L}$ gyrase are shown. Error bars represent the SD of at least three independent experiments.

Some cross-resistance between the GyrA^{S83L} fluoroquinolone resistance mutation and gepotidacin was also observed at the enzyme level (Figure 6.3, left panel, red). Once again, high potency and decreased efficacy were observed. However, the maximal cleavage induced by gepotidacin (~12%) was still considerably higher than that seen with GyrA^{P35L}.

As reported previously, GyrA^{S83L} was highly resistant to ciprofloxacin (Figure 6.3, right panel, red). Virtually no double-stranded DNA cleavage was observed up to 100 μM drug. Some cross-resistance was also observed with the gepotidacin-resistant GyrA^{P35L} enzyme (Figure 6.3, right panel, blue). Although the potency remained close to that of WT, maximal cleavage at 100 μM ciprofloxacin dropped from ~27% to ~10%. The decreased efficacy of ciprofloxacin against GyrA^{P35L} is consistent with the 8-fold resistance seen in cellular studies (Table 6.1) and suggests that resistance is tracking with cleavage enhancement rather than inhibition of catalytic activity.

Effects of gepotidacin on the DNA decatenation activities of WT and mutant E. coli topoisomerase IV

Gepotidacin inhibited DNA decatenation catalyzed by *E. coli* topoisomerase IV at low concentrations (IC_{50} ≈ 0.3 μM) (Figure 6.4, left panel). Once again, although the potency of the NBTI in this reaction differed somewhat from cleavage, this may be due to the difference in assay conditions between the two reactions. The potency of the NBTI against the resistant ParC^{D79N} mutation dropped approximately 5-fold (IC_{50} ≈ 1.5 μM), which could be contributing to cellular resistance. Similar to results with DNA cleavage, the inhibition of DNA decatenation by gepotidacin with ParC^{S80L} topoisomerase IV was similar to WT.

As seen with gyrase, higher concentrations of ciprofloxacin were required to inhibit DNA decatenation (IC_{50} ≈ 3 μM) as compared to gepotidacin (Figure 6.4, right panel). Consistent with a previous report,[202] the fluoroquinolone resistance mutation did not affect the ability of ciprofloxacin to inhibit topoisomerase IV catalytic activity considerably. The NBTI resistance mutation (ParC^{D79N}) displayed cross-resistance to the fluoroquinolone, raising the IC_{50} of ciprofloxacin to ~ 2-fold (7.5 μM)

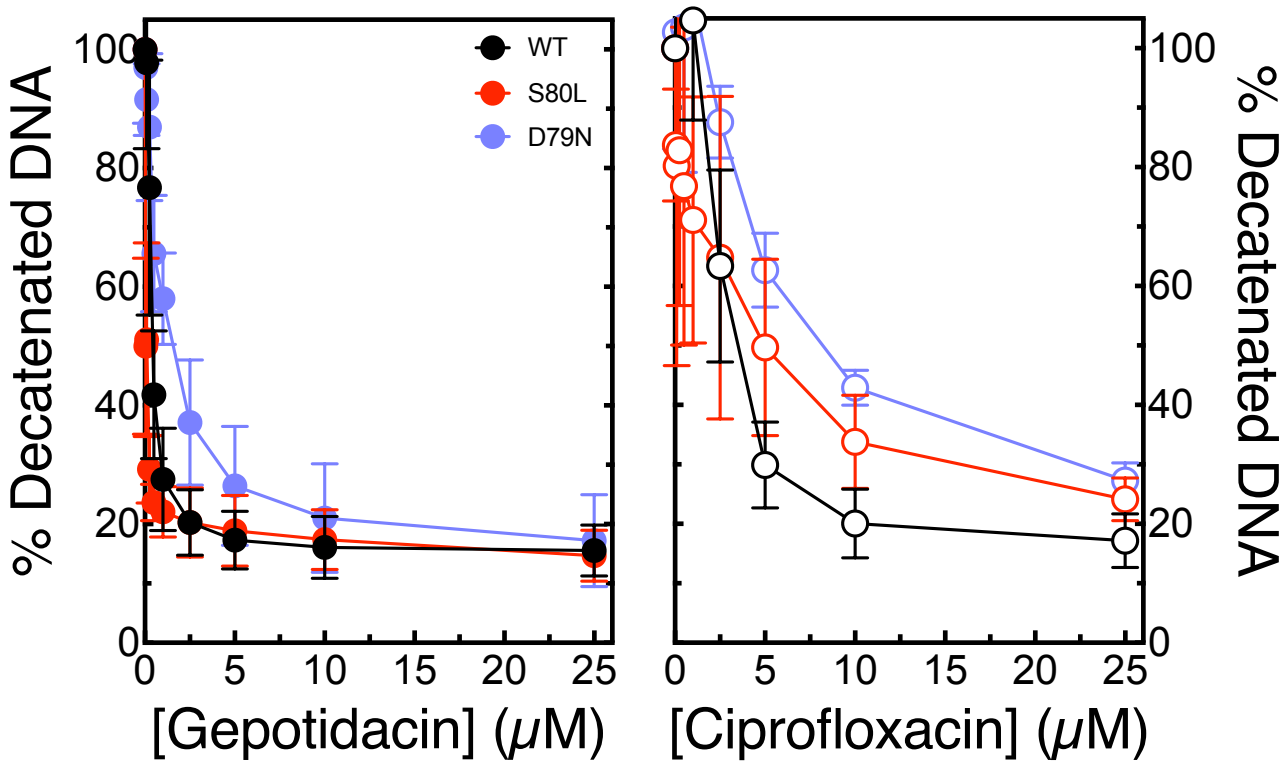

Figure 6.4. Gepotidacin inhibits DNA decatenation catalyzed by wild-type (WT), fluoroquinolone-resistant, and NBTI-resistant *E. coli* topoisomerase IV. The effects of gepotidacin on the decatenation of kDNA DNA by WT (black), fluoroquinolone-resistant ParC^{S80L} (red), and NBTI-resistant ParC^{D79N} (blue) are shown on the left. In comparison, the effects of ciprofloxacin on these enzymes are shown on the right. Error bars represent the SD of at least three independent experiments.

drug. This cross-resistance was not observed in cellular studies. However, this would not have been expected, as gyrase is the primary cellular target for fluoroquinolones in *E. coli*.

Effects of gepotidacin on the DNA cleavage activities of WT and mutant E. coli topoisomerase IV

Gepotidacin was a potent enhancer of DNA cleavage mediated by *E. coli* topoisomerase IV ($CC_{50} \approx 0.025$ μM), inducing maximal levels of single-stranded DNA cleavage of nearly 40% between 0.5 and 1 μM compound (Figure 6.5, left, closed black). Furthermore, gepotidacin induced no double-stranded breaks. Under the conditions employed, *E. coli* topoisomerase IV generates high levels of double-stranded DNA breaks (~10%) even in the absence of external poisons. Because of this high background level of DNA cleavage (in contrast to gyrase), the suppression of double-stranded breaks is obvious (Figure 6.5 left, open black). The suppression of double-stranded breaks has been reported previously.[234, 235, 242]

Gepotidacin was more potent and induced higher levels of single-stranded DNA breaks with *E. coli* topoisomerase IV than was observed for double-stranded breaks with ciprofloxacin ($CC_{50} \approx 2.5$ μM maximal cleavage) (Figure 6.5, right, open black). Single-stranded DNA breaks arose at similar concentrations of ciprofloxacin, suggesting that the affinity of the fluoroquinolone for the two scissile bonds in topoisomerase IV is similar.

Similar to results with the NBTI-resistant mutation in *E. coli* gyrase, gepotidacin maintained high potency against the $ParC^{D79N}$ mutant topoisomerase IV with greatly reduced levels of maximal single-stranded DNA cleavage (~40% to ~18%) (Figure 6.6, left, blue). Yet again, this demonstrates that the mutation that is associated with resistance in cells alters the interaction between the NBTI and topoisomerase IV *in vitro*, and suggests that resistance results from a lack of proper positioning of the NBTI in the cleavage complex rather than a lack of affinity. In contrast to the NBTI-resistant mutant, gepotidacin maintained high activity (potency and maximal cleavage) against the fluoroquinolone-resistant topoisomerase IV $ParC^{S80L}$ mutant enzyme.

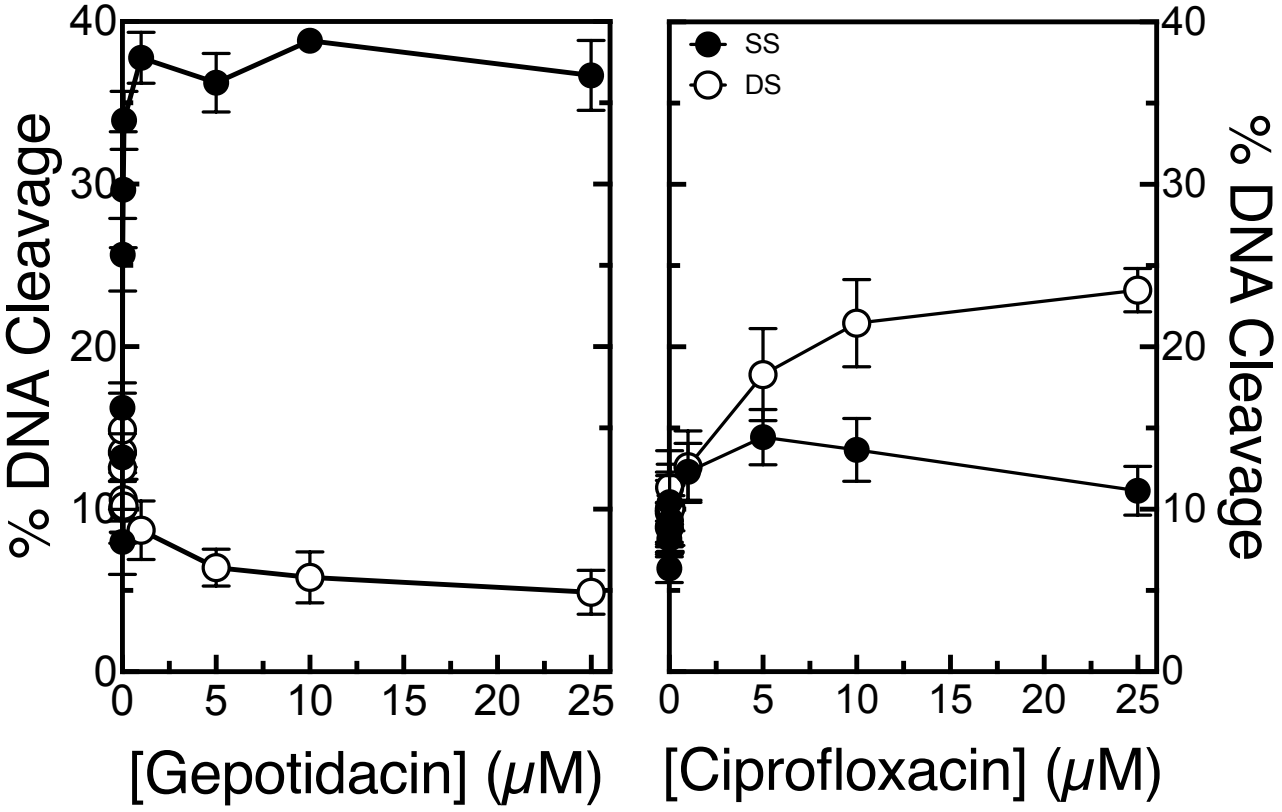

Figure 6.5. Effects of gepotidacin on DNA cleavage mediated by WT *E. coli* topoisomerase IV. The effects of gepotidacin on single-stranded (SS, filled circles) and double-stranded (DS, empty circles) DNA cleavage mediated by WT *E. coli* topoisomerase IV are shown on the left. Corresponding data with ciprofloxacin is on the right. Error bars represent the SD of at least three independent experiments.

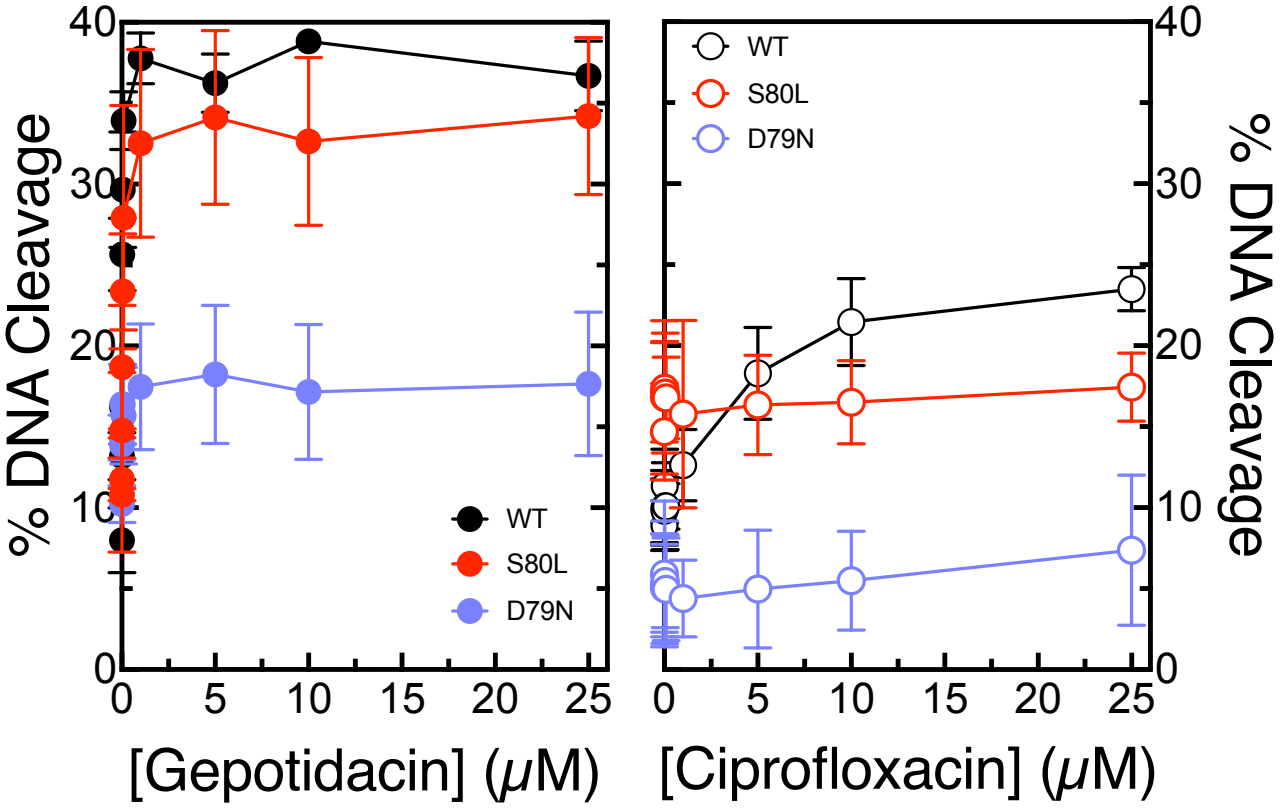

Figure 6.6. Effects of gepotidacin on DNA cleavage mediated by WT, fluoroquinolone-resistant, and NBTI-resistant *E. coli* topoisomerase IV. The effects of gepotidacin on single-stranded (SS, filled circles, left) and ciprofloxacin on double-stranded (DS, empty circles, right) DNA cleavage mediated by WT (black), fluoroquinolone-resistant GyrA^{S80L} (red), and NBTI-resistant GyrA^{D79N} gyrase are shown. Error bars represent the SD of at least three independent experiments.

As reported previously, ciprofloxacin induced less DNA scission with the topoisomerase IV containing the ParC^{S80L} fluoroquinolone resistance mutation (Figure 6.6, right, red). Ciprofloxacin also displayed substantial cross-resistance against the ParC^{D79N} topoisomerase IV mutant. Once again, the lack of cross-resistance in cells is likely due to the fact that gyrase, rather than topoisomerase IV, is the primary cellular target for fluoroquinolones in *E. coli*.

Effects of gepotidacin on N. gonorrhoeae gyrase and topoisomerase IV activity

A previous study compared the effects of gepotidacin and ciprofloxacin on WT *N. gonorrhoeae* (FA1090E) cells and isogenic strains that harbored mutations in gyrase (GyrA^{A92T}, FA1090E-1), topoisomerase IV (ParC^{D86N}, FA1090E-2), or both (GyrA^{A92T} and ParC^{D86N}, FA1090E-3) that were observed in resistant clinical isolates (Table 6.2).[289] It should be noted that the ParC^{D86N} in *N. gonorrhoeae* topoisomerase IV is equivalent to that seen in *E. coli* topoisomerase IV, while the gyrase mutants are not equivalent.

Results of the cellular studies with *N. gonorrhoeae* are seen in Table 6.2. Evidence for dual-targeting of gyrase and topoisomerase IV were less definitive than those seen with *E. coli* (Table 6.1). Once again, ciprofloxacin was considerably more potent than gepotidacin in cultured cells (MIC 0.004 μg/mL). However, levels of resistance in the doubly-mutated strain (FA1090E-3) were considerably lower than observed in *E. coli* (16- vs 128-fold) and 4-fold resistance was observed in the gyrase mutant alone (FA1090E-1).

Because of the clinical trials of gepotidacin against gonorrhea and to reconcile differences between results seen with *E. coli*, it is critical to examine interactions between the NBTI and the type II enzymes from *N. gonorrhoeae*. As a first step, the effects of gepotidacin on the catalytic and DNA cleavage activities of WT gyrase and topoisomerase IV from *N. gonorrhoeae* were assessed.

	Mutation		MIC (μg/mL)			
N. gonorrhoeae	GyrA	ParC	Gepotidacin	Fold	Ciprofloxacin	Fold
FA1090E	WT	WT	0.25	NA	0.004	NA
FA1090E-1	A92T	WT	0.5	2	0.002	0.5
FA1090E-2	WT	D86N	0.25	1	0.004	1
FA1090E-3	**A92T**	**D86N**	**4**	**16**	**0.002**	**0.5**

Table 6.2. Gepotidacin MIC values against *N. gonorrhoeae* FA1090E NBTI target mutants. The MIC values of gepotidacin and ciprofloxacin against WT cells or cells with a presumed NBTI-resistance mutation in gyrase ($GyrA^{A92T}$), topoisomerase IV ($ParC^{D86N}$), or both ($GyrA^{A92T}$, $ParC^{D86N}$) were determined by broth dilution. The fold change from the WT strain FA1090E is given for comparison. It should be noted that the WT strain FA1090E contained an $mtrR_{-79}$ efflux allele. Data are adapted from a GlaxoSmithKline poster.[289] NA = not applicable.

Effects of gepotidacin on the DNA supercoiling activities of WT N. gonorrhoeae gyrase

Gepotidacin inhibited DNA supercoiling catalyzed by *N. gonorrhoeae* gyrase at low μM concentrations ($IC_{50} \approx 1.2$ μM) (Figure 6.7, left, black). However, the compound appeared to be ~10-fold less potent than observed against gyrase from *E. coli*. Compared to gepotidacin ciprofloxacin was more potent with an IC_{50} value of ~0.3 μM.

Effects of gepotidacin on the DNA cleavage activities of WT and mutant N. gonorrhoeae gyrase

As seen in Figure 6.8 (left panel, black), gepotidacin was a potent enhancer of DNA cleavage mediated by *N. gonorrhoeae* gyrase. Once again, only single-stranded DNA breaks were enhanced even at concentrations up to 200 μM gepotidacin (not shown). The CC_{50} was approximately 0.7 μM.

Ciprofloxacin induced primarily double-stranded breaks but was much less potent than gepotidacin ($CC_{50} \approx 7$ μM) (Figure 6.8, right panel). However, maximal levels of DNA cleavage (~26%) were higher than observed with gepotidacin (~16%). Single-stranded breaks induced by ciprofloxacin were less pronounced with the *N. gonorrhoeae* (as compared to *E. coli*) gyrase.

The effects of gepotidacin on the DNA single-stranded cleavage activity of gyrase harboring the mutation $GyrA^{A92T}$ is shown in Figure 6.8 (left panel, blue). The NBTI maintained its potency but the efficacy of the compound was reduced considerably from a maximal cleavage of ~16% (WT, black) to ~8% (A92T, blue). This finding confirms that $GyrA^{A92T}$ confers resistance at the enzyme level. However, this resistance is less than seen with the *E. coli* $GyrA^{P35L}$ resistance mutation. This may contribute to the low overall resistance observed in cellular studies with *N. gonorrhoeae*. The gyrase $GyrA^{D95G}$ fluoroquinolone resistance mutation showed little to no cross-reactivity with the NBTI (D95G, red).

The $GyrA^{D95G}$ fluoroquinolone resistance mutation conferred low levels of resistance against ciprofloxacin (Figure 6.8, right panel, red). The CC_{50} was ~2-fold higher than seen with WT gyrase and maximal levels of DNA cleavage were equivalent. Furthermore, the activity of ciprofloxacin against the

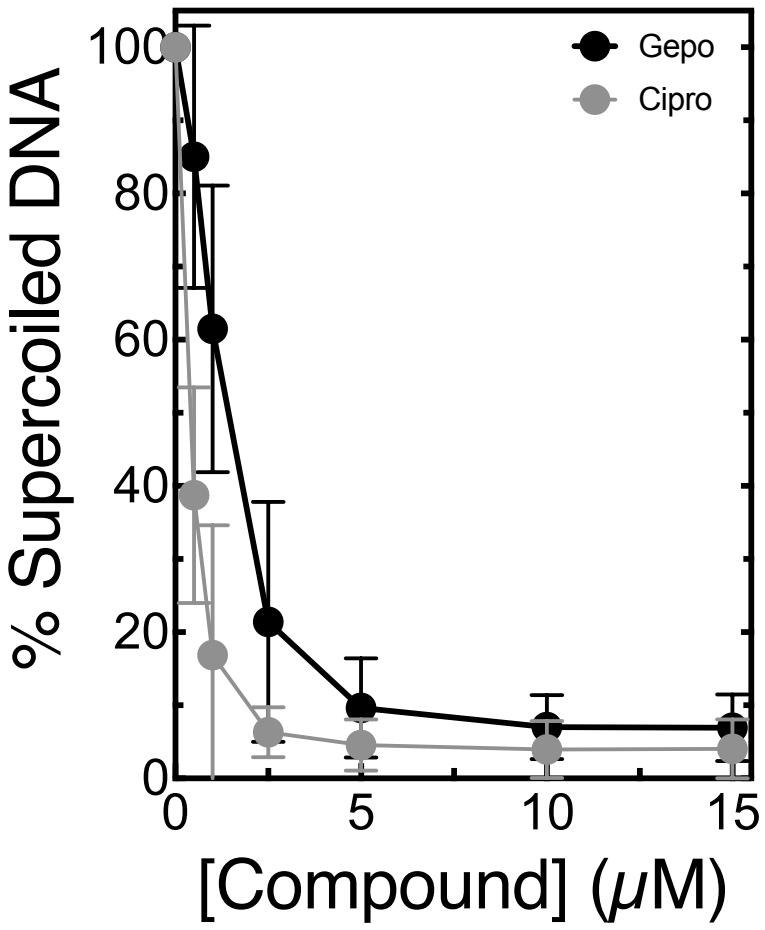

Figure 6.7. Gepotidacin inhibits DNA supercoiling catalyzed by wild-type WT *N. gonorrhoeae* gyrase. The effects of gepotidacin (black) and ciprofloxacin (grey) on the supercoiling of relaxed DNA by WT gyrase are shown. Error bars represent the SD of at least three independent experiments.

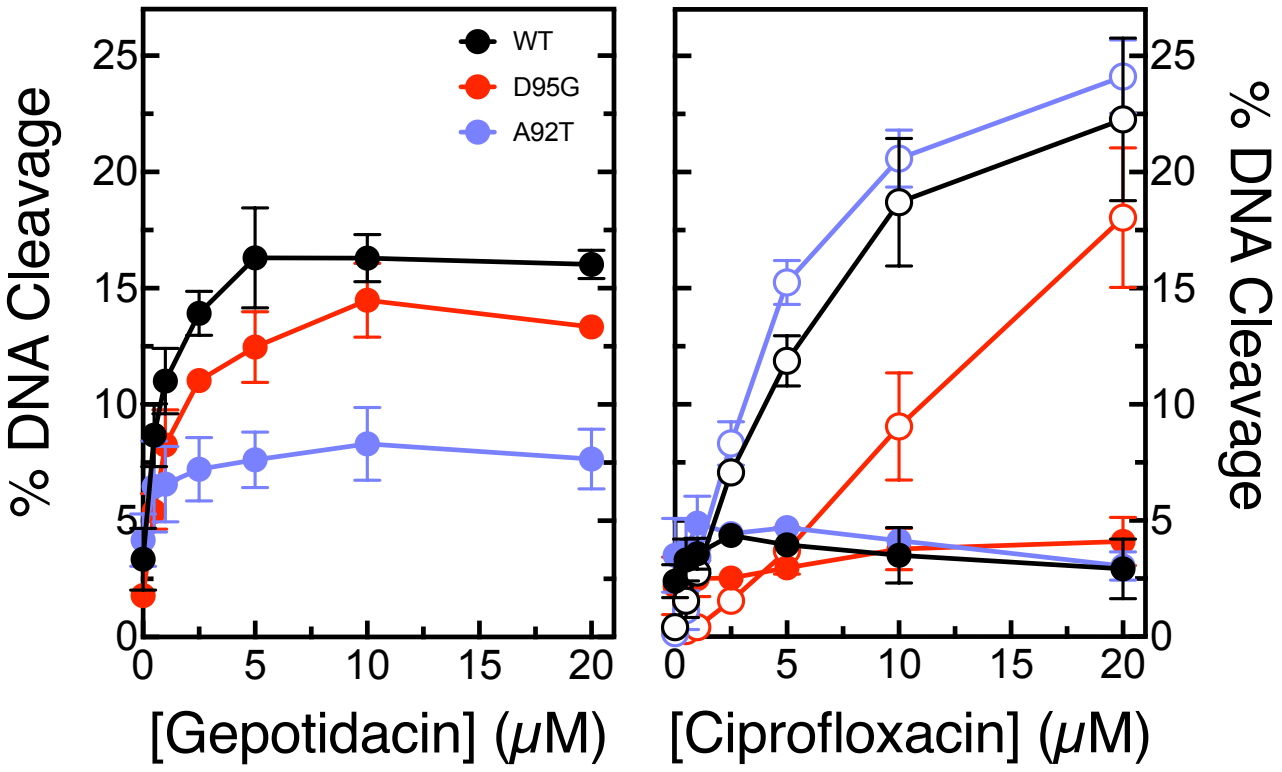

Figure 6.8. Effects of gepotidacin on DNA cleavage mediated by WT, fluoroquinolone-resistant, and NBTI-resistant *N. gonorrhoeae* gyrase. The effects of gepotidacin on single-stranded (SS, filled circles, left) and ciprofloxacin on double-stranded (DS, empty circles, right) DNA cleavage mediated by WT (black), fluoroquinolone-resistant GyrA^{D95G} (red), and NBTI-resistant GyrA^{A92T} gyrase are shown. Error bars represent the SD of at least three independent experiments.

NBTI resistance mutation was similar to WT (A92T, blue). Note that the effects of the resistance mutation on DNA supercoiling have yet to be assessed.

Effects of gepotidacin on the DNA decatenation activities of WT N. gonorrhoeae topoisomerase IV

Gepotidacin inhibited DNA decatenation catalyzed by *N. gonorrhoeae* topoisomerase IV at low μM concentrations ($IC_{50} \approx 2.1$ μM) (Figure 6.9, left panel). Although higher than the IC_{50} value observed with *E. coli* topoisomerase IV, the NBTI was considerably more potent against *N. gonorrhoeae* topoisomerase IV than was ciprofloxacin ($IC_{50} \approx 12$ μM). Note that information for drug-resistant *N. gonorrhoeae* is not yet available.

Effects of gepotidacin on the DNA cleavage activities of WT N. gonorrhoeae topoisomerase IV

Gepotidacin induced only single-stranded DNA breaks mediated by *N. gonorrhoeae* topoisomerase IV with a CC_{50} of ~0.5 μM and a maximal cleavage level of ~23% (Figure 6.10, left panel). In both respects, the NBTI was less active against *N. gonorrhoeae* topoisomerase IV than it was against the *E. coli* enzyme. Although gepotidacin was more potent against the *N. gonorrhoeae* type II enzyme than ciprofloxacin ($CC_{50} \approx 11$ μM), the fluoroquinolone induced slightly higher levels of double-stranded DNA breaks.

Conclusions

Gepotidacin is the most clinically advanced NBTI and is currently in Phase III clinical trials against uncomplicated UTIs (primarily due to *E. coli* infection) and uncomplicated urogenital gonorrhea (due to *N. gonorrhoeae*). However, nothing is known about how gepotidacin interacts with its proposed cellular targets, gyrase and topoisomerase IV. The current work was undertaken to address this critical issue.

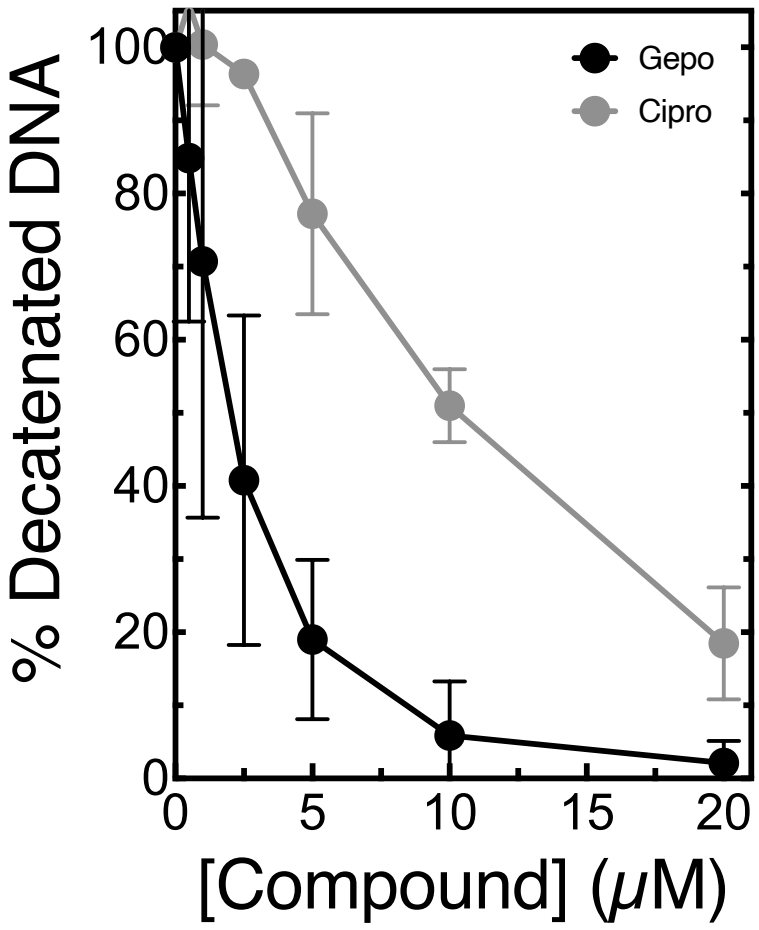

Figure 6.9. Gepotidacin inhibits DNA supercoiling catalyzed by wild-type WT *N. gonorrhoeae* topoisomerase IV. The effects of gepotidacin (black) and ciprofloxacin (grey) on the decatenation of kDNA by WT topoisomerase IV are shown. Error bars represent the SD of at least three independent experiments.

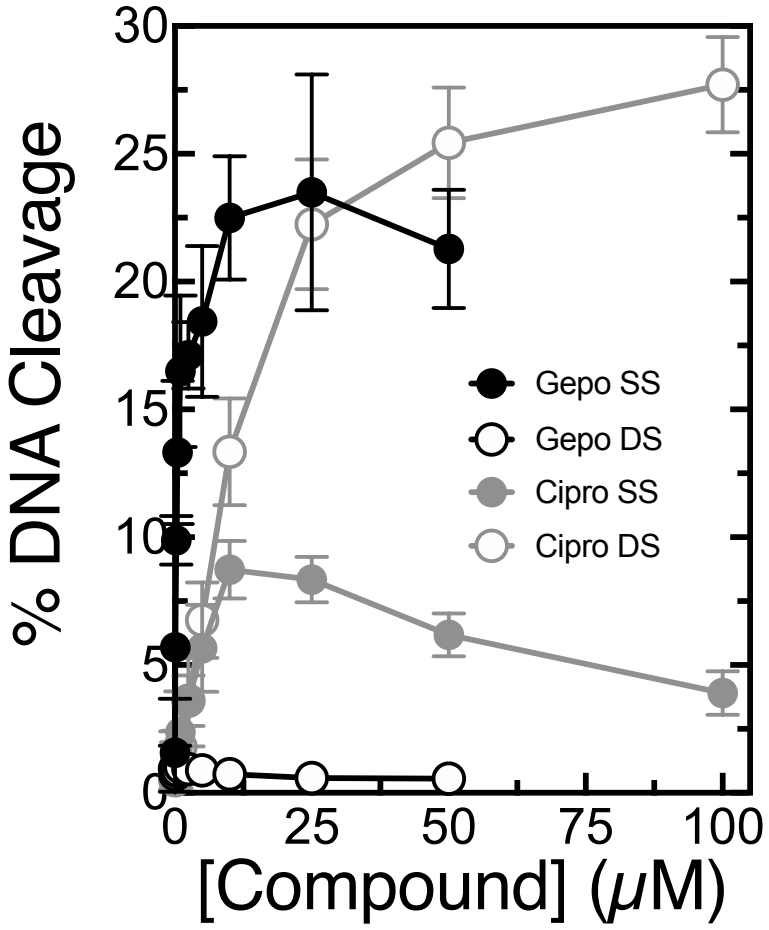

Figure 6.10. Effects of gepotidacin on DNA cleavage mediated by WT *N. gonorrhoeae* topoisomerase IV. The effects of gepotidacin on single-stranded (SS, filled circles) and double-stranded (DS, empty circles) DNA cleavage mediated by WT *E. coli* topoisomerase IV are shown in black. Corresponding data with ciprofloxacin is in grey. Error bars represent the SD of at least three independent experiments.

Cellular studies based on data from resistant clinical isolates indicate that resistance tracks with mutations in gyrase and topoisomerase IV in both *E. coli* and *N. gonorrhoeae*. Furthermore, the studies with *E. coli* provide strong evidence that gepotidacin targets both enzymes in a balanced manner. Resistant clinical isolates always contained mutations in both gyrase and topoisomerase IV. In addition, this result was recapitulated in studies with cultured isogenic strains of *E. coli*. No resistance was observed with mutation of gyrase or topoisomerase IV alone, while the strain that encoded mutations in both enzymes was 128-fold resistant to the NBTI. Gepotidacin was also found to target gyrase and topoisomerase IV in cultured *N. gonorrhoeae* strains but evidence for dual-targeting was less definitive.

In both species, ciprofloxacin appeared to be more potent than gepotidacin. The underlying basis for this finding is unclear; however, based on the present *in vitro* experiments it does not appear to reflect a weaker interaction of the NBTI with the bacterial type II topoisomerases.

In most cases with fluoroquinolones, there is not a direct correlation between cellular targeting and *in vitro* interactions of these drugs with their gyrase and topoisomerase IV targets. Frequently, stronger interactions are observed with topoisomerase IV, while genetic studies suggest that gyrase is the primary cellular target. The basis for this discrepancy is not known. It may be that gyrase is a potentially more lethal target because of its actions ahead of replication forks; inhibition of the enzyme causes a block to a critical cellular function and cleavage complexes are more likely to be converted to DNA strand breaks that must be repaired by DNA recombination pathways. Ultimately, the relationships between cellular and *in vitro* studies are further complicated by the fact that the lethal actions of fluoroquinolones have never been fully described. It is still an open question as to whether these drugs kill cells by inducing a DNA damage response or by robbing the cell of the essential functions of gyrase/topoisomerase IV. Alternatively, it may be a combination of both.

Parallel studies comparing cellular and *in vitro* data have yet to be carried out for NBTIs. Therefore, the effects of gepotidacin on the catalytic activities and DNA cleavage reaction of gyrase and topoisomerase IV were assessed. The compound was highly active against all of the enzymes examined.

With *E. coli*, gepotidacin was a more potent (~3-fold) inhibitor of gyrase-catalyzed supercoiling than it was of topoisomerase IV-catalyzed decatenation. However, it induced higher levels of DNA cleavage with topoisomerase IV at lower drug concentrations. In contrast to *E. coli*, gepotidacin displayed similar attributes for the inhibition of catalytic activity and the induction of DNA cleavage with *N. gonorrhoeae* gyrase and topoisomerase IV. Whereas these data provide incontrovertible evidence for the actions of gepotidacin against the type II topoisomerases from these species, they further point to the complicated relationships involved in cellular targeting.

Although the cellular studies demonstrated that mutations in gyrase and topoisomerase IV lead to resistance against gepotidacin, the basis for that resistance was unknown. For example, mutations could alter enzyme stability or interactions with cellular repair machinery rather than altering interactions with the compound. Therefore, the effects of gepotidacin on the catalytic activity and DNA cleavage reaction of the bacterial type II topoisomerases were examined. Gepotidacin showed decreased activity against both the GyrA^{P35L} and ParC^{D79N} mutants from *E. coli* gyrase and topoisomerase IV, respectively. Less potent inhibition of supercoiling/decatenation and lower levels of DNA cleavage were observed with these enzymes. Thus, the resistance mutations directly impair interactions between gepotidacin and the type II topoisomerases. Similarly, although with *N. gonorrhoeae* there is only cleavage data for GyrA^{A92T}, gepotidacin also generated fewer single-stranded breaks with the mutant gyrase (albeit with high potency). At the present time, it is not clear whether these mutations act primarily by decreasing gepotidacin binding or by altering its conformation in the active site of gyrase and topoisomerase IV. Further drug binding studies will be required to distinguish between these two possibilities.

To a large extent, gepotidacin appears to overcome common mutations in gyrase and topoisomerase IV that cause fluoroquinolone resistance. Single-stranded DNA breaks induced by the NBTI with *E. coli* GyrA^{S83L} were decreased. However, the compound inhibited DNA supercoiling catalyzed by the mutant gyrase with WT activity. Moreover, in all respects gepotidacin displayed WT activity against ParC^{S80L} *E.*

coli topoisomerase IV. Therefore, the compound may maintain activity against infections that are no longer susceptible to treatment with fluoroquinolones.

Ciprofloxacin was considerably more potent an inhibitor of supercoiling by *E. coli* GyrA^{P35L} but DNA cleavage was reduced considerably. The fluoroquinolone cross-resistance observed in cells harboring this NBTI-resistant enzyme may reflect this reduction in DNA cleavage. Although ParC^{D79N} *E. coli* topoisomerase IV was highly resistant to ciprofloxacin *in vitro*, this was not reflected in the cellular studies. However, this is consistent with the fact that gyrase, not topoisomerase IV, is the primary lethal target for fluoroquinolones in *E. coli*. Therefore, fluoroquinolones may retain clinically-viable activity against strains that contain NBTI-resistance mutations, at least in topoisomerase IV.

In conclusion, these studies provide strong evidence for the targeting of gyrase and topoisomerase IV by gepotidacin in *E. coli* and *N. gonorrhoeae*. Furthermore, they link clinically-relevant resistance mutations to interactions between the compound and type II topoisomerases in these species. These findings lay the groundwork for future mechanistic studies with gepotidacin and support its mechanism of action as an antibacterial agent.

CHAPTER VII

CONCLUSIONS AND IMPLICATIONS

The fields of cancer therapy and bacterial disease treatment seem, in many ways, to be on completely opposite ends of the biomedical spectrum. The former attempts to rid humans of their own compromised cells and tissues, while the latter promises eradication of foreign bodies from the human form. In reality, the two fields are much more related, and interrelated, than that. Both seek to kill the "bad" (cancerous or pathogenic) cells without harming the "good" (normal or commensal) cells. Unfortunately, current cancer therapeutic and antibacterial approaches struggle to deliver on both counts. Cancer therapies are highly toxic – unfortunately their toxicities (such as cardiomyopathy, myelosuppression, and treatment-related leukemias) are not limited to the "bad" cells. Antibacterials have a different problem – they are losing effectiveness as bacterial resistance increases.

This dissertation has sought to define potential solutions to the off-target effects of chemotherapy regimens and the rising rates of antimicrobial resistance with respect to type II topoisomerases as molecular targets. In particular, I have focused on the effects of anticancer and antibacterial compounds on these essential enzymes.

Minimizing Off-target Effects of Etoposide

Etoposide is a classic example of an important drug with terrible side effects. Its activity against the type II topoisomerases, hTIIα and hTIIβ, has been studied extensively.[63, 133, 147 137, 145, 151] The drug acts as a topoisomerase II poison, enhancing enzyme-mediated DNA scission and triggering DNA repair and cell death pathways. Unfortunately, the DNA repair pathways can lead to rearrangements in the *MLL* and *PML* genes, which can ultimately lead to secondary leukemias.[64, 132, 143, 154-156]

Consequently, the etoposide derivative F14512 was developed to minimize these adverse effects. As many cancer types have active polyamine transport, the compound replaces the C4 sugar substituent of etoposide with a spermine substituent to increase the preferential uptake of F14512 by cancer cells capable of polyamine transport.[237, 24] Importantly, the compound was shown to be a more efficacious type II topoisomerase poison than the parent drug etoposide as a result of this linkage.[245, 250] Although NMR studies indicated that the spermine moiety of F14512 did not interact with the enzyme alone,[250] modeling studies suggested that it could interact in the ternary complex (enzyme-DNA-drug).[244]

To further assess the role of the polyamine substitution, I analyzed the effects of F14512 and five other etoposide-polyamine hybrids, with varying C4 polyamine substituents, on hTIIα and hTIIβ. As Chapter III describes, these derivatives induced higher levels of cleavage with both enzymes than did etoposide. Additionally, the hybrids were more active against the β isoform. Modeling studies suggest that this differential activity may result from the enhanced specificity of interactions with a glutamine residue (Gln778) in hTIIβ that corresponds to a methionine residue in hTIIα (Met762).

The high activity of F14512 and the other hybrids against human type II topoisomerases is promising. However, there is one major caveat. The first is that studies have linked the leukemogenic properties of etoposide and other topoisomerase-targeting anticancer drugs to hTIIβ.[64, 132, 143, 154-156] The fact that these etoposide-polyamine hybrids preferentially enhance DNA cleavage mediated by the β isoform could lead to adverse effects.

F14512 has been in clinical trials for human refractory/relapsing AMLs[266] and canine lymphomas.[267, 290] Both studies have shown favorable safety profiles and anticancer activity. However, a Phase I dose-escalation study of F14512 in patients with platinum-refractory ovarian cancer was stopped due to dose-limiting toxicities, including neutropenia.[291]

It remains to be seen whether F14512 will progress through clinical approval. Despite the inconclusiveness of the clinical trial results, the enzymology and modeling studies presented in Chapter III inform future drug design for specificity toward the α isoform of human type II topoisomerase.[292,

[293]Toward that end, future work with the etoposide-polyamine hybrids will assess the effects of mutating the key Gln778 in hTIIβ to a methionine. Correspondingly, Met762 of hTIIα will be mutated to a glutamine. Effects of these mutations on the activity of the compounds will provide further insight into the binding pockets and inform hTIIα-specific anticancer drug development.

Overcoming Fluoroquinolone Resistance

By 2050, global antimicrobial resistance-related deaths may rise to 10 million annually.[209] Some of the most urgent and serious threats, according to the CDC, include *N. gonorrhoeae*, *M. tuberculosis*, and Enterobacteriaceae (*E. coli*). These bacteria, along with a Gram-positive comparator, *B. anthracis*, have been included in the studies reported in this dissertation. As discussed earlier, fluoroquinolones have been a critically important drug class for use against these and other bacterial infections. However, rising rates of fluoroquinolone resistance has undercut the utility of this antibacterial class.[48, 110, 169, 170, 173, 183-185]

The fluoroquinolones exert their antibacterial effects against the type II topoisomerases, gyrase and topoisomerase IV.[110, 168-170, 173, 176-178] Target-mediated resistance to fluoroquinolones has been demonstrated to occur as a result of mutations in the quinolone-resistance determining region (QRDR) specifically in a conserved serine and an acidic residue four amino acids downstream.[193-196] Structural studies showed that the QRDR is near the DNA cleavage/ligation active site of the type II enzymes and that the two commonly mutated amino acids in this region appeared to anchor a water-metal ion bridge to the drugs.[179, 180] Subsequent biochemical studies and crystal structures confirmed that two fluoroquinolone molecules bind to the A subunits of gyrase and topoisomerase IV in this way and stabilize double-stranded DNA cleavage.[79, 181, 202-204, 199-201]

However, utilization of the bridge is highly drug- and enzyme-dependent. For example, the water-metal ion bridge appears to support fluoroquinolone binding in *B. anthracis* gyrase and topoisomerase IV as well as *M. tuberculosis* gyrase. However, the bridge may be more important for fluoroquinolone

positioning in *E. coli* topoisomerase IV.[202] This highlights an important fact: fluoroquinolones are a broad-spectrum class of antibacterials, but their exact mechanisms of action cannot be generalized.

A major focus of this dissertation has been characterizing the effects of two compounds from an emerging class of antibacterials. The NBTIs, like fluoroquinolones, target bacterial type II topoisomerases and stabilize enzyme-mediated cleavage complex stabilization.[181, 221, 228-235] However, NBTIs do not utilize the water-metal ion bridge. Furthermore, a single NBTI molecule binds in the 2-fold axis of the protein[181, 234-236] and stabilizes only single-stranded DNA breaks.[234, 235, 236]

Chapter V reports my characterization of the first of these compounds, GSK126. We conclude that NBTIs work in a bimodal fashion, both capable of inhibiting gyrase/topoisomerase IV catalytic activity and of stabilizing cleavage complexes. However, the relative importance of these mechanisms to antibacterial activity differs between the three species used. This variability is reminiscent of the differential functioning of the water-metal ion bridge in fluoroquinolone action.

GSK126 was a potent inhibitor of catalytic activity in gyrase and topoisomerase IV from *E. coli* and *B. anthracis* as well as gyrase from *M. tuberculosis*. The compound also maintained activity, to some degree, against the corresponding fluoroquinolone resistant mutants. Additionally, the compound enhanced only single-stranded DNA cleavage with all of the enzymes examined. This observation agreed with other NBTI mechanistic studies.[234, 235, 236] In terms of cleavage, GSK126 maintained activity with all but the fluoroquinolone resistant *E. coli* enzymes.

Against *E. coli*, GSK126 appears to mediate cell kill by inhibiting enzymatic catalysis and thereby robbing cells of the critical activity of gyrase and topoisomerase IV. Conversely, enhancement of gyrase-mediated DNA breaks may play a larger role in GSK126 killing of *M. tuberculosis*. Data with *B. anthracis* are more balanced and do not suggest one mode over the other. Clearly, the fact that NBTIs target the same enzymes across a wide range of bacterial species means little in terms of their molecular actions. The mechanism by which they manifest their antibacterial properties in distinct species may be fundamentally different.

This work suggests that GSK126 may have clinical potential. One important consideration for antibacterials is off-target effects in humans, one measure of which is human ether-à-go-go-related gene (hERG) channel inhibition. These potassium channels are involved in electrical signal propagation in the heart; inhibition can lead to arrythmias, long QT syndrome, or even sudden cardiac death. The acceptable limit for FDA drug approval is >30 μM.[294] The MGI derivatives of GSK126 inhibited hERG channels with an IC_{50} of <2 μM; however, GSK126 had an IC_{50} >50 μM.[237] Despite the lack of hERG channel inhibition, GSK126 has not been a focus of further clinical development.

Mechanistic *in vitro* studies with wild-type and resistant enzymes will have to be coupled with parallel cellular studies to develop a set of "rules" that describe the actions of NBTIs. To that end, Chapter VI examines the activities of gepotidacin, a first-in-class NBTI in clinical trials, against the clinically-relevant bacteria *E. coli* and *N. gonorrhoeae* and the type II topoisomerases from these species.

Cellular studies based on data from resistant clinical isolates indicate that resistance tracks with mutations in gyrase and topoisomerase IV in both *E. coli* and *N. gonorrhoeae*. The biochemical evidence supports this hypothesis. Furthermore, the studies with *E. coli* provide strong evidence that gepotidacin targets both enzymes in a balanced manner, as no resistance was observed with mutated gyrase or topoisomerase IV alone, either in clinical isolates or in cultured isogenic strains, while the strain that encoded mutations in both enzymes was 128-fold resistant to the NBTI. Gepotidacin was also found to target gyrase and topoisomerase IV in cultured *N. gonorrhoeae* strains but evidence for dual-targeting was less definitive.

Gepotidacin was a potent inhibitor of both WT DNA supercoiling and decatenation in both species. The compound also induced only single-stranded breaks, as has been observed with other NBTIs. In terms of fluoroquinolone resistance, gepotidacin overcame mutations conferring fluoroquinolone resistance in all cases except for *E. coli* gyrase cleavage enhancement. When assessed against the *E. coli* enzymes harboring the mutations isolated from clinical trials, gepotidacin showed decreased activity. Resistant

mutant enzyme studies in *N. gonorrhoeae* are still ongoing but show gepotidacin maintaining high activity against the fluoroquinolone resistance mutation, and not the NBTI resistance mutation, in gyrase.

The combined cellular and biochemical findings are important as they support three main points: 1) gepotidacin targets gyrase and topoisomerase IV in *E. coli* and *N. gonorrhoeae*, 2) the resistance mutations found in clinical isolates alter gepotidacin-enzyme interactions and confer resistance at the enzyme level, and 3) gepotidacin exhibits well-balanced dual targeting in *E. coli*. Future studies will investigate the mechanism through which single-stranded breaks are enhanced while double-stranded scission is suppressed. To accomplish this, we will employ NBTIs that have been shown to enhance double-stranded cleavage for comparative studies and set up an oligonucleotide system for strand cleavage monitoring. Additionally, two major questions in the topoisomerase field remain. Do fluoroquinolones and NBTIs kill cells through gyrase and topoisomerase IV catalytic inhibition or through stabilization of DNA breaks? Furthermore, which is more detrimental to a cell: single- or double-stranded topoisomerase cleavage complexes? Cellular studies, including *In vivo* complex of enzyme bioassays, will be used to address these points.

Taken all together, the studies presented in Chapters V and VI make key contributions to the field. Firstly, they provide further *in vitro* evidence for the gyrase/topoisomerase IV targeting of a novel class of antibacterials. Secondly, they define the actions of GSK126 and gepotidacin against WT, fluoroquinolone-resistant, and NBTI-resistant enzymes. Moreover, the results of this dissertation suggest that at least one member of the NBTI class is a clinically-promising agent for supplementing the loss of fluoroquinolone utility. If gepotidacin completes Phase III clinical trials against UTIs, uncomplicated urogenital gonorrhea, or both, it will be the first new drug class to enter the antibacterial field since 1986. in decades.[218-220]

REFERENCES

[1] Alberts, B. (2015) *Molecular Biology of the Cell*, Sixth edition. ed., Garland Science, Taylor and Francis Group, New York, NY.

[2] Genome, N. R. C. U. C. o. M. a. S. t. H. (1988) Introduction, In *Mapping and Sequencing the Human Genome*, National Academies Press (US), Washington (DC).

[3] Bates, A. D., and Maxwell, A. (2005) *DNA Topology*, Oxford University Press, New York, USA.

[4] Buck, D. (2009) DNA topology, In *Proceedings of Symposia in Applied Mathematics: Applications of Knot Theory* (Buck, D., and Flapan, E., Eds.), pp 47-80, American Mathematical Society, Providence.

[5] Liu, Z., Deibler, R. W., Chan, H. S., and Zechiedrich, L. (2009) The why and how of DNA unlinking, *Nucleic Acids Res. 37*, 661-671.

[6] Irobalieva, R. N., Fogg, J. M., Catanese, D. J., Jr., Sutthibutpong, T., Chen, M., Barker, A. K., Ludtke, S. J., Harris, S. A., Schmid, M. F., Chiu, W., and Zechiedrich, L. (2015) Structural diversity of supercoiled DNA, *Nat Commun 6*, 8440.

[7] Finzi, L., and Olson, W. K. (2016) The emerging role of DNA supercoiling as a dynamic player in genomic structure and function, *Biophys. Rev. 8*, 1-3.

[8] Bendich, A. J., and Drlica, K. (2000) Prokaryotic and eukaryotic chromosomes: what's the difference?, *Bioessays 22*, 481-486.

[9] Wang, J. C. (2002) Cellular roles of DNA topoisomerases: a molecular perspective, *Nat. Rev. Mol. Cell Biol. 3*, 430-440.

[10] Espeli, O., and Marians, K. J. (2004) Untangling intracellular DNA topology, *Mol. Microbiol. 52*, 925-931.

[11] Deweese, J. E., Osheroff, M. A., and Osheroff, N. (2008) DNA topology and topoisomerases: teaching a "knotty" subject, *Biochem. Mol. Biol. Educ. 37*, 2-10.

[12] Chen, S. H., Chan, N. L., and Hsieh, T. S. (2013) New mechanistic and functional insights into DNA topoisomerases, *Annu. Rev. Biochem. 82*, 139-170.

[13] Ashley, R. E., and Osheroff, N. (2016) Regulation of DNA topology by topoisomerases: mathematics at the molecular level, In *Knots, Low-Dimensional Topology and Applications* (Adams, C. C., Gordon, C. M., Jones, V. F. R., Kauffman, L. H., Lambropoulou, S., Millett, K. C., Przytycki, J. H., Ricca, R., and Sazadanovic, R., Eds.), Springer, Greece.

[14] Pommier, Y., Sun, Y., Huang, S. N., and Nitiss, J. L. (2016) Roles of eukaryotic topoisomerases in transcription, replication and genomic stability, *Nat. Rev. Mol. Cell Biol. 17*, 703-721.

[15] Seol, Y., and Neuman, K. C. (2016) The dynamic interplay between DNA topoisomerases and DNA topology, *Biophys. Rev. 8*, 101-111.

[16] Flapan, E. (2000) DNATopology, In *When topology meets chemistry: A topological look at molecular chirality*, pp 198-232, Cambridge University Press.

[17] Bauer, W. R., Crick, F. H., and White, J. H. (1980) Supercoiled DNA, *Sci. Am. 243*, 100-113.

[18] White, J. H., and Cozzarelli, N. R. (1984) A simple topological method for describing stereoisomers of DNA catenanes and knots, *Proc. Natl. Acad. Sci. U. S. A. 81*, 3322-3326.

[19] Vologodskii, A. V., and Cozzarelli, N. R. (1994) Conformational and thermodynamic properties of supercoiled DNA, *Annu. Rev. Biophys. Biomol. Struct. 23*, 609-643.

[20] Shore, D., and Baldwin, R. L. (1983) Energetics of DNA twisting. II. Topoisomer analysis, *J. Mol. Biol. 170*, 983-1007.

[21] Kirkegaard, K., and Wang, J. C. (1985) Bacterial DNA topoisomerase I can relax positively supercoiled DNA containing a single-stranded loop, *J. Mol. Biol. 185*, 625-637.

[22] Awate, S., and Brosh, R. M., Jr. (2017) Interactive Roles of DNA Helicases and Translocases with the Single-Stranded DNA Binding Protein RPA in Nucleic Acid Metabolism, *Int. J. Mol. Sci. 18*.

[23] Bjorkegren, C., and Baranello, L. (2018) DNA Supercoiling, Topoisomerases, and Cohesin: Partners in Regulating Chromatin Architecture?, *Int. J. Mol. Sci. 19*.
[24] Liu, L. F., and Wang, J. C. (1978) *Micrococcus luteus* DNA gyrase: active components and a model for its supercoiling of DNA, *Proc. Natl. Acad. Sci. U. S. A. 75*, 2098-2102.
[25] Reece, R. J., and Maxwell, A. (1991) The C-terminal domain of the *Escherichia coli* DNA gyrase A subunit is a DNA-binding protein, *Nucleic Acids Res. 19*, 1399-1405.
[26] Hobson, M. J., Bryant, Z., and Berger, J. M. (2020) Modulated control of DNA supercoiling balance by the DNA-wrapping domain of bacterial gyrase, *Nucleic Acids Res. 48*, 2035-2049.
[27] Liu, L. F., and Wang, J. C. (1987) Supercoiling of the DNA template during transcription, *Proc. Natl. Acad. Sci. U. S. A. 84*, 7024-7027.
[28] Kuzminov, A. (2018) When DNA topology turns deadly - RNA polymerases dig in their R-loops to stand their ground: new positive and negative (super)twists in the replication-transcription conflict, *Trends Genet. 34*, 111-120.
[29] Koster, D. A., Crut, A., Shuman, S., Bjornsti, M. A., and Dekker, N. H. (2010) Cellular strategies for regulating DNA supercoiling: a single-molecule perspective, *Cell 142*, 519-530.
[30] Santos-Pereira, J. M., and Aguilera, A. (2015) R loops: new modulators of genome dynamics and function, *Nat Rev Genet 16*, 583-597.
[31] Chakraborty, P. (2020) New insight into the biology of R-loops, *Mutat. Res. 821*, 111711.
[32] Adams, C. (2009) A brief introduction to knot theory from the physical point of view, In *Proceedings of Symposia in Applied Mathematics: Applications of Knot Theory* (Buck, D., and Flapan, E., Eds.), pp 1-20, American Mathematical Society, Providence.
[33] Falaschi, A., Abdurashidova, G., Sandoval, O., Radulescu, S., Biamonti, G., and Riva, S. (2007) Molecular and structural transactions at human DNA replication origins, *Cell Cycle 6*, 1705-1712.
[34] Vos, S. M., Tretter, E. M., Schmidt, B. H., and Berger, J. M. (2011) All tangled up: how cells direct, manage and exploit topoisomerase function, *Nat. Rev. Mol. Cell Biol. 12*, 827-841.
[35] Postow, L., Crisona, N. J., Peter, B. J., Hardy, C. D., and Cozzarelli, N. R. (2001) Topological challenges to DNA replication: conformations at the fork, *Proc. Natl. Acad. Sci. U. S. A. 98*, 8219-8226.
[36] Schalbetter, S. A., Mansoubi, S., Chambers, A. L., Downs, J. A., and Baxter, J. (2015) Fork rotation and DNA precatenation are restricted during DNA replication to prevent chromosomal instability, *Proc. Natl. Acad. Sci. U. S. A. 112*, E4565-4570.
[37] Deweese, J. E., and Osheroff, N. (2009) The DNA cleavage reaction of topoisomerase II: wolf in sheep's clothing, *Nucleic Acids Res. 37*, 738-749.
[38] Gentry, A. C., and Osheroff, N. (2013) DNA Topoisomerases: Type II, In *The Encyclopedia of Biological Chemistry* (Lennarz W.J., a. L. M. D., Ed.), pp 163-168, Academic Press, Waltham, MA.
[39] Bush, N. G., Evans-Roberts, K., and Maxwell, A. (2015) DNA topoisomerases, *EcoSal Plus 6*.
[40] Dalvie, E. D., and Osheroff, N. (2021) DNA topoisomerases: type II, In *The Encyclopedia of Biological Chemistry* (Jez, J. M., Ed.) in press ed., Elsevier, Inc.
[41] McKie, S. J., Neuman, K. C., and Maxwell, A. (2021) DNA topoisomerases: Advances in understanding of cellular roles and multi-protein complexes via structure-function analysis, *Bioessays 43*, e2000286.
[42] Vann, K. R., Oviatt, A. A., and Osheroff, N. (2021) Topoisomerase II Poisons: Converting Essential Enzymes into Molecular Scissors, *Biochemistry 60*, 1630-1641.
[43] Wang, J. C. (1971) Interaction between DNA and an Escherichia coli protein omega, *J. Mol. Biol. 55*, 523-533.
[44] Wang, J. C. (1996) DNA topoisomerases, *Annu. Rev. Biochem. 65*, 635-692.

[45] Champoux, J. J. (2001) DNA topoisomerases: structure, function, and mechanism, *Annu. Rev. Biochem. 70*, 369-413.
[46] Schoeffler, A. J., and Berger, J. M. (2005) Recent advances in understanding structure-function relationships in the type II topoisomerase mechanism, *Biochem. Soc. Trans. 33*, 1465-1470.
[47] McClendon, A. K., and Osheroff, N. (2007) DNA topoisomerase II, genotoxicity, and cancer, *Mutat. Res. 623*, 83-97.
[48] Aldred, K. J., Kerns, R. J., and Osheroff, N. (2014) Mechanism of quinolone action and resistance, *Biochemistry 53*, 1565-1574.
[49] Bermejo, R., Doksani, Y., Capra, T., Katou, Y. M., Tanaka, H., Shirahige, K., and Foiani, M. (2007) Top1- and Top2-mediated topological transitions at replication forks ensure fork progression and stability and prevent DNA damage checkpoint activation, *Genes Dev. 21*, 1921-1936.
[50] Suski, C., and Marians, K. J. (2008) Resolution of converging replication forks by RecQ and topoisomerase III, *Mol. Cell 30*, 779-789.
[51] Berger, J. M., Gamblin, S. J., Harrison, S. C., and Wang, J. C. (1996) Structure and mechanism of DNA topoisomerase II, *Nature 379*, 225-232.
[52] Berger, J. M., Fass, D., Wang, J. C., and Harrison, S. C. (1998) Structural similarities between topoisomerases that cleave one or both DNA strands, *Proc. Natl. Acad. Sci. U. S. A. 95*, 7876-7881.
[53] Dong, K. C., and Berger, J. M. (2007) Structural basis for gate-DNA recognition and bending by type IIA topoisomerases, *Nature 450*, 1201-1205.
[54] Schmidt, B. H., Osheroff, N., and Berger, J. M. (2012) Structure of a topoisomerase II-DNA-nucleotide complex reveals a new control mechanism for ATPase activity, *Nat. Struct. Mol. Biol. 19*, 1147-1154.
[55] Chen, S. F., Huang, N. L., Lin, J. H., Wu, C. C., Wang, Y. R., Yu, Y. J., Gilson, M. K., and Chan, N. L. (2018) Structural insights into the gating of DNA passage by the topoisomerase II DNA-gate, *Nat Commun 9*, 3085.
[56] Jackson, A. P., Maxwell, A., and Wigley, D. B. (1991) Preliminary crystallographic analysis of the ATP-hydrolysing domain of the Escherichia coli DNA gyrase B protein, *J. Mol. Biol. 217*, 15-17.
[57] Wigley, D. B., Davies, G. J., Dodson, E. J., Maxwell, A., and Dodson, G. (1991) Crystal structure of an N-terminal fragment of the DNA gyrase B protein, *Nature 351*, 624-629.
[58] Morais Cabral, J. H., Jackson, A. P., Smith, C. V., Shikotra, N., Maxwell, A., and Liddington, R. C. (1997) Crystal structure of the breakage-reunion domain of DNA gyrase, *Nature 388*, 903-906.
[59] Laponogov, I., Pan, X. S., Veselkov, D. A., McAuley, K. E., Fisher, L. M., and Sanderson, M. R. (2010) Structural basis of gate-DNA breakage and resealing by type II topoisomerases, *PLoS One 5*, e11338.
[60] Vanden Broeck, A., Lotz, C., Ortiz, J., and Lamour, V. (2019) Cryo-EM structure of the complete E. coli DNA gyrase nucleoprotein complex, *Nat Commun 10*, 4935.
[61] Nitiss, J. L. (2009) DNA topoisomerase II and its growing repertoire of biological functions, *Nat. Rev. Cancer 9*, 327-337.
[62] Pommier, Y., Leo, E., Zhang, H., and Marchand, C. (2010) DNA topoisomerases and their poisoning by anticancer and antibacterial drugs, *Chem. Biol. 17*, 421-433.
[63] Pommier, Y. (2013) Drugging topoisomerases: lessons and challenges, *ACS Chem. Biol. 8*, 82-95.
[64] Pendleton, M., Lindsey, R. H., Jr., Felix, C. A., Grimwade, D., and Osheroff, N. (2014) Topoisomerase II and leukemia, *Ann. N. Y. Acad. Sci. 1310*, 98-110.
[65] McKie, S. J., Maxwell, A., and Neuman, K. C. (2020) Mapping DNA topoisomerase binding and cleavage genome wide using next-generation sequencing techniques, *Genes (Basel) 11*.

[66] Wendorff, T. J., Schmidt, B. H., Heslop, P., Austin, C. A., and Berger, J. M. (2012) The structure of DNA-bound human topoisomerase IIα: conformational mechanisms for coordinating inter-subunit interactions with DNA cleavage, *J. Mol. Biol. 424*, 109-124.
[67] Laponogov, I., Veselkov, D. A., Crevel, I. M., Pan, X. S., Fisher, L. M., and Sanderson, M. R. (2013) Structure of an 'open' clamp type II topoisomerase-DNA complex provides a mechanism for DNA capture and transport, *Nucleic Acids Res. 41*, 9911-9923.
[68] Gellert, M., Mizuuchi, K., O'Dea, M. H., and Nash, H. A. (1976) DNA gyrase: an enzyme that introduces superhelical turns into DNA, *Proc. Natl. Acad. Sci. U. S. A. 73*, 3872-3876.
[69] Goto, T., and Wang, J. C. (1982) Yeast DNA topoisomerase II. An ATP-dependent type II topoisomerase that catalyzes the catenation, decatenation, unknotting, and relaxation of double-stranded DNA rings, *J. Biol. Chem. 257*, 5866-5872.
[70] Maxwell, A., and Gellert, M. (1984) The DNA dependence of the ATPase activity of DNA gyrase, *J. Biol. Chem. 259*, 14472-14480.
[71] Kato, J., Nishimura, Y., Imamura, R., Niki, H., Hiraga, S., and Suzuki, H. (1990) New topoisomerase essential for chromosome segregation in *E. coli*, *Cell 63*, 393-404.
[72] Deweese, J. E., Burgin, A. B., and Osheroff, N. (2008) Human topoisomerase IIα uses a two-metal-ion mechanism for DNA cleavage, *Nucleic Acids Res. 36*, 4883-4893.
[73] Schmidt, B. H., Burgin, A. B., Deweese, J. E., Osheroff, N., and Berger, J. M. (2010) A novel and unified two-metal mechanism for DNA cleavage by type II and IA topoisomerases, *Nature 465*, 641-644.
[74] Zechiedrich, E. L., and Osheroff, N. (1990) Eukaryotic topoisomerases recognize nucleic acid topology by preferentially interacting with DNA crossovers, *EMBO J. 9*, 4555-4562.
[75] Kirchhausen, T., Wang, J. C., and Harrison, S. C. (1985) DNA gyrase and its complexes with DNA: direct observation by electron microscopy, *Cell 41*, 933-943.
[76] Roca, J., and Wang, J. C. (1992) The capture of a DNA double helix by an ATP-dependent protein clamp: a key step in DNA transport by type II DNA topoisomerases, *Cell 71*, 833-840.
[77] Lindsey, R. H., Jr., Pendleton, M., Ashley, R. E., Mercer, S. L., Deweese, J. E., and Osheroff, N. (2014) Catalytic core of human topoisomerase IIα: insights into enzyme-DNA interactions and drug mechanism, *Biochemistry 53*, 6595-65602.
[78] Lee, S., Jung, S. R., Heo, K., Byl, J. A., Deweese, J. E., Osheroff, N., and Hohng, S. (2012) DNA cleavage and opening reactions of human topoisomerase IIα are regulated via Mg^{2+}-mediated dynamic bending of gate-DNA, *Proc. Natl. Acad. Sci. U. S. A. 109*, 2925-2930.
[79] Bax, B. D., Murshudov, G., Maxwell, A., and Germe, T. (2019) DNA topoisomerase inhibitors: trapping a DNA-cleaving machine in motion, *J. Mol. Biol. 431*, 3427-3449.
[80] Lee, I., Dong, K. C., and Berger, J. M. (2013) The role of DNA bending in type IIA topoisomerase function, *Nucleic Acids Res. 41*, 5444-5456.
[81] Jang, Y., Son, H., Lee, S. W., Hwang, W., Jung, S. R., Byl, J. A. W., Osheroff, N., and Lee, S. (2019) Selection of DNA cleavage sites by topoisomerase II results from enzyme-induced flexibility of DNA, *Cell Chem Biol 26*, 502-511 e503.
[82] Deweese, J. E., and Osheroff, N. (2009) Coordinating the two protomer active sites of human topoisomerase IIα: nicks as topoisomerase II poisons, *Biochemistry 48*, 1439-1441.
[83] Harkins, T. T., and Lindsley, J. E. (1998) Pre-steady-state analysis of ATP hydrolysis by *Saccharomyces cerevisiae* DNA topoisomerase II. 1. A DNA-dependent burst in ATP hydrolysis, *Biochemistry 37*, 7292-7298.
[84] Aravind, L., Leipe, D. D., and Koonin, E. V. (1998) Toprim--a conserved catalytic domain in type IA and II topoisomerases, DnaG-type primases, OLD family nucleases and RecR proteins, *Nucleic Acids Res. 26*, 4205-4213.

[85] West, K. L., Meczes, E. L., Thorn, R., Turnbull, R. M., Marshall, R., and Austin, C. A. (2000) Mutagenesis of E477 or K505 in the B' domain of human topoisomerase II beta increases the requirement for magnesium ions during strand passage, *Biochemistry 39*, 1223-1233.
[86] Noble, C. G., and Maxwell, A. (2002) The role of GyrB in the DNA cleavage-religation reaction of DNA gyrase: a proposed two metal-ion mechanism, *J. Mol. Biol. 318*, 361-371.
[87] Osheroff, N. (1987) Role of the divalent cation in topoisomerase II mediated reactions, *Biochemistry 26*, 6402-6406.
[88] Osheroff, N., and Zechiedrich, E. L. (1987) Calcium-promoted DNA cleavage by eukaryotic topoisomerase II: trapping the covalent enzyme-DNA complex in an active form, *Biochemistry 26*, 4303-4309.
[89] Fortune, J. M., and Osheroff, N. (2000) Topoisomerase II as a target for anticancer drugs: when enzymes stop being nice, *Prog. Nucleic Acid Res. Mol. Biol. 64*, 221-253.
[90] Tse, Y. C., Kirkegaard, K., and Wang, J. C. (1980) Covalent bonds between protein and DNA. Formation of phosphotyrosine linkage between certain DNA topoisomerases and DNA, *J. Biol. Chem. 255*, 5560-5565.
[91] Liu, L. F., Rowe, T. C., Yang, L., Tewey, K. M., and Chen, G. L. (1983) Cleavage of DNA by mammalian DNA topoisomerase II, *J. Biol. Chem. 258*, 15365-15370.
[92] Sander, M., and Hsieh, T. (1983) Double strand DNA cleavage by type II DNA topoisomerase from Drosophila melanogaster, *J. Biol. Chem. 258*, 8421-8428.
[93] Zechiedrich, E. L., Christiansen, K., Andersen, A. H., Westergaard, O., and Osheroff, N. (1989) Double-stranded DNA cleavage/religation reaction of eukaryotic topoisomerase II: evidence for a nicked DNA intermediate, *Biochemistry 28*, 6229-6236.
[94] Liu, L. F. (1989) DNA topoisomerase poisons as antitumor drugs, *Annu. Rev. Biochem. 58*, 351-375.
[95] Levine, C., Hiasa, H., and Marians, K. J. (1998) DNA gyrase and topoisomerase IV: biochemical activities, physiological roles during chromosome replication, and drug sensitivities, *Biochim. Biophys. Acta 1400*, 29-43.
[96] Wang, J. C. (1998) Moving one DNA double helix through another by a type II DNA topoisomerase: the story of a simple molecular machine, *Q. Rev. Biophys. 31*, 107-144.
[97] Austin, C. A., Lee, K. C., Swan, R. L., Khazeem, M. M., Manville, C. M., Cridland, P., Treumann, A., Porter, A., Morris, N. J., and Cowell, I. G. (2018) TOP2B: the first thirty years, *Int. J. Mol. Sci. 19*.
[98] Drake, F. H., Hofmann, G. A., Bartus, H. F., Mattern, M. R., Crooke, S. T., and Mirabelli, C. K. (1989) Biochemical and pharmacological properties of p170 and p180 forms of topoisomerase II, *Biochemistry 28*, 8154-8160.
[99] Woessner, R. D., Mattern, M. R., Mirabelli, C. K., Johnson, R. K., and Drake, F. H. (1991) Proliferation- and cell cycle-dependent differences in expression of the 170 kilodalton and 180 kilodalton forms of topoisomerase II in NIH-3T3 cells, *Cell Growth Differ. 2*, 209-214.
[100] Padget, K., Pearson, A. D., and Austin, C. A. (2000) Quantitation of DNA topoisomerase IIα and β in human leukaemia cells by immunoblotting, *Leukemia 14*, 1997-2005.
[101] Yu, X., Davenport, J. W., Urtishak, K. A., Carillo, M. L., Gosai, S. J., Kolaris, C. P., Byl, J. A. W., Rappaport, E. F., Osheroff, N., Gregory, B. D., and Felix, C. A. (2017) Genome-wide TOP2A DNA cleavage is biased toward translocated and highly transcribed loci, *Genome Res. 27*, 1238-1249.
[102] Heintzman, D. R., Campos, L. V., Byl, J. A. W., Osheroff, N., and Dewar, J. M. (2019) Topoisomerase II is crucial for fork convergence during vertebrate replication termination, *Cell Rep 29*, 422-436 e425.

[103] Grue, P., Grasser, A., Sehested, M., Jensen, P. B., Uhse, A., Straub, T., Ness, W., and Boege, F. (1998) Essential mitotic functions of DNA topoisomerase IIα are not adopted by topoisomerase IIβ in human H69 cells, *J. Biol. Chem. 273*, 33660-33666.
[104] Christensen, M. O., Larsen, M. K., Barthelmes, H. U., Hock, R., Andersen, C. L., Kjeldsen, E., Knudsen, B. R., Westergaard, O., Boege, F., and Mielke, C. (2002) Dynamics of human DNA topoisomerases IIα and IIβ in living cells, *J. Cell Biol. 157*, 31-44.
[105] Yang, X., Li, W., Prescott, E. D., Burden, S. J., and Wang, J. C. (2000) DNA topoisomerase IIβ and neural development, *Science 287*, 131-134.
[106] Ju, B. G., Lunyak, V. V., Perissi, V., Garcia-Bassets, I., Rose, D. W., Glass, C. K., and Rosenfeld, M. G. (2006) A topoisomerase IIβ-mediated dsDNA break required for regulated transcription, *Science 312*, 1798-1802.
[107] Chen, W., Qiu, J., and Shen, Y. M. (2012) Topoisomerase IIα, rather than IIβ, is a promising target in development of anti-cancer drugs, *Drug Discov. Ther. 6*, 230-237.
[108] Cole, S. T., and Barrell, B. G. (1998) Analysis of the genome of *Mycobacterium tuberculosis* H37Rv, *Novartis Found. Symp. 217*, 160-172; discussion 172-167.
[109] Tomb, J. F., White, O., Kerlavage, A. R., Clayton, R. A., Sutton, G. G., Fleischmann, R. D., Ketchum, K. A., Klenk, H. P., Gill, S., Dougherty, B. A., Nelson, K., Quackenbush, J., Zhou, L., Kirkness, E. F., Peterson, S., Loftus, B., Richardson, D., Dodson, R., Khalak, H. G., Glodek, A., McKenney, K., Fitzegerald, L. M., Lee, N., Adams, M. D., Hickey, E. K., Berg, D. E., Gocayne, J. D., Utterback, T. R., Peterson, J. D., Kelley, J. M., Cotton, M. D., Weidman, J. M., Fujii, C., Bowman, C., Watthey, L., Wallin, E., Hayes, W. S., Borodovsky, M., Karp, P. D., Smith, H. O., Fraser, C. M., and Venter, J. C. (1997) The complete genome sequence of the gastric pathogen *Helicobacter pylori*, *Nature 388*, 539-547.
[110] Anderson, V. E., and Osheroff, N. (2001) Type II topoisomerases as targets for quinolone antibacterials: turning Dr. Jekyll into Mr. Hyde, *Curr. Pharm. Des. 7*, 337-353.
[111] Gibson, E. G., Ashley, R. E., Kerns, R. J., and Osheroff, N. (2018) Fluoroquinolone interactions with bacterial type II topoisomerases and target-mediated drug resistance, In *Antimicrobial Resistance and Implications for the 21st Century* (Drlica, K., Shlaes, D., and Fong, I. W., Eds.), pp 507-529, Springer, New York.
[112] Gellert, M. (2000) Dr. Martin Gellert Oral History 2000, In *The Office of NIH History and Stetten Museum* (Park, B. S., Ed.), NIH.
[113] Liu, L. F., and Wang, J. C. (1978) DNA-DNA gyrase complex: the wrapping of the DNA duplex outside the enzyme, *Cell 15*, 979-984.
[114] Kampranis, S. C., and Maxwell, A. (1996) Conversion of DNA gyrase into a conventional type II topoisomerase, *Proc. Natl. Acad. Sci. U. S. A. 93*, 14416-14421.
[115] Ullsperger, C., and Cozzarelli, N. R. (1996) Contrasting enzymatic acitivites of topoisomerase IV and DNA gyrase from *Escherichia coli*, *J. Biol. Chem. 271*, 31549-31555.
[116] Kramlinger, V. M., and Hiasa, H. (2006) The "GyrA-box" is required for the ability of DNA gyrase to wrap DNA and catalyze the supercoiling reaction, *J. Biol. Chem. 281*, 3738-3742.
[117] Ashley, R. E., Dittmore, A., McPherson, S. A., Turnbough, C. L., Jr., Neuman, K. C., and Osheroff, N. (2017) Activities of gyrase and topoisomerase IV on positively supercoiled DNA, *Nucleic Acids Res.*, in press.
[118] Stracy, M., Wollman, A. J. M., Kaja, E., Gapinski, J., Lee, J. E., Leek, V. A., McKie, S. J., Mitchenall, L. A., Maxwell, A., Sherratt, D. J., Leake, M. C., and Zawadzki, P. (2019) Single-molecule imaging of DNA gyrase activity in living Escherichia coli, *Nucleic Acids Res. 47*, 210-220.
[119] Weidlich, D., and Klostermeier, D. (2020) Functional interactions between gyrase subunits are optimized in a species-specific manner, *J. Biol. Chem. 295*, 2299-2312.

[120] Hirsch, J., and Klostermeier, D. (2021) What makes a type IIA topoisomerase a gyrase or a Topo IV?, *Nucleic Acids Res. 49*, 6027-6042.
[121] Marians, K. J. (1987) DNA gyrase-catalyzed decatenation of multiply linked DNA dimers, *J. Biol. Chem. 262*, 10362-10368.
[122] Sugino, A., and Cozzarelli, N. R. (1980) The intrinsic ATPase of DNA gyrase, *J. Biol. Chem. 255*, 6299-6306.
[123] Drlica, K. (1992) Control of bacterial DNA supercoiling, *Mol. Microbiol. 6*, 425-433.
[124] Wang, X., Reyes-Lamothe, R., and Sherratt, D. J. (2008) Modulation of *Escherichia coli* sister chromosome cohesion by topoisomerase IV, *Genes Dev. 22*, 2426-2433.
[125] Zawadzki, P., Stracy, M., Ginda, K., Zawadzka, K., Lesterlin, C., Kapanidis, A. N., and Sherratt, D. J. (2015) The localization and action of topoisomerase IV in *Escherichia coli* chromosome segregation is coordinated by the SMC complex, MukBEF, *Cell Rep. 13*, 2587-2596.
[126] Zechiedrich, E. L., and Cozzarelli, N. R. (1995) Roles of topoisomerase IV and DNA gyrase in DNA unlinking during replication in *Escherichia coli*., *Genes Dev. 9*, 2859-2869.
[127] Crisona, N. J., Strick, T. R., Bensimon, D., Croquette, V., and Cozzarelli, N. R. (2000) Preferential relaxation of positively supercoiled DNA by *E. coli* topoisomerase IV in single-molecule and ensemble measurements, *Genes Dev. 14*, 2881-2892.
[128] Neuman, K. C., Charvin, G., Bensimon, D., and Croquette, V. (2009) Mechanisms of chiral discrimination by topoisomerase IV, *Proc. Natl. Acad. Sci. U. S. A. 106*, 6986-6991.
[129] Sissi, C., and Palumbo, M. (2010) In front of and behind the replication fork: bacterial type IIA topoisomerases, *Cell. Mol. Life Sci. 67*, 2001-2024.
[130] Markovits, J., Pommier, Y., Kerrigan, D., Covey, J. M., Tilchen, E. J., and Kohn, K. W. (1987) Topoisomerase II-mediated DNA breaks and cytotoxicity in relation to cell proliferation and the cell cycle in NIH 3T3 fibroblasts and L1210 leukemia cells, *Cancer Res. 47*, 2050-2055.
[131] D'Arpa, P., Beardmore, C., and Liu, L. F. (1990) Involvement of nucleic acid synthesis in cell killing mechanisms of topoisomerase poisons, *Cancer Res. 50*, 6919-6924.
[132] Felix, C. A., Kolaris, C. P., and Osheroff, N. (2006) Topoisomerase II and the etiology of chromosomal translocations, *DNA Repair (Amst.) 5*, 1093-1108.
[133] Nitiss, J. L. (2009) Targeting DNA topoisomerase II in cancer chemotherapy, *Nat. Rev. Cancer 9*, 338-350.
[134] O'Sullivan, D. M., Hinds, J., Butcher, P. D., Gillespie, S. H., and McHugh, T. D. (2008) *Mycobacterium tuberculosis* DNA repair in response to subinhibitory concentrations of ciprofloxacin, *J. Antimicrob. Chemother. 62*, 1199-1202.
[135] Andoh, T., and Ishida, R. (1998) Catalytic inhibitors of DNA topoisomerase II, *Biochim. Biophys. Acta 1400*, 155-171.
[136] Larsen, A. K., Escargueil, A. E., and Skladanowski, A. (2003) Catalytic topoisomerase II inhibitors in cancer therapy, *Pharmacol. Ther. 99*, 167-181.
[137] Osheroff, N. (1989) Effect of antineoplastic agents on the DNA cleavage/religation reaction of eukaryotic topoisomerase II: inhibition of DNA religation by etoposide, *Biochemistry 28*, 6157-6160.
[138] Kane, R. C., McGuinn, W. D., Jr., Dagher, R., Justice, R., and Pazdur, R. (2008) Dexrazoxane (Totect): FDA review and approval for the treatment of accidental extravasation following intravenous anthracycline chemotherapy, *Oncologist 13*, 445-450.
[139] Pommier, Y., and Marchand, C. (2012) Interfacial inhibitors: targeting macromolecular complexes, *Nat. Rev. Drug Discov. 11*, 25-36.
[140] Mistry, A. R., Felix, C. A., Whitmarsh, R. J., Mason, A., Reiter, A., Cassinat, B., Parry, A., Walz, C., Wiemels, J. L., Segal, M. R., Ades, L., Blair, I. A., Osheroff, N., Peniket, A. J., Lafage-Pochitaloff, M., Cross, N. C., Chomienne, C., Solomon, E., Fenaux, P., and Grimwade, D.

(2005) DNA topoisomerase II in therapy-related acute promyelocytic leukemia, *N. Engl. J. Med. 352*, 1529-1538.
[141] Hasan, S. K., Mays, A. N., Ottone, T., Ledda, A., La Nasa, G., Cattaneo, C., Borlenghi, E., Melillo, L., Montefusco, E., Cervera, J., Stephen, C., Satchi, G., Lennard, A., Libura, M., Byl, J. A., Osheroff, N., Amadori, S., Felix, C. A., Voso, M. T., Sperr, W. R., Esteve, J., Sanz, M. A., Grimwade, D., and Lo-Coco, F. (2008) Molecular analysis of t(15;17) genomic breakpoints in secondary acute promyelocytic leukemia arising after treatment of multiple sclerosis, *Blood 112*, 3383-3390.
[142] Joannides, M., and Grimwade, D. (2010) Molecular biology of therapy-related leukaemias, *Clin. Transl. Oncol. 12*, 8-14.
[143] Joannides, M., Mays, A. N., Mistry, A. R., Hasan, S. K., Reiter, A., Wiemels, J. L., Felix, C. A., Coco, F. L., Osheroff, N., Solomon, E., and Grimwade, D. (2011) Molecular pathogenesis of secondary acute promyelocytic leukemia, *Mediterr. J. Hematol. Infect. Dis. 3*, e2011045.
[144] Wu, C. C., Li, Y. C., Wang, Y. R., Li, T. K., and Chan, N. L. (2013) On the structural basis and design guidelines for type II topoisomerase-targeting anticancer drugs, *Nucleic Acids Res. 41*, 10630-10640.
[145] Wu, C. C., Li, T. K., Farh, L., Lin, L. Y., Lin, T. S., Yu, Y. J., Yen, T. J., Chiang, C. W., and Chan, N. L. (2011) Structural basis of type II topoisomerase inhibition by the anticancer drug etoposide, *Science 333*, 459-462.
[146] Hande, K. R. (1998) Etoposide: four decades of development of a topoisomerase II inhibitor, *Eur. J. Cancer 34*, 1514-1521.
[147] Baldwin, E. L., and Osheroff, N. (2005) Etoposide, topoisomerase II and cancer, *Curr. Med. Chem. Anticancer Agents 5*, 363-372.
[148] Loike, J. D., Brewer, C. F., Sternlicht, H., Gensler, W. J., and Horwitz, S. B. (1978) Structure-activity study of the inhibition of microtubule assembly in vitro by podophyllotoxin and its congeners, *Cancer Res. 38*, 2688-2693.
[149] Willmore, E., Frank, A. J., Padget, K., Tilby, M. J., and Austin, C. A. (1998) Etoposide targets topoisomerase IIalpha and IIbeta in leukemic cells: isoform-specific cleavable complexes visualized and quantified in situ by a novel immunofluorescence technique, *Mol. Pharmacol. 54*, 78-85.
[150] Burden, D. A., Kingma, P. S., Froelich-Ammon, S. J., Bjornsti, M. A., Patchan, M. W., Thompson, R. B., and Osheroff, N. (1996) Topoisomerase II-etoposide interactions direct the formation of drug-induced enzyme-DNA cleavage complexes, *J. Biol. Chem. 271*, 29238-29244.
[151] Bromberg, K. D., Burgin, A. B., and Osheroff, N. (2003) A two-drug model for etoposide action against human topoisomerase IIα, *J. Biol. Chem. 278*, 7406-7412.
[152] Wilstermann, A. M., Bender, R. P., Godfrey, M., Choi, S., Anklin, C., Berkowitz, D. B., Osheroff, N., and Graves, D. E. (2007) Topoisomerase II - drug interaction domains: identification of substituents on etoposide that interact with the enzyme, *Biochemistry 46*, 8217-8225.
[153] Bender, R. P., Jablonksy, M. J., Shadid, M., Romaine, I., Dunlap, N., Anklin, C., Graves, D. E., and Osheroff, N. (2008) Substituents on etoposide that interact with human topoisomerase IIα in the binary enzyme-drug complex: contributions to etoposide binding and activity, *Biochemistry 47*, 4501-4509.
[154] Azarova, A. M., Lyu, Y. L., Lin, C. P., Tsai, Y. C., Lau, J. Y., Wang, J. C., and Liu, L. F. (2007) Roles of DNA topoisomerase II isozymes in chemotherapy and secondary malignancies, *Proc. Natl. Acad. Sci. U. S. A. 104*, 11014-11019.
[155] Cowell, I. G., Sondka, Z., Smith, K., Lee, K. C., Manville, C. M., Sidorczuk-Lesthuruge, M., Rance, H. A., Padget, K., Jackson, G. H., Adachi, N., and Austin, C. A. (2012) Model for MLL translocations in therapy-related leukemia involving topoisomerase IIβ-mediated DNA strand breaks and gene proximity, *Proc. Natl. Acad. Sci. U. S. A. 109*, 8989-8994.

[156] Cowell, I. G., and Austin, C. A. (2012) Mechanism of generation of therapy related leukemia in response to anti-topoisomerase II agents, *Int. J. Environ. Res. Public Health 9*, 2075-2091.
[157] Lyu, Y. L., Kerrigan, J. E., Lin, C. P., Azarova, A. M., Tsai, Y. C., Ban, Y., and Liu, L. F. (2007) Topoisomerase IIβ mediated DNA double-strand breaks: implications in doxorubicin cardiotoxicity and prevention by dexrazoxane, *Cancer Res. 67*, 8839-8846.
[158] Osborne, C. S., Chakalova, L., Brown, K. E., Carter, D., Horton, A., Debrand, E., Goyenechea, B., Mitchell, J. A., Lopes, S., Reik, W., and Fraser, P. (2004) Active genes dynamically colocalize to shared sites of ongoing transcription, *Nat. Genet. 36*, 1065-1071.
[159] Cook, P. R. (2010) A model for all genomes: the role of transcription factories, *J. Mol. Biol. 395*, 1-10.
[160] Strissel, P. L., Strick, R., Tomek, R. J., Roe, B. A., Rowley, J. D., and Zeleznik-Le, N. J. (2000) DNA structural properties of AF9 are similar to MLL and could act as recombination hot spots resulting in MLL/AF9 translocations and leukemogenesis, *Hum. Mol. Genet. 9*, 1671-1679.
[161] Zhang, Y., Strissel, P., Strick, R., Chen, J., Nucifora, G., Le Beau, M. M., Larson, R. A., and Rowley, J. D. (2002) Genomic DNA breakpoints in AML1/RUNX1 and ETO cluster with topoisomerase II DNA cleavage and DNase I hypersensitive sites in t(8;21) leukemia, *Proc. Natl. Acad. Sci. U. S. A. 99*, 3070-3075.
[162] Zhang, S., Liu, X., Bawa-Khalfe, T., Lu, L. S., Lyu, Y. L., Liu, L. F., and Yeh, E. T. (2012) Identification of the molecular basis of doxorubicin-induced cardiotoxicity, *Nat. Med. 18*, 1639-1642.
[163] Toyoda, E., Kagaya, S., Cowell, I. G., Kurosawa, A., Kamoshita, K., Nishikawa, K., Iiizumi, S., Koyama, H., Austin, C. A., and Adachi, N. (2008) NK314, a topoisomerase II inhibitor that specifically targets the alpha isoform, *J. Biol. Chem. 283*, 23711-23720.
[164] Ortega, J. A., Arencibia, J. M., Minniti, E., Byl, J. A. W., Franco-Ulloa, S., Borgogno, M., Genna, V., Summa, M., Bertozzi, S. M., Bertorelli, R., Armirotti, A., Minarini, A., Sissi, C., Osheroff, N., and De Vivo, M. (2020) Novel, potent, and druglike tetrahydroquinazoline inhibitor that is highly selective for human topoisomerase II α over β, *J. Med. Chem. 63*, 12873-12886.
[165] Shapiro, A. B., and Austin, C. A. (2014) A high-throughput fluorescence anisotropy-based assay for human topoisomerase II beta-catalyzed ATP-dependent supercoiled DNA relaxation, *Anal. Biochem. 448*, 23-29.
[166] Roca, J., Ishida, R., Berger, J. M., Andoh, T., and Wang, J. C. (1994) Antitumor bisdioxopiperazines inhibit yeast DNA topoisomerase II by trapping the enzyme in the form of a closed protein clamp, *Proc. Natl. Acad. Sci. U. S. A. 91*, 1781-1785.
[167] Hasinoff, B. B., Patel, D., and Wu, X. (2020) The Role of Topoisomerase IIbeta in the Mechanisms of Action of the Doxorubicin Cardioprotective Agent Dexrazoxane, *Cardiovasc. Toxicol. 20*, 312-320.
[168] Hooper, D. C. (1999) Mode of action of fluoroquinolones, *Drugs 58 Suppl. 2*, 6-10.
[169] Hooper, D. C. (2001) Mechanisms of action of antimicrobials: focus on fluoroquinolones, *Clin. Infect. Dis. 32 Suppl. 1*, S9-S15.
[170] Drlica, K., Hiasa, H., Kerns, R., Malik, M., Mustaev, A., and Zhao, X. (2009) Quinolones: action and resistance updated, *Curr. Top. Med. Chem. 9*, 981-998.
[171] (2012) Outpatient quinolone use, *The Center for Disease Dynamics, Economics & Policy*, Resistance Map.
[172] Hooper, D. C. (1998) Clinical applications of quinolones, *Biochim. Biophys. Acta 1400*, 45-61.
[173] Andriole, V. T. (2005) The quinolones: past, present, and future, *Clin. Infect. Dis. 41 Suppl. 2*, S113-119.
[174] Lesher, G. Y., Froelich, E. J., Gruett, M. D., Bailey, J. H., and Brundage, R. P. (1962) 1,8-Naphthyridine derivatives. A new class of chemotherapeutic agents, *J. Med. Pharm. Chem. 91*, 1063-1065.

[175] Bayer HealthCare Pharmaceuticals. CIPRO (ciprofloxacin) [package insert]. U.S. Food and Drug Administration website. https://www.accessdata.fda.gov/drugsatfda_docs/label/2016/019537s086lbl.pdf Revised July 2016.
[176] Shen, L. L., Mitscher, L. A., Sharma, P. N., O'Donnell, T. J., Chu, D. W., Cooper, C. S., Rosen, T., and Pernet, A. G. (1989) Mechanism of inhibition of DNA gyrase by quinolone antibacterials: a cooperative drug--DNA binding model, *Biochemistry 28*, 3886-3894.
[177] Mitscher, L. A. (2005) Bacterial topoisomerase inhibitors: quinolone and pyridone antibacterial agents, *Chem. Rev. 105*, 559-592.
[178] Drlica, K., Malik, M., Kerns, R. J., and Zhao, X. (2008) Quinolone-mediated bacterial death, *Antimicrob. Agents Chemother. 52*, 385-392.
[179] Laponogov, I., Sohi, M. K., Veselkov, D. A., Pan, X. S., Sawhney, R., Thompson, A. W., McAuley, K. E., Fisher, L. M., and Sanderson, M. R. (2009) Structural insight into the quinolone-DNA cleavage complex of type IIA topoisomerases, *Nat. Struct. Mol. Biol. 16*, 667-669.
[180] Wohlkonig, A., Chan, P. F., Fosberry, A. P., Homes, P., Huang, J., Kranz, M., Leydon, V. R., Miles, T. J., Pearson, N. D., Perera, R. L., Shillings, A. J., Gwynn, M. N., and Bax, B. D. (2010) Structural basis of quinolone inhibition of type IIA topoisomerases and target-mediated resistance, *Nat. Struct. Mol. Biol. 17*, 1152-1153.
[181] Bax, B. D., Chan, P. F., Eggleston, D. S., Fosberry, A., Gentry, D. R., Gorrec, F., Giordano, I., Hann, M. M., Hennessy, A., Hibbs, M., Huang, J., Jones, E., Jones, J., Brown, K. K., Lewis, C. J., May, E. W., Saunders, M. R., Singh, O., Spitzfaden, C. E., Shen, C., Shillings, A., Theobald, A. J., Wohlkonig, A., Pearson, N. D., and Gwynn, M. N. (2010) Type IIA topoisomerase inhibition by a new class of antibacterial agents, *Nature 466*, 935-940.
[182] Vanden Broeck, A., McEwen, A. G., Chebaro, Y., Potier, N., and Lamour, V. (2019) Structural Basis for DNA Gyrase Interaction with Coumermycin A1, *J. Med. Chem. 62*, 4225-4231.
[183] Emmerson, A. M., and Jones, A. M. (2003) The quinolones: decades of development and use, *J. Antimicrob. Chemother. 51 Suppl 1*, 13-20.
[184] Martinez-Martinez, L., Pascual, A., Garcia, I., Tran, J., and Jacoby, G. A. (2003) Interaction of plasmid and host quinolone resistance, *J. Antimicrob. Chemother. 51*, 1037-1039.
[185] Hooper, D. C., and Jacoby, G. A. (2015) Mechanisms of drug resistance: quinolone resistance, *Ann. N. Y. Acad. Sci. 1354*, 12-31.
[186] Norrby, S. R. (1989) Ciprofloxacin in the treatment of acute and chronic osteomyelitis: a review, *Scand. J. Infect. Dis. Suppl. 60*, 74-78.
[187] CDC. (2013) Antibiotic Resistance Threats in the United States.
[188] Davies, J., and Davies, D. (2010) Origins and evolution of antibiotic resistance, *Microbiol. Mol. Biol. Rev. 74*, 417-433.
[189] Tran, J. H., and Jacoby, G. A. (2002) Mechanism of plasmid-mediated quinolone resistance, *Proc. Natl. Acad. Sci. USA 99*, 5638-5642.
[190] Tran, J. H., Jacoby, G. A., and Hooper, D. C. (2005) Interaction of the plasmid-encoded quinolone resistance protein QnrA with Escherichia coli topoisomerase IV, *Antimicrob. Agents Chemother. 49*, 3050-3052.
[191] Tran, J. H., Jacoby, G. A., and Hooper, D. C. (2005) Interaction of the plasmid-encoded quinolone resistance protein Qnr with Escherichia coli DNA gyrase, *Antimicrob. Agents Chemother. 49*, 118-125.
[192] Yamane, K., Wachino, J., Suzuki, S., Kimura, K., Shibata, N., Kato, H., Shibayama, K., Konda, T., and Arakawa, Y. (2007) New plasmid-mediated fluoroquinolone efflux pump, QepA, found in an Escherichia coli clinical isolate, *Antimicrob. Agents Chemother. 51*, 3354-3360.

[193] Price, L. B., Vogler, A., Pearson, T., Busch, J. D., Schupp, J. M., and Keim, P. (2003) *In vitro* selection and characterization of *Bacillus anthracis* mutants with high-level resistance to ciprofloxacin, *Antimicrob. Agents Chemother. 47*, 2362-2365.
[194] Morgan-Linnell, S. K., Becnel Boyd, L., Steffen, D., and Zechiedrich, L. (2009) Mechanisms accounting for fluoroquinolone resistance in *Escherichia coli* clinical isolates, *Antimicrob. Agents Chemother. 53*, 235-241.
[195] Malik, M., Marks, K. R., Mustaev, A., Zhao, X., Chavda, K., Kerns, R. J., and Drlica, K. (2011) Fluoroquinolone and quinazolinedione activities against wild-type and gyrase mutant strains of *Mycobacterium smegmatis*, *Antimicrob. Agents Chemother. 55*, 2335-2343.
[196] Malik, M., Mustaev, A., Schwanz, H. A., Luan, G., Shah, N., Oppegard, L. M., de Souza, E. C., Hiasa, H., Zhao, X., Kerns, R. J., and Drlica, K. (2016) Suppression of gyrase-mediated resistance by C7 aryl fluoroquinolones, *Nucleic Acids Res. 44*, 3304-3316.
[197] Khodursky, A. B., Zechiedrich, E. L., and Cozzarelli, N. R. (1995) Topoisomerase IV is a target of quinolones in *Escherichia coli*, *Proc. Natl. Acad. Sci. U. S. A. 92*, 11801-11805.
[198] Hiasa, H. (2002) The Glu-84 of the ParC subunit plays critical roles in both topoisomerase IV-quinolone and topoisomerase IV-DNA interactions, *Biochemistry 41*, 11779-11785.
[199] Aldred, K. J., McPherson, S. A., Turnbough, C. L., Kerns, R. J., and Osheroff, N. (2013) Topoisomerase IV-quinolone interactions are mediated through a water-metal ion bridge: mechanistic basis of quinolone resistance, *Nucleic Acids Res. 41*, 4628-4639.
[200] Aldred, K. J., McPherson, S. A., Wang, P., Kerns, R. J., Graves, D. E., Turnbough, C. L., and Osheroff, N. (2012) Drug interactions with *Bacillus anthracis* topoisomerase IV: biochemical basis for quinolone action and resistance, *Biochemistry 51*, 370-381.
[201] Aldred, K. J., Schwanz, H. A., Li, G., McPherson, S. A., Turnbough, C. L., Kerns, R. J., and Osheroff, N. (2013) Overcoming target-mediated quinolone resistance in topoisomerase IV by introducing metal-ion-independent drug–enzyme interactions, *ACS Chem. Biol.*, 2660-2668.
[202] Aldred, K. J., Breland, E. J., Vlčková, V., Strub, M. P., Neuman, K. C., Kerns, R. J., and Osheroff, N. (2014) Role of the water-metal ion bridge in mediating interactions between quinolones and *Escherichia coli* topoisomerase IV, *Biochemistry 53*, 5558-5567.
[203] Aldred, K. J., Blower, T. R., Kerns, R. J., Berger, J. M., and Osheroff, N. (2016) Fluoroquinolone interactions with *Mycobacterium tuberculosis* gyrase: enhancing drug activity against wild-type and resistant gyrase, *Proc. Natl. Acad. Sci. U. S. A. 113*, E839-E846.
[204] Ashley, R. E., Lindsey, R. H., Jr., McPherson, S. A., Turnbough, C. L., Jr., Kerns, R. J., and Osheroff, N. (2017) Interactions between quinolones and *Bacillus anthracis* gyrase and the basis of drug resistance, *Biochemistry 56*, 4191-4200.
[205] Aldred, K. J., Schwanz, H. A., Li, G., Williamson, B. H., McPherson, S. A., Turnbough, C. L., Jr., Kerns, R. J., and Osheroff, N. (2015) Activity of quinolone CP-115,955 against bacterial and human type II topoisomerases is mediated by different interactions, *Biochemistry 54*, 1278-1286.
[206] CDC. (2019) Antibiotic Resistance Threats in the United States.
[207] Organization, W. H. (2015) Global Action Plan on Antimicrobial Resistance.
[208] Antimicrobial Resistance, C. (2022) Global burden of bacterial antimicrobial resistance in 2019: a systematic analysis, *Lancet 399*, 629-655.
[209] O'Neill, J. (2014)

Antimicrobial Resistance: Tackling a Crisis for the Health and Wealth of Nations

, In *The Review on Antimicrobial Resistance*, London.
[210] (2004) Bad bugs, no drugs: As antibiotic discover stagnates, a public health crisis brews, *The Infectious Diseases Society of America*.
[211] WHO. (2016) World Health Organization sexually transmitted infections (STIs) fact sheet.

[212] Whelan, J., Abbing-Karahagopian, V., Serino, L., and Unemo, M. (2021) Gonorrhoea: a systematic review of prevalence reporting globally, *BMC Infect. Dis. 21*, 1152.
[213] CDC. (2016) Gonorrheae - 2016 STD surveillance report.
[214] CDC. (2018) Sexually transmitted disease surveillance 2018.
[215] CDC. (2017) Gonorrhea - CDC Fact Sheet (Detailed Version).
[216] Fleming, D. T. a. W., J.N. (1999) From epidemiological synergy to public health policy and practice: the contribution of sexually transmitted diseases to sexual transmission of HIV infection, *Sex. Transm. Infect. 75*, 3-17.
[217] CDC. (2006) Update to CDC's Sexually Transmitted Diseases Treatment Guidelines, 2006: fluoroquinolones no longer recommended for treatment of gonococcal infections, In *MMWR*, pp 332-336.
[218] Ventola, C. L. (2015) The antibiotic resistance crisis: part 1: causes and threats, *P T 40*, 277-283.
[219] Trusts, T. P. C. (2016) A scientific roadmap for antibiotic discovery, The Pew Charitable Trusts, 2016.
[220] Miethke, M., Pieroni, M., Weber, T., Bronstrup, M., Hammann, P., Halby, L., Arimondo, P. B., Glaser, P., Aigle, B., Bode, H. B., Moreira, R., Li, Y., Luzhetskyy, A., Medema, M. H., Pernodet, J. L., Stadler, M., Tormo, J. R., Genilloud, O., Truman, A. W., Weissman, K. J., Takano, E., Sabatini, S., Stegmann, E., Brotz-Oesterhelt, H., Wohlleben, W., Seemann, M., Empting, M., Hirsch, A. K. H., Loretz, B., Lehr, C. M., Titz, A., Herrmann, J., Jaeger, T., Alt, S., Hesterkamp, T., Winterhalter, M., Schiefer, A., Pfarr, K., Hoerauf, A., Graz, H., Graz, M., Lindvall, M., Ramurthy, S., Karlen, A., van Dongen, M., Petkovic, H., Keller, A., Peyrane, F., Donadio, S., Fraisse, L., Piddock, L. J. V., Gilbert, I. H., Moser, H. E., and Muller, R. (2021) Towards the sustainable discovery and development of new antibiotics, *Nat Rev Chem 5*, 726-749.
[221] Dougherty, T. J., Nayar, A., Newman, J. V., Hopkins, S., Stone, G. G., Johnstone, M., Shapiro, A. B., Cronin, M., Reck, F., and Ehmann, D. E. (2014) NBTI 5463 is a novel bacterial type II topoisomerase inhibitor with activity against gram-negative bacteria and *in vivo* efficacy, *Antimicrob. Agents Chemother. 58*, 2657-2664.
[222] Hiasa, H. (2018) DNA topoisomerases as targets for antibacterial agents, *Methods Mol. Biol. 1703*, 47-62.
[223] Huband, M. D., Bradford, P. A., Otterson, L. G., Basarab, G. S., Kutschke, A. C., Giacobbe, R. A., Patey, S. A., Alm, R. A., Johnstone, M. R., Potter, M. E., Miller, P. F., and Mueller, J. P. (2015) *In vitro* antibacterial activity of AZD0914, a new spiropyrimidinetrione DNA gyrase/topoisomerase inhibitor with potent activity against Gram-positive, fastidious Gram-Negative, and atypical bacteria, *Antimicrob. Agents Chemother. 59*, 467-474.
[224] Kern, G., Palmer, T., Ehmann, D. E., Shapiro, A. B., Andrews, B., Basarab, G. S., Doig, P., Fan, J., Gao, N., Mills, S. D., Mueller, J., Sriram, S., Thresher, J., and Walkup, G. K. (2015) Inhibition of *Neisseria gonorrhoeae* type II topoisomerases by the novel spiropyrimidinetrione AZD0914, *J. Biol. Chem. 290*, 20984-20994.
[225] Giacobbe, R. A., Huband, M. D., deJonge, B. L., and Bradford, P. A. (2017) Effect of susceptibility testing conditions on the *in vitro* antibacterial activity of ETX0914, *Diagn. Microbiol. Infect. Dis. 87*, 139-142.
[226] Coates, W. J., Gwynn, M.N., Hatton, I.K., Masters, P.J., Pearson, N.D., Rahman, S.S., Slocombe, B., and Warrack, J.D. (1999) Preparation of piperidinylalkylquinolines as antibacterials, In *United States Patent W09937635*.
[227] Gomez, L., Hack, M. D., Wu, J., Wiener, J. J., Venkatesan, H., Santillan, A., Jr., Pippel, D. J., Mani, N., Morrow, B. J., Motley, S. T., Shaw, K. J., Wolin, R., Grice, C. A., and Jones, T. K. (2007) Novel pyrazole derivatives as potent inhibitors of type II topoisomerases. Part 1: synthesis and preliminary SAR analysis, *Bioorg. Med. Chem. Lett. 17*, 2723-2727.

[228] Black, M. T., Stachyra, T., Platel, D., Girard, A. M., Claudon, M., Bruneau, J. M., and Miossec, C. (2008) Mechanism of action of the antibiotic NXL101, a novel nonfluoroquinolone inhibitor of bacterial type II topoisomerases, *Antimicrob. Agents Chemother. 52*, 3339-3349.
[229] Surivet, J. P., Zumbrunn, C., Rueedi, G., Hubschwerlen, C., Bur, D., Bruyere, T., Locher, H., Ritz, D., Keck, W., Seiler, P., Kohl, C., Gauvin, J. C., Mirre, A., Kaegi, V., Dos Santos, M., Gaertner, M., Delers, J., Enderlin-Paput, M., and Boehme, M. (2013) Design, synthesis, and characterization of novel tetrahydropyran-based bacterial topoisomerase inhibitors with potent anti-gram-positive activity, *J. Med. Chem. 56*, 7396-7415.
[230] Singh, S. B., Kaelin, D. E., Wu, J., Miesel, L., Tan, C. M., Meinke, P. T., Olsen, D., Lagrutta, A., Bradley, P., Lu, J., Patel, S., Rickert, K. W., Smith, R. F., Soisson, S., Wei, C., Fukuda, H., Kishii, R., Takei, M., and Fukuda, Y. (2014) Oxabicyclooctane-linked novel bacterial topoisomerase inhibitors as broad spectrum antibacterial agents, *ACS Med. Chem. Lett. 5*, 609-614.
[231] Biedenbach, D. J., Bouchillon, S. K., Hackel, M., Miller, L. A., Scangarella-Oman, N. E., Jakielaszek, C., and Sahm, D. F. (2016) *In vitro* activity of gepotidacin, a novel triazaacenaphthylene bacterial topoisomerase inhibitor, against a broad spectrum of bacterial pathogens, *Antimicrob. Agents Chemother. 60*, 1918-1923.
[232] Charrier, C., Salisbury, A. M., Savage, V. J., Duffy, T., Moyo, E., Chaffer-Malam, N., Ooi, N., Newman, R., Cheung, J., Metzger, R., McGarry, D., Pichowicz, M., Sigerson, R., Cooper, I. R., Nelson, G., Butler, H. S., Craighead, M., Ratcliffe, A. J., Best, S. A., and Stokes, N. R. (2017) Novel bacterial topoisomerase inhibitors with potent broad-spectrum activity against drug-resistant bacteria, *Antimicrob. Agents Chemother. 61*, e02100-02116.
[233] Mitton-Fry, M. J., Brickner, S. J., Hamel, J. C., Barham, R., Brennan, L., Casavant, J. M., Ding, X., Finegan, S., Hardink, J., Hoang, T., Huband, M. D., Maloney, M., Marfat, A., McCurdy, S. P., McLeod, D., Subramanyam, C., Plotkin, M., Reilly, U., Schafer, J., Stone, G. G., Uccello, D. P., Wisialowski, T., Yoon, K., Zaniewski, R., and Zook, C. (2017) Novel 3-fluoro-6-methoxyquinoline derivatives as inhibitors of bacterial DNA gyrase and topoisomerase IV, *Bioorg. Med. Chem. Lett. 27*, 3353-3358.
[234] Gibson, E. G., Blower, T. R., Cacho, M., Bax, B., Berger, J. M., and Osheroff, N. (2018) Mechanism of action of *Mycobacterium tuberculosis* gyrase inhibitors: a novel class of gyrase poisons, *ACS Infect. Dis. 4*, 1211-1222.
[235] Gibson, E. G., Bax, B., Chan, P. F., and Osheroff, N. (2019) Mechanistic and structural basis for the actions of the antibacterial gepotidacin against *Staphylococcus aureus* gyrase, *ACS Infect. Dis. 5*, 570-581.
[236] Kolaric, A., Anderluh, M., and Minovski, N. (2020) Two Decades of Successful SAR-Grounded Stories of the Novel Bacterial Topoisomerase Inhibitors (NBTIs), *J. Med. Chem. 63*, 5664-5674.
[237] Blanco, D., Perez-Herran, E., Cacho, M., Ballell, L., Castro, J., Gonzalez Del Rio, R., Lavandera, J. L., Remuinan, M. J., Richards, C., Rullas, J., Vazquez-Muniz, M. J., Woldu, E., Zapatero-Gonzalez, M. C., Angulo-Barturen, I., Mendoza, A., and Barros, D. (2015) *Mycobacterium tuberculosis* gyrase inhibitors as a new class of antitubercular drugs, *Antimicrob. Agents Chemother. 59*, 1868-1875.
[238] Li, L., Okumu, A. A., Nolan, S., English, A., Vibhute, S., Lu, Y., Hervert-Thomas, K., Seffernick, J. T., Azap, L., Cole, S. L., Shinabarger, D., Koeth, L. M., Lindert, S., Yalowich, J. C., Wozniak, D. J., and Mitton-Fry, M. J. (2019) 1,3-dioxane-linked bacterial topoisomerase inhibitors with enhanced antibacterial activity and reduced hERG inhibition, *ACS Infect. Dis. 5*, 1115-1128.
[239] Partnership, G. A. R. a. D. (2021) A Multi-center, Randomized, Open-label, Non Inferiority Trial to Evaluate the Efficacy and Safety of a Single, Oral Dose of Zoliflodacin Compared to a Combination of a Single Intramuscular Dose of Ceftriaxone and a Single Oral Dose of Azithromycin in the Treatment of Patients With Uncomplicated Gonorrhoea, ClinTrials.gov.

[240] Gibson, E. G., Oviatt, A. A., and Osheroff, N. (2020) Two-Dimensional Gel Electrophoresis to Resolve DNA Topoisomers, *Methods Mol. Biol. 2119*, 15-24.
[241] Oviatt, A. A., Kuriappan, J. A., Minniti, E., Vann, K. R., Onuorah, P., Minarini, A., De Vivo, M., and Osheroff, N. (2018) Polyamine-containing etoposide derivatives as poisons of human type II topoisomerases: Differential effects on topoisomerase IIalpha and IIbeta, *Bioorg. Med. Chem. Lett. 28*, 2961-2968.
[242] Gibson, E. G., Oviatt, A. A., Cacho, M., Neuman, K. C., Chan, P. F., and Osheroff, N. (2019) Bimodal Actions of a Naphthyridone/Aminopiperidine-Based Antibacterial That Targets Gyrase and Topoisomerase IV, *Biochemistry 58*, 4447-4455.
[243] Englund, P. T. (1978) The replication of kinetoplast DNA networks in *Crithidia fasciculata*, *Cell 14*, 157-168.
[244] Palermo, G., Minniti, E., Greco, M. L., Riccardi, L., Simoni, E., Convertino, M., Marchetti, C., Rosini, M., Sissi, C., Minarini, A., and De Vivo, M. (2015) An optimized polyamine moiety boosts the potency of human type II topoisomerase poisons as quantified by comparative analysis centered on the clinical candidate F14512, *Chem. Commun. (Camb.) 51*, 14310-14313.
[245] Barret, J. M., Kruczynski, A., Vispe, S., Annereau, J. P., Brel, V., Guminski, Y., Delcros, J. G., Lansiaux, A., Guilbaud, N., Imbert, T., and Bailly, C. (2008) F14512, a potent antitumor agent targeting topoisomerase II vectored into cancer cells via the polyamine transport system, *Cancer Res. 68*, 9845-9853.
[246] Worland, S. T., and Wang, J. C. (1989) Inducible overexpression, purification, and active site mapping of DNA topoisomerase II from the yeast *Saccharomyces cerevisiae*, *J. Biol. Chem. 264*, 4412-4416.
[247] Kingma, P. S., Greider, C. A., and Osheroff, N. (1997) Spontaneous DNA lesions poison human topoisomerase IIα and stimulate cleavage proximal to leukemic 11q23 chromosomal breakpoints, *Biochemistry 36*, 5934-5939.
[248] Fortune, J. M., and Osheroff, N. (1998) Merbarone inhibits the catalytic activity of human topoisomerase IIα by blocking DNA cleavage, *J. Biol. Chem. 273*, 17643-17650.
[249] Byl, J. A., Fortune, J. M., Burden, D. A., Nitiss, J. L., Utsugi, T., Yamada, Y., and Osheroff, N. (1999) DNA topoisomerases as targets for the anticancer drug TAS-103: primary cellular target and DNA cleavage enhancement, *Biochemistry 38*, 15573-15579.
[250] Gentry, A. C., Pitts, S. L., Jablonsky, M. J., Bailly, C., Graves, D. E., and Osheroff, N. (2011) Interactions between the etoposide derivative F14512 and human type II topoisomerases: implications for the C4 spermine moiety in promoting enzyme-mediated DNA cleavage, *Biochemistry 50*, 3240-3249.
[251] Wang, Y. R., Chen, S. F., Wu, C. C., Liao, Y. W., Lin, T. S., Liu, K. T., Chen, Y. S., Li, T. K., Chien, T. C., and Chan, N. L. (2017) Producing irreversible topoisomerase II-mediated DNA breaks by site-specific Pt(II)-methionine coordination chemistry, *Nucleic Acids Res. 45*, 10920.
[252] Sastry, G. M., Adzhigirey, M., Day, T., Annabhimoju, R., and Sherman, W. (2013) Protein and ligand preparation: parameters, protocols, and influence on virtual screening enrichments, *J. Comput. Aided Mol. Des. 27*, 221-234.
[253] Friesner, R. A., Murphy, R. B., Repasky, M. P., Frye, L. L., Greenwood, J. R., Halgren, T. A., Sanschagrin, P. C., and Mainz, D. T. (2006) Extra precision glide: docking and scoring incorporating a model of hydrophobic enclosure for protein-ligand complexes, *J. Med. Chem. 49*, 6177-6196.
[254] Farid, R., Day, T., Friesner, R. A., and Pearlstein, R. A. (2006) New insights about HERG blockade obtained from protein modeling, potential energy mapping, and docking studies, *Bioorg. Med. Chem. 14*, 3160-3173.
[255] Sherman, W., Day, T., Jacobson, M. P., Friesner, R. A., and Farid, R. (2006) Novel procedure for modeling ligand/receptor induced fit effects, *J. Med. Chem. 49*, 534-553.

[256] Dong, S., McPherson, S. A., Wang, Y., Li, M., Wang, P., Turnbough, C. L., Jr., and Pritchard, D. G. (2010) Characterization of the enzymes encoded by the anthrose biosynthetic operon of *Bacillus anthracis*, *J. Bacteriol. 192*, 5053-5062.
[257] Maxwell, A., and Howells, A. J. (1999) Overexpression and purification of bacterial DNA gyrase, *Methods Mol. Biol. 94*, 135-144.
[258] Peng, H., and Marians, K. J. (1993) *Escherichia coli* topoisomerase IV. Purification, characterization, subunit structure, and subunit interactions, *J. Biol. Chem. 268*, 24481-24490.
[259] Corbett, K. D., Schoeffler, A. J., Thomsen, N. D., and Berger, J. M. (2005) The structural basis for substrate specificity in DNA topoisomerase IV, *J. Mol. Biol. 351*, 545-561.
[260] Blower, T. R., Williamson, B. H., Kerns, R. J., and Berger, J. M. (2016) Crystal structure and stability of gyrase-fluoroquinolone cleaved complexes from *Mycobacterium tuberculosis*, *Proc. Natl. Acad. Sci. U. S. A. 113*, 1706-1713.
[261] Anderson, V. E., Gootz, T. D., and Osheroff, N. (1998) Topoisomerase IV catalysis and the mechanism of quinolone action, *J. Biol. Chem. 273*, 17879-17885.
[262] Ashley, R. E., Blower, T. R., Berger, J. M., and Osheroff, N. (2017) Recognition of DNA Supercoil Geometry by *Mycobacterium tuberculosis* Gyrase, *Biochemistry 56*, 5440-5448.
[263] McClendon, A. K., Rodriguez, A. C., and Osheroff, N. (2005) Human topoisomerase IIα rapidly relaxes positively supercoiled DNA: implications for enzyme action ahead of replication forks, *J. Biol. Chem. 280*, 39337-39345.
[264] Chaires, J. B. (1990) Biophysical chemistry of the daunomycin-DNA interaction, *Biophys. Chem. 35*, 191-202.
[265] Graves, D. E. (1999) Drug-DNA interactions, In *Protocols in DNA topology and DNA topoisomerases* (Bjornsti, M. A., Osheroff, N., Ed.), pp 785-792, Humana Press, Newark, New Jersey.
[266] Kruczynski, A., Pillon, A., Creancier, L., Vandenberghe, I., Gomes, B., Brel, V., Fournier, E., Annereau, J. P., Currie, E., Guminski, Y., Bonnet, D., Bailly, C., and Guilbaud, N. (2013) F14512, a polyamine-vectorized anti-cancer drug, currently in clinical trials exhibits a marked preclinical anti-leukemic activity, *Leukemia 27*, 2139-2148.
[267] Tierny, D., Serres, F., Segaoula, Z., Bemelmans, I., Bouchaert, E., Petain, A., Brel, V., Couffin, S., Marchal, T., Nguyen, L., Thuru, X., Ferre, P., Guilbaud, N., and Gomes, B. (2015) Phase I Clinical Pharmacology Study of F14512, a New Polyamine-Vectorized Anticancer Drug, in Naturally Occurring Canine Lymphoma, *Clin. Cancer Res. 21*, 5314-5323.
[268] Kruczynski, A., Vandenberghe, I., Pillon, A., Pesnel, S., Goetsch, L., Barret, J. M., Guminski, Y., Le Pape, A., Imbert, T., Bailly, C., and Guilbaud, N. (2011) Preclinical activity of F14512, designed to target tumors expressing an active polyamine transport system, *Invest. New Drugs 29*, 9-21.
[269] Ross, W., Rowe, T., Glisson, B., Yalowich, J., and Liu, L. (1984) Role of topoisomerase II in mediating epipodophyllotoxin-induced DNA cleavage, *Cancer Res. 44*, 5857-5860.
[270] Chow, K. C., Macdonald, T. L., and Ross, W. E. (1988) DNA binding by epipodophyllotoxins and N-acyl anthracyclines: implications for mechanism of topoisomerase II inhibition, *Mol. Pharmacol. 34*, 467-473.
[271] Bombarde, O., Larminat, F., Gomez, D., Frit, P., Racca, C., Gomes, B., Guilbaud, N., and Calsou, P. (2017) The DNA-Binding Polyamine Moiety in the Vectorized DNA Topoisomerase II Inhibitor F14512 Alters Reparability of the Consequent Enzyme-Linked DNA Double-Strand Breaks, *Mol. Cancer Ther. 16*, 2166-2177.
[272] Bandele, O. J., and Osheroff, N. (2008) The efficacy of topoisomerase II-targeted anticancer agents reflects the persistence of drug-induced cleavage complexes in cells, *Biochemistry 47*, 11900-11908.

[273] Zdraljevic, S., Strand, C., Seidel, H. S., Cook, D. E., Doench, J. G., and Andersen, E. C. (2017) Natural variation in a single amino acid substitution underlies physiological responses to topoisomerase II poisons, *PLoS Genet 13*, e1006891.
[274] Ortega, J. A., Riccardi, L., Minniti, E., Borgogno, M., Arencibia, J. M., Greco, M. L., Minarini, A., Sissi, C., and De Vivo, M. (2018) Pharmacophore Hybridization To Discover Novel Topoisomerase II Poisons with Promising Antiproliferative Activity, *J. Med. Chem. 61*, 1375-1379.
[275] Bax, B. D., Murshudov, G., Maxwell, A., and Germe, T. (2019) DNA topoisomerase inhibitors: trapping a DNA-cleaving machine in motion, *J. Mol. Biol. 431*, 3427-3449.
[276] Cole, S. T., Brosch, R., Parkhill, J., Garnier, T., Churcher, C., Harris, D., Gordon, S. V., Eiglmeier, K., Gas, S., Barry, C. E., 3rd, Tekaia, F., Badcock, K., Basham, D., Brown, D., Chillingworth, T., Connor, R., Davies, R., Devlin, K., Feltwell, T., Gentles, S., Hamlin, N., Holroyd, S., Hornsby, T., Jagels, K., Krogh, A., McLean, J., Moule, S., Murphy, L., Oliver, K., Osborne, J., Quail, M. A., Rajandream, M. A., Rogers, J., Rutter, S., Seeger, K., Skelton, J., Squares, R., Squares, S., Sulston, J. E., Taylor, K., Whitehead, S., and Barrell, B. G. (1998) Deciphering the biology of *Mycobacterium tuberculosis* from the complete genome sequence, *Nature 393*, 537-544.
[277] Surivet, J. P., Zumbrunn, C., Rueedi, G., Bur, D., Bruyere, T., Locher, H., Ritz, D., Seiler, P., Kohl, C., Ertel, E. A., Hess, P., Gauvin, J. C., Mirre, A., Kaegi, V., Dos Santos, M., Kraemer, S., Gaertner, M., Delers, J., Enderlin-Paput, M., Weiss, M., Sube, R., Hadana, H., Keck, W., and Hubschwerlen, C. (2015) Novel tetrahydropyran-based bacterial topoisomerase inhibitors with potent anti-gram positive activity and improved safety profile, *J. Med. Chem. 58*, 927-942.
[278] Tan, C. M., Gill, C. J., Wu, J., Toussaint, N., Yin, J., Tsuchiya, T., Garlisi, C. G., Kaelin, D., Meinke, P. T., Miesel, L., Olsen, D. B., Lagrutta, A., Fukuda, H., Kishii, R., Takei, M., Oohata, K., Takeuchi, T., Shibue, T., Takano, H., Nishimura, A., Fukuda, Y., and Singh, S. B. (2016) *In vitro* and *in vivo* characterization of the novel oxabicyclooctane-linked bacterial topoisomerase inhibitor AM-8722, a selective, potent inhibitor of bacterial DNA gyrase, *Antimicrob. Agents Chemother. 60*, 4830-4839.
[279] Surivet, J. P., Zumbrunn, C., Bruyere, T., Bur, D., Kohl, C., Locher, H. H., Seiler, P., Ertel, E. A., Hess, P., Enderlin-Paput, M., Enderlin-Paput, S., Gauvin, J. C., Mirre, A., Hubschwerlen, C., Ritz, D., and Rueedi, G. (2017) Synthesis and characterization of tetrahydropyran-based bacterial topoisomerase inhibitors with antibacterial activity against gram-negative bacteria, *J. Med. Chem. 60*, 3776-3794.
[280] Pitts, S. L., Liou, G. F., Mitchenall, L. A., Burgin, A. B., Maxwell, A., Neuman, K. C., and Osheroff, N. (2011) Use of divalent metal ions in the DNA cleavage reaction of topoisomerase IV, *Nucleic Acids Res. 39*, 4808-4817.
[281] Magaro, G., Prati, F., Garofalo, B., Corso, G., Furlotti, G., Apicella, C., Mangano, G., D'Atanasio, N., Robinson, D., Di Giorgio, F. P., and Ombrato, R. (2019) Virtual screening approach and investigation of structure-activity relationships to discover novel bacterial topoisomerase inhibitors targeting gram-positive and gram-negative pathogens, *J. Med. Chem. 62*, 7445-7472.
[282] Miles, T. J., Hennessy, A. J., Bax, B., Brooks, G., Brown, B. S., Brown, P., Cailleau, N., Chen, D., Dabbs, S., Davies, D. T., Esken, J. M., Giordano, I., Hoover, J. L., Huang, J., Jones, G. E., Sukmar, S. K., Spitzfaden, C., Markwell, R. E., Minthorn, E. A., Rittenhouse, S., Gwynn, M. N., and Pearson, N. D. (2013) Novel hydroxyl tricyclics (e.g., GSK966587) as potent inhibitors of bacterial type IIA topoisomerases, *Bioorg. Med. Chem. Lett. 23*, 5437-5441.
[283] Miles, T. J., Hennessy, A. J., Bax, B., Brooks, G., Brown, B. S., Brown, P., Cailleau, N., Chen, D., Dabbs, S., Davies, D. T., Esken, J. M., Giordano, I., Hoover, J. L., Jones, G. E., Kusalakumari Sukmar, S. K., Markwell, R. E., Minthorn, E. A., Rittenhouse, S., Gwynn, M. N., and Pearson,

N. D. (2016) Novel tricyclics (e.g., GSK945237) as potent inhibitors of bacterial type IIA topoisomerases, *Bioorg. Med. Chem. Lett. 26*, 2464-2469.
[284] Jacobsson, S., Golparian, D., Scangarella-Oman, N., and Unemo, M. (2018) In vitro activity of the novel triazaacenaphthylene gepotidacin (GSK2140944) against MDR Neisseria gonorrhoeae, *J. Antimicrob. Chemother. 73*, 2072-2077.
[285] Scangarella-Oman, N. E., Hossain, M., Dixon, P. B., Ingraham, K., Min, S., Tiffany, C. A., Perry, C. R., Raychaudhuri, A., Dumont, E. F., Huang, J., Hook, E. W., 3rd, and Miller, L. A. (2018) Microbiological Analysis from a Phase 2 Randomized Study in Adults Evaluating Single Oral Doses of Gepotidacin in the Treatment of Uncomplicated Urogenital Gonorrhea Caused by Neisseria gonorrhoeae, *Antimicrob. Agents Chemother. 62*.
[286] Taylor, S. N., Morris, D. H., Avery, A. K., Workowski, K. A., Batteiger, B. E., Tiffany, C. A., Perry, C. R., Raychaudhuri, A., Scangarella-Oman, N. E., Hossain, M., and Dumont, E. F. (2018) Gepotidacin for the Treatment of Uncomplicated Urogenital Gonorrhea: A Phase 2, Randomized, Dose-Ranging, Single-Oral Dose Evaluation, *Clin. Infect. Dis. 67*, 504-512.
[287] GlaxoSmithKline. (2021) A Phase III, Randomized, Multicenter, Parallel-Group, Double-Blind, Double-Dummy Study in Adolescent and Adult Female Participants Comparing the Efficacy and Safety of Gepotidacin to Nitrofurantoin in the Treatment of Uncomplicated Urinary Tract Infection (Acute Cystitis), ClinTrials.gov.
[288] GlaxoSmithKline. (2022) A Phase III, Randomized, Multicenter, Open-Label Study in Adolescent and Adult Participants Comparing the Efficacy and Safety of Gepotidacin to Ceftriaxone Plus Azithromycin in the Treatment of Uncomplicated Urogenital Gonorrhea Caused by Neisseria Gonorrhoeae, ClinTrials.gov.
[289] Chan, P., Ingraham, K., Min, S., Scangarella-Oman, N., Rittenhouse, S., and Huang, J. (2020) Genetic evidence that gepotidacin shows well-balanced dual targeting against DNA gyrase and topoisomerase IV in *Neisseria gonorrhoeae*, In *IDWeek*, Virtual.
[290] Boye, P., Floch, F., Serres, F., Segaoula, Z., Hordeaux, J., Pascal, Q., Coste, V., Courapied, S., Bouchaert, E., Rybicka, A., Mazuy, C., Marescaux, L., Geeraert, K., Fournel-Fleury, C., Duhamel, A., Machuron, F., Ferre, P., Petain, A., Guilbaud, N., Tierny, D., and Gomes, B. (2020) Randomized, double-blind trial of F14512, a polyamine-vectorized anticancer drug, compared with etoposide phosphate, in dogs with naturally occurring lymphoma, *Oncotarget 11*, 671-686.
[291] Leary, A., Le Tourneau, C., Varga, A., Sablin, M. P., Gomez-Roca, C., Guilbaud, N., Petain, A., Pavlyuk, M., and Delord, J. P. (2019) Phase I dose-escalation study of F14512, a polyamine-vectorized topoisomerase II inhibitor, in patients with platinum-refractory or resistant ovarian cancer, *Invest. New Drugs 37*, 693-701.
[292] Kuriappan, J. A., Osheroff, N., and De Vivo, M. (2019) Smoothed Potential MD Simulations for Dissociation Kinetics of Etoposide To Unravel Isoform Specificity in Targeting Human Topoisomerase II, *J. Chem. Inf. Model. 59*, 4007-4017.
[293] Ortega, J. A., Arencibia, J. M., Minniti, E., Byl, J. A. W., Franco-Ulloa, S., Borgogno, M., Genna, V., Summa, M., Bertozzi, S. M., Bertorelli, R., Armirotti, A., Minarini, A., Sissi, C., Osheroff, N., and De Vivo, M. (2020) Novel, Potent, and Druglike Tetrahydroquinazoline Inhibitor That Is Highly Selective for Human Topoisomerase II alpha over beta, *J. Med. Chem. 63*, 12873-12886.
[294] Park, E., Willard, J., Bi, D., Fiszman, M., Kozeli, D., and Koerner, J. (2013) The impact of drug-related QT prolongation on FDA regulatory decisions, *Int. J. Cardiol. 168*, 4975-4976.